Advanced Studies in Characterization of Pyrolysis Products from Live Vegetation

Mahsa Alizadeh

A dissertation submitted to the faculty of
Brigham Young University
in partial fulfillment of the requirements for the degree of

Doctor of Philosophy

Thomas H. Fletcher, Chair
Morris D. Argyle
Bradley C. Bundy
Andrew Fry
David O. Lignell

Department of Chemical and Biological Engineering

Brigham Young University

Advanced Studies in Characterization of Pyrolysis Products from Live Vegetation

Mahsa Alizadeh
Department of Chemical and Biological Engineering
Doctor of Philosophy

BYU ENGINEERING

Abstract

Fire is a naturally occurring element in many ecosystems which can have both positive and negative effects. However, in recent years the frequency of the fires and the area they affect has increased. The rapid spread of wildland fires coupled with the limited resources available to forest services to manage wildland fires highlights the urgency for accurate prediction of fire spread.

Fire prediction models enable the fire management services to predict the spread of fire and prioritize firefighting efforts more effectively. Understanding reactions and mechanisms occurring during wildland fires improves the fire prediction models. During wildland fires, the biomass covering forest beds undergoes pyrolysis prior to combustion due to exposure to high temperatures. Pyrolysis is the thermal decomposition of biomass, which does not require oxygen. Volatiles generated during pyrolysis may react with oxygen and contribute to the fire spread. Detailed examination of the volatiles released during pyrolysis of the foliage provides valuable information which later can be used to improve fire prediction models.

In this research, the pyrolysis behavior of plant species from three U.S. regions (southern California, northern Utah, and the southeastern U.S.) with frequent wildfires is studied. The temperature and heating rates were selected carefully, 725 °C and 180 °C/s respectively, to mimic those of wildfires. A flat flame burner was used to provide a high temperature and high heating rate zone for pyrolysis experiments. This setup was used for pyrolysis of plant samples from southern California, northern Utah, and co-pyrolysis of chamise and scrub oak. Tar was collected during pyrolysis and co-pyrolysis experiments and was analyzed by a gas chromatography mass spectrometry (GC/MS) system. To identify the high molecular weight compounds in tar from pyrolysis of Utah juniper and long leaf pine litter, the collected tar was analyzed by high performance liquid chromatography (HPLC). Gas analysis was achieved by gas chromatography thermal conductivity detector (GC/TCD). To investigate tar compounds in various flame heights, pine needles were used as fuel and samples were collected from three different regions inside the flame:

near the base, the intermittent region and the plume region. These tar samples were later analyzed by GC/MS.

The results from this research show that the slight disparities in the tar yield of plants from different U.S. regions (southeastern U.S., northern Utah, and southern California) is likely due to inherent chemical and physical differences between various plant species. Similar to tar, the differences in the yields of light gases from plant species is due to biomass type. Further analysis of tar from all plants showed that, with the exception of manzanita foliage and its twigs, aromatics are the major constituents of tar. This research showed that despite similarities in the chemical composition of tar from various species, it is necessary to collect and analyze tar from any specific biomass to have a better understanding of its composition.

CO, CO_2, CH_4, and H_2 were the major constituents of pyrolysis gases on a wt % basis. CO was the main component of the light gases succeeded by CO_2, CH_4, and H_2 on a wt % basis.

High heating value of tar and light gases released during pyrolysis of all plant species was estimated. The contribution of tar to the HHV of volatiles was 82 to 92% which shows the importance of tar identification to estimate the impact of pyrolysis of biomass prior to combustion of foliage. Co-pyrolysis of chamise and scrub oak did not result in any significant synergistic effects as the chemical composition of the two plant species are similar to each other.

Keywords: pyrolysis, wildfires, live vegetation, biomass, tar, light gases

Acknowledgement

I would like to thank Dr. Thomas Fletcher for his mentorship, patience and kindness for the duration of my Ph.D. studies. Thank you for all your guidance and for giving me the opportunity to be in your research group.

I want to thank all undergraduate students for helping me during this research: Adam Fletcher, Sebastian Flores, Garret Johnson, Maxfield Crawford, Ann Marie Garner, Schuyler Duke, and Ricardo Moreno. Thank you for being such amazing lab mates and doing meticulous work in the lab. I enjoyed working with you and I truly appreciate your help. I also want to express my gratitude to Madi Johnston for helping me with HPLC experiments.

I would also like to thank the faculty who taught me in class and Dr. Argyle, Dr. Bundy, Dr. Fry, and Dr. Lignell for serving on my committee and helping me with this research.

I would like to express my gratitude to Dr. David Weise for helping me with sample collection and statistical analysis during this research. I would like to thank Dr. Morris Argyle for letting me use the gas chromatography thermal conductivity system for the duration of this research.

I acknowledge my deep thanks to my husband, Mahmood Rahmati, for his love and support during graduate school. I wouldn't have been able to focus on my research if you had not sacrificed so much time and energy. You are an amazing soulmate.

Table of Contents

List of Figures

List of Tables

Nomenclature

GC/MS	Gas chromatography mass spectrometry
HPLC	High performance liquid chromatography
GC/TCD	Gas chromatography thermal conductivity detector
USDA	United States Department of Agriculture
CPD	Chemical Percolation Devolatilization
PAH	Poly Aromatic Hydrocarbon
HHV	High Heating Value
α	Stoichiometric amount of oxygen
SSE	sum of squared error,
MSE	mean square error
AIC	Akaike Information Criterion
FDS	Fire Dynamics Simulator
WFDS	Wildland-Urban Interface Fire Dynamics Simulator
GPyro	Generalized Pyrolysis Model
CFD	Computational Fluid Dynamics
daf	dry- ash free
tig	Time to ignition(tig)
Tig	Ignition Temperature
mH2O	mass of moisture per mass of each sample
S.E. U.S.	southeastern United States
N. Utah	northern Utah
S. CA	southern California
wt%	weight percentage
FFB	Flat flame burner

NIST	National Institute of Standards and Technology
UHP	Ultra-High Purity
PVF	Polyvinyl fluoride
UV/Vis	Ultraviolet / Visible
ANOVA	Analysis of variance
TGA	Thermogravimetric analysis
β	mass fraction of chamise
WEEE	waste electrical and electronic equipment
HDPE	High-density polyethylene
z	Distance above the top of the fuel bed

1 Introduction

Fire is a naturally occurring phenomenon which may have both positive and negative effects on the ecosystem. However, in recent years, multiple factors, such as development in the wildland-urban boundary, deforestation and reforestation, invasive species, climate change and fire suppression, have led to increasingly destructive fires (Fusco et al., 2019; Pereira et al., 2021). Wildland fires are complex, multi-phase, and multi-scale phenomena that are affected by various factors such as environmental conditions (wind speed, air temperature, humidity), heat-transfer processes, and the physical and chemical properties of the foliage covering forest beds. This makes modeling wildfires challenging (Sullivan, 2009a). In recent decades, the number of the wildfires in U.S., the area they affect, and their adverse economic impacts have increased (Keeley and Syphard, 2016). The rapid spread of wildland fires coupled with the limited resources available to forest services to manage wildland fires highlights the urgency for accurate prediction of fire spread (Taylor et al., 2013).

Fire prediction models enable the fire management services to anticipate the spread of fire and prioritize firefighting efforts more effectively (Finney et al., 2012). Understanding reactions and mechanisms occurring during wildland fires is necessary to improve the models used to predict fire spread (Finney et al., 2021). Before combustion, the vegetation on forest beds undergoes pyrolysis as they are exposed to high temperatures. The bonds between molecules and atoms of the vegetation start to break releasing volatile compounds. Pyrolysis is the thermal decomposition of solid fuels that generates light gases, tar, and char (Shafizadeh, 1982). Detailed information on pyrolysis of vegetation such as the yields of tar and light gases, concentration of compounds in tar and light gases and the heat generated as the released compounds combust is valuable as it affects fire.

Many pyrolysis studies simplify the fuel by either using a surrogate such as cellulose, hemicellulose or lignin or by focusing on a single biomass type. The studies on diverse vegetation are rare (Di Blasi, 2008). Southern California, semi-arid ecosystem of northern Utah and southeastern U.S. all experience frequent wildfires. These areas are all covered with various types of plant species with different ratios of cellulose, hemicellulose and

lignin. These variations in their biochemical characteristics along with differences in the physical characteristics may result in disparities in the yields and chemical composition of pyrolysis products released as these plant species are exposed to high temperatures. Detailed understanding of pyrolysis products (their chemical composition and the yields) is critical for improving fire spread wildfire models (Mueller et al., 2021). Despite its role in soot formation, flame stability and gas-phase reactions, detailed studies on tar from pyrolysis of biomass are scarce (Evans and Milne, 1987; Wang et al., 2018; Apicella et al., 2020).

Another limitation in previous pyrolysis studies is their operating conditions and pre-treatment of samples; most of these studies are performed under controlled conditions at low heating rates that are different from those observed during wildfires (Greenberg et al., 2006; Zhang et al., 2020). Moreover, the samples are pre-treated prior to experiments to ensure reproducibility of the results (Boon et al., 1982; Susott, 1982; Tao, 2020). These conditions do not represent the high-temperature and high heating rate environment experienced in a wildland fire. Due to these issues, extrapolating results from these previous studies to real world wildland fires is challenging.

Forest beds are almost always covered with more than one type of biomass so during wildfires, this biomass blend is exposed to high temperatures, leading to potential synergistic effects that may affect pyrolysis of the vegetation and subsequently, the wildfires. Investigating the potential synergistic effects of co-pyrolysis of two types of biomass would improve our understanding of wildfires.

The focus of this dissertation is on studying the pyrolysis behavior of plant species from three U.S. regions (southern California, northern Utah, and the southeastern U.S.) with frequent wildfires. The temperature and heating rates were selected carefully, 725 °C and 180 °C/s respectively, to mimic those of wildfires. Butler et al. (2004) reported temperatures between 800°C to 1000°C during prescribed wildland fires. The experimental setup used to maintain a high temperature and high heating rate zone for pyrolysis experiments was a flat flame burner. This setup was used for pyrolysis of plant samples from southern California and northern Utah. Co-pyrolysis of chamise and scrub oak, two plant species from southern California, was also investigated using the flat flame burner. Tar was collected during pyrolysis and co-pyrolysis experiments and was analyzed by a gas chromatography mass spectrometry (GC/MS) system. To identify the high molecular weight compounds in tar from pyrolysis of Utah juniper and long leaf pine litter, the collected tar was analyzed by high performance liquid chromatography (HPLC). Gas analysis was achieved by gas chromatography thermal conductivity detector (GC/TCD). To investigate tar compounds present at various flame heights, pine

needles were used as fuel and samples were collected from three different regions inside the flame: near the base, the intermittent region and the plume region. These tar samples were later analyzed by GC/MS. The experimental setup for this part of the project was in the burn building of United States Department of Agriculture (USDA) Forest Service Pacific Southwest Research Station in Riverside, California. This was a comprehensive, experimentally grounded analysis of pyrolysis behavior of plant species that aimed to narrow the knowledge gaps in previous studies by performing the experiments in temperatures and heating rates that are observed during wildfires. The results from this research can be used to improve physical-based fire propagation models.

This dissertation first includes a literature review which discusses the published work regarding pyrolysis of live vegetation and its effect on the propagation of wildland fires. The literature review is structured into six distinct sections: (1) plant structure and its biochemical composition; (2) pyrolysis of biomass and its influence on wildfires; (3) pyrolysis products; (4) high heating value of pyrolysis products; (5) modeling wildfires and (6) previous research on pyrolysis of live vegetation. Following the literature review, the objective and tasks of this project are thoroughly explained (Chapter 3). Chapter 4 involves the description of the experiments. Chapters 5-6 discuss the gas and tar species evolved during rapid pyrolysis of southern California chaparral and northern Utah shrubs. Chapter 7 provides a comprehensive analysis of pyrolysis of selected plant samples from southern California, northern Utah, and southeastern U.S. to suggest components for physics-based wildland fire models. Chapter 8 discusses co-pyrolysis of two different types of biomass (chamise and scrub oak). Chapter 9 is on analysis of tars from a flame above a moving pine needle bed. The last chapter of this dissertation (Chapter 10) involves summaries and conclusions of the project.

2 Literature Review

This chapter reviews the published work regarding pyrolysis of live vegetation and its effect on the propagation of wildland fires. The literature review is structured into six distinct sections: (1) plant structure and its biochemical composition; (2) pyrolysis of biomass and its influence on wildfires; (3) pyrolysis products; (4) high heating value of pyrolysis products; (5) modeling wildfires, and (6) previous research on pyrolysis of live vegetation.

2.1 Plant Structure and Its Biochemical Composition

All organic matter of plant origin is referred to as plant biomass. Plant biomass can be classified into two groups: structural components and non-structural components. Structural components of biomass are sometimes referred to as lignocellulosic material (McKendry, 2002). Lignocellulosic biomass is made of 40-60 wt % cellulose, 15-30 wt % hemicellulose and approximately 10-25 wt % lignin. The structure and relative proportion of these components vary across species and plant parts, influencing the thermal degradation behavior of vegetation during heating and combustion. Non-structural components include proteins and amino acids, starch and soluble sugars (glucose and fructose), inorganic minerals and ashes, and extractives (resins, oils, waxes, lipids, etc.). Concentration of compounds classified as extractives has been reported to be up to 15 wt % of such biomass (Taylor et al., 2013; Wang et al., 2017). However, extractive yields reported for live vegetation may be as high as 58% (Matt et al., 2020). The extractives affect the pyrolysis reactions and the composition of pyrolysis products as their general composition varies between different species and even within one plant family between different seasons (Guo et al., 2010; Dietenberger et al., 2020). To better understand the effect of each compound classified as extractives on pyrolysis of biomass, first the concentration of each of these specific compounds in the biomass must be determined. Extraction of compounds classified as extractives has been widely discussed by Matt et al. (2020). Figure 2.1 shows cellulose, hemicellulose, and lignin in plant cells.

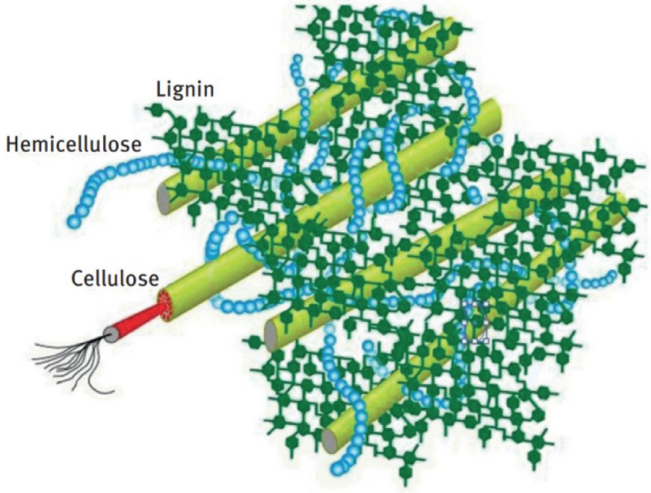

Figure 2.1: intertwined structure of cellulose, hemicellulose, and lignin in plant cells (Wang et al., 2017).

Cellulose, a linear macromolecular biopolymer made of glucose monomer units, is the most abundant compound found in biomass. The abundance of cellulose in various biomass is different, varying between 45% for woody biomass to 80- 95% in cotton, flax and chemical pulp (Wang et al., 2017). The complex chemical structure of cellulose can be formulated as $(C_6H_{10}O_5)_n$ in which n is the degree of polymerization. The cellulose polymer chains (made up of glucose monomers) connect inter and intramolecularly through hydrogen bonding and form higher order aggregates known as microfibrils. Figure 2.2 shows cellulose building units. These microfibrils develop semi-crystalline structures, containing both high order (crystalline) and low order (amorphous) areas that affect their mechanical stiffness, water permeability, and thermal stability. The crystalline areas provide mechanical strength and rigidity to plant cells, whereas the amorphous parts contribute to flexibility and facilitate cellulose reactivity; including interactions with hemicellulose and lignin (Klemm et al., 2005). Due to higher levels of intramolecular hydrogen bonds in the crystalline region, this area has higher thermal stability compared to amorphous areas. Pyrolysis of cellulose and the influence of its degree of polymerization on the yield of pyrolysis products and the compounds released has been studied (Yang et al., 2007; Bai et al., 2013; Wang et al., 2017; Ansari et al., 2019). However, it is worth mentioning that in most cases, due to complexity of cellulose structure, other compounds such as glucose, methyl cellobiose, cellotriose or cyclodextrin were used as cellulose surrogates (Wang et al., 2017).

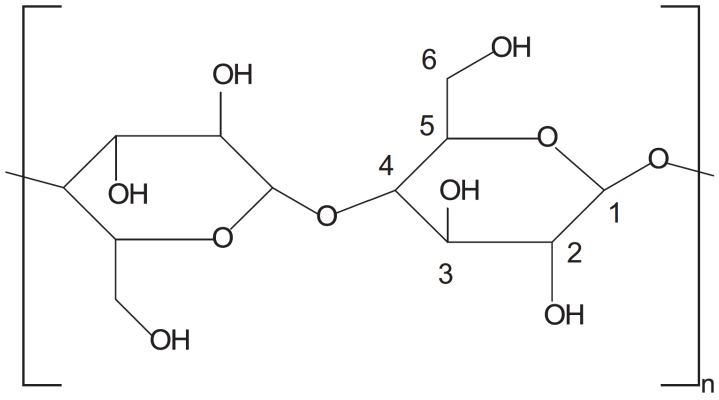

Figure 2.2: Cellulose building units (Collard and Blin, 2014).

Hemicellulose is a combination of various heterogeneous polysaccharides which may structurally vary from each other. Based on differences in structure, these polysaccharides are divided into four groups of xylans, mannans, xyloglucans, and b-1,3;1,4-glucans (Zhou et al., 2017). The ratios of each of these polysaccharides are different in various biomass types. Hemicellulose is cross-linked to lignin and cellulose in plant structures. It links cellulose microfibrils to each other, adding rigidity to cells. This makes extraction of hemicellulose from natural resources very challenging. Therefore, some researchers have opted for xylan to investigate hemicellulose pyrolysis (Shafizadeh et al., 1972; Yang et al., 2006; Shen et al., 2010a; Shen et al., 2010b; Wang et al., 2013; Stefanidis et al., 2014). Similar to cellulose pyrolysis, choosing a surrogate compound for hemicellulose resolves the extraction issues. However, the effect of other compounds in cellulose or hemicellulose on the pyrolysis reactions remains unexplored.

Lignin is a heterogeneous biopolymer present in the cell wall contributing to the structural support and resistance of plant cells against penetration of chemicals and microbes (Klemm et al., 2005). Lignin is made of three different types of lignols all made from phenyl propane monomer units. These lignols are p-hydroxyphenyl (H), guaiacyl (4-hydroxy-3-methoxyphenyl, G) and syringyl (3,5-dimethoxy-4-hydroxyphenyl). These monomer units are bonded by various ether bonds (C–O) and condensed (C–C) linkages, yielding a chemically heterogeneous structure for lignins. Figure 2.3 shows a partial structure of hardwood lignin. These heterogeneous features of lignin affect its behavior during pyrolysis reactions. The ratio of lignols varies between different types of biomass. Moreover, lignin levels in the cells of a specific plant increase as they mature. The prevalent ether bonds (β-O-4 and α-O-4) are less thermally

stable and start to break at relatively lower temperatures while the C-C bonds (β-5, 5-5 and β-β) are more resistant and break at higher temperatures. As a result, lignin decomposes over a broad temperature window and generates a more diverse set of products.

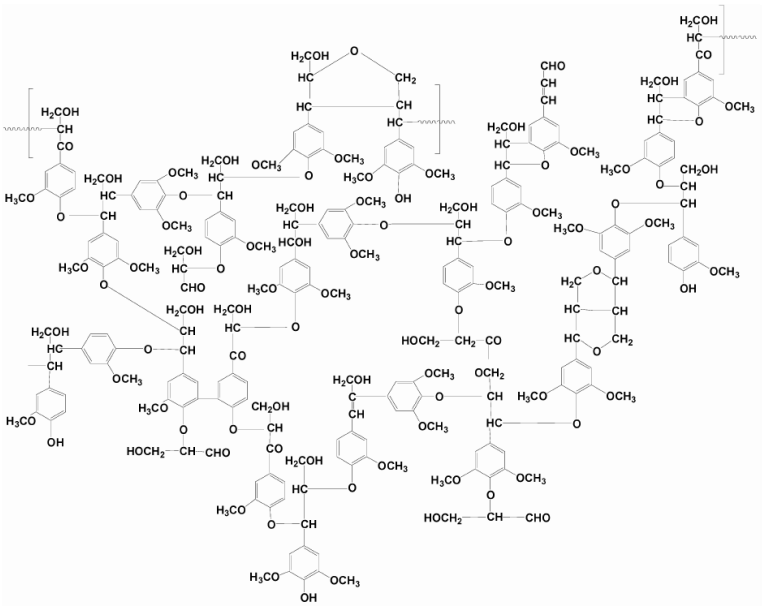

Figure 2.3: Partial structure of lignin (Brebu and Vasile, 2010).

Research performed by Yang et al. (2007) at low heating rates suggests that reaction mechanisms related to biomass pyrolysis may be categorized into three main steps: hemicellulose decomposition, cellulose decomposition, and lignin decomposition. Lewis and Fletcher (2013) predicted pyrolysis yields of sawdust particles as they were exposed to high heating rates (gas temperatures of 1163-1433 K) and low residence times (23-102 ms). They used CPD (Chemical Percolation Devolatilization) model and considered biomass as a weighted sum of cellulose, hemicellulose, and lignin. They also supplemented their model with a tar-cracking submodel to account for secondary tar cracking above 500°C. Their approach successfully predicted the yields of pyrolysis products regardless of the reactor type. Biagini and Tognotti (2014) studied kinetics of pyrolysis of 37 different materials concluding that the kinetic parameters of biomass might be derived from the kinetic parameters of three main biomass constituents (cellulose, hemicellulose and lignin). However, there is some contradicting evidence showing possible interactions between compounds released during thermal decomposition of biomass (Manyà et al., 2003; Zhou et al., 2014).

2.2 Pyrolysis of Biomass and Its Influence on Wildfires

During wildland fires, as a result of elevated temperatures, the vegetation on forest beds undergo complex processes which can be categorized into the following: 1) water evaporation, 2) pyrolysis of biomass releasing volatiles, 3) combustion of the released volatile compounds, and 4) smoldering and glowing combustion (Yokelson et al., 1996; Wang et al., 2017). Smoke generation is also of importance. Comprehensive investigation of wildland fires is possible only if a comprehensive study of each of these steps is performed.

Pyrolysis is defined as thermal decomposition of biomass that does not require O_2 (Uddin et al., 2018). Gases released during pyrolysis combust with O_2 present in the air releasing heat. This exothermic combustion process increases the temperature of surrounding leaves promoting fire spread (Porterie et al., 2007; Rahimi Borujerdi et al., 2022). Pyrolysis of the materials prior to combustion is an important step during fires as the compounds released during pyrolysis combust and propagate the fires. Information on the compounds released during pyrolysis such as concentration, rate of generation and the heat produced is valuable as it affects fire.

Moisture removal from the surface of the biomass is the first process occurring as biomass is exposed to high temperatures. The biomass constituents (mainly cellulose, hemicellulose, and lignin) then undergo initial thermal decomposition that releases low molecular weight volatile compounds. Compounds released during primary pyrolysis of biomass can be classified as: light gases (e.g., CO, CO_2, and H_2), light hydrocarbons (e.g., CH_4, C_2H_4), condensable gases (tars), and solid residue (char) (Gómez-Barea and Leckner, 2010). If the temperatures continue to rise, some of the released compounds start to participate in secondary reactions generating higher molecular weight compounds (Jegers and Klein, 1985; Caballero et al., 1997; Patwardhan et al., 2011; Zhou et al., 2013; Xiong et al., 2019). The predominant reactions occurring during primary pyrolysis of biomass are bond cleavage and depolymerization of the biomass chemical structure. Secondary pyrolysis involves both homogeneous and heterogeneous reactions between volatile compounds (light gases and tar) released during primary pyrolysis and char surfaces. The main reactions and processes occurring during secondary pyrolysis are: tar cracking, dehydrogenation and deoxygenation (Di Blasi, 2008; Ranzi et al., 2008), aromatization and PAH formation (Shafizadeh, 1982; Marsh et al., 2004; Di Blasi et al., 2014), reforming and radical recombination (Ranzi et al., 2008), and tar–char and gas–char interactions (Antal and Grønli, 2003; Di Blasi, 2008). Comparing the composition of light gases and tars collected from primary pyrolysis of biomass to those collected after secondary pyrolysis

shows drastic differences such as lower yields of tar, higher yields of light gases and more aromatics or soot precursors.

2.3 Pyrolysis Products

Pyrolysis results in three major classes of products: tar, light gases, and char. Tar is the mixture of compounds condensable at room temperature. Light gases remain gas at room temperatures and are mainly constituted of CO, CO_2, CH_4, and H_2. Char refers to the carbon-rich solid residue remaining after pyrolysis. Pyrolysis yield and characteristics of its products are influenced by numerous parameters including biomass type, prior pretreatments, pyrolysis atmosphere and temperature, heating rate, and residence time (Kan et al., 2016; Wang et al., 2017). Pyrolysis temperature has been widely studied as a key operating factor during pyrolysis of biomass. Product yields such as tar, permanent gases and char yield, composition of compounds released into these products are affected by temperature. Char yield decreases as temperature increases. This is due to thermal degradation of some of the higher molecular weight compounds present in char releasing lower molecular weight chemicals into the tar and gas phase. Tar yield reaches a maximum at a temperature between 630 and 730 K depending on heating rate. Further increase in temperature facilitates bond breakage in some of the tar compounds generating lower molecular weight chemicals. This secondary reaction process increases gas yield while tar yield decreases (Demirbas, 2007).

Heating rate and residence time affect the pyrolysis process. Since pyrolysis is bond breakage due to exposure of the biomass to high temperatures, its rate depends on how quickly the temperature at the reaction interface reaches the desired value. Higher heating rates will facilitate faster increase in temperature. Physical and chemical properties of the biomass, such as its thickness, its thermal conductivity, moisture content and chemical composition affect the heat transfer to the reaction interface. At a specific heating rate, the inner temperature at a certain depth of the leaf will be lower for biomass species with higher moisture content. When leaves are exposed to heat, a portion of the energy will evaporate the moisture. This will reduce the heat available for possible thermal degradation. There have been numerous studies investigating possible correlations between the biomass characteristics and pyrolysis products (Kan et al., 2016). There is some evidence that the ratio of major biopolymers in biomass (i.e., cellulose, hemicellulose and lignin) plays an important role in pyrolysis behavior of species such as pyrolysis product yields and concentration of various compounds in tar and permanent gases. Pyrolysis of each of the major components of biomass (cellulose, hemicellulose and lignin) happens through different reactions mechanisms generating different compounds. Cellulose and hemicellulose promote tar

generation while lignin contributes to char production. Pyrolysis of biomass with higher lignin content may result in generation of higher molecular weight tar (Kan et al., 2016). The relative ratios of cellulose, hemicellulose and lignin vary in different types of biomass which can be determined experimentally.

2.4 High Heating Value (HHV) of Pyrolysis Products

High heating value (HHV), sometimes referred to as high calorific value or heat of combustion, is the energy released during complete combustion of a unit quantity of fuel (initially at 25°C) in oxygen after the temperature of the products return to 25°C. The HHV value assumes that liquid water is the pyrolysis product at 25°C. HHV for a specific fuel (such as coal) can be measured by a bomb calorimeter in an experimental setup. Estimating the high heating value of a fuel provides researchers with valuable information about the energy content of a specific fuel, enabling researchers to classify and compare various fuel types. Higher values of HHV mean that the energy released during complete combustion of the fuel will be higher making the combustion more favorable. Estimating HHV of volatile pyrolysis products (tar and gases) provides us with information on the energy released into the flame front as the volatile compounds combust. Having better estimates of HHVs of tar and light gases also improves model inputs for physics-based fire simulators like WFDS or GPyro (Finney et al., 2012).

Since both gas species and tar species yields were measured quantitatively in this research, HHVs of both light gas and tar were computed for each plant species, and these values were blended into a composite HHV for total volatiles for each plant species.

$$HHV_{volatiles} = (yield_{tar} \times HHV_{tar}) + (yield_{light\ gas} \times HHV_{light\ gas}) \quad (2.1)$$

The HHVs for light gases released during pyrolysis were calculated by multiplying high heating values associated with each individual gas component (CO, CO_2, CH_4, and H_2) by their respective mole percentages. The HHV of tar was estimated by multiplying high heating values associated with each individual tar component by their respective mole percentages. This is an estimation because there are more species in the tar that were below the detection limit of the GC/MS instrument. Also, HHVs of all detected tar compounds are not readily available since they may not have been measured experimentally by a bomb calorimeter. This problem is similar to that observed by researchers who have tried to estimate the HHV of coal and coal tars. There are several correlations suggested in the literature to estimate the HHVs of these compounds based on their organic elemental composition (CHONS) as presented in Table 2.1. Most of these correlations were first developed to predict HHVs of coal but were later

modified to be used for coal tars and biomass. In these correlations, C, H, O, N, and S are the weight percentage of each element in the parent fuel and the coefficients are estimated according to the complete combustion of the fuel:

$$C_aH_bO_cN_dS_e + \alpha\, O_2 \rightarrow a\, CO_2 + \frac{b}{2} H_2O + \frac{d}{2} N_2 + e\, SO_2 \quad (2.2)$$

where α is the stoichiometric amount of oxygen needed for complete combustion of the fuel.

Table 2.1: Correlations for prediction of HHV(kJ/kg) of the fuel based on their elemental composition (adapted from (Richards et al., 2021)).

Correlation Name	Correlation
Dulong	$\Delta Hc = aC + b\left(H - \frac{O}{8}\right) + cS$
Steuer	$\Delta Hc = a\left(C - \frac{30}{8}\right) + b\left(\frac{30}{8}\right) + c\left(H - \frac{O}{16}\right) + dS$
Strache-Lant	$\Delta Hc = aC + bH + cO + dS$
D'Huart , Boie	
Seylor	$\Delta Hc = aC + bH + cO^2 + dS$
Gumz,Channiwala	$\Delta Hc = aC + bH + cN + dS + eO$
Dulong-Berthelot	$\Delta Hc = aC + bH - \frac{c(N + O - 1)}{8} + dS$
IGT	$\Delta Hc = aC + bH + c + d(O + N)$
VDI	$\Delta Hc = aC + b(H - \frac{O}{8})$+cS+dH
Given	$\Delta Hc = aC + bH + cO + dS + e$
Mott and Spooner	$\Delta Hc = aC + bH + cO + dS$ for coals with oxygen content below 15% $\Delta Hc = aC + bH + eO + fO^2 + gS$ for coals with oxygen content over 15%

These models were examined against existing data on HHV of coal and biomass using various measures of fit. These measures included: the sum of squared error (SSE), the mean square error (MSE), and the Akaike Information Criterion (AIC). The differences between AIC calculated for two different models helps select the model that fits the data well but is not too complex. Using these measures of fit to compare various models, Richards et. al (2021) suggested to use correlation provided by Mott and Spooner to calculate HHVs of biomass.

2.5 Modeling Wildfires

Modeling the propagation of wildfires is remarkably challenging due to complexities of the reactions and mechanism responsible for the nature of the fire. The ignition and propagation of wildland fires involve intricate processes and sophisticated mechanisms across multiple scales ranging from micrometer-level phenomena (e.g. pyrolysis on the surface of the fuel) to large-scale influences such as wind and landscape topography which affect fire spread on the scale of several kilometers. Various classifications of wildfire propagation models are proposed based on what phenomena, scales and modeling techniques are accounted for (Collin et al., 2011). One of the most commonly used methods to classify fire behavior models is proposed by Sullivan. He categorized fire behavior models along a spectrum ranging from empirical to fully physics-based models based on the model's dependence on physical principles versus empirical data. Models are categorized as physics-based models, empirical models, and quasi-physical (hybrid) models (Sullivan, 2009a, b).

Physics-based models, such as Fire Dynamics Simulator (FDS), Wildland-Urban Interface Fire Dynamics Simulator (WFDS), FIRETEC and Generalized Pyrolysis model(GPyro) use physics-based equations such as Navier Stokes and heat transfer correlations to describe the behavior of the fluid and temperature variations during complex reactions occurring in fires (Mell et al., 2010; Morvan, 2011; Hoffman et al., 2016; Grasso and Innocente, 2020; Zhou et al., 2021). Equations governing the kinetics of chemical mechanisms and reactions may be utilized by physical based models to:

1. predict the compounds generated during fires and their effect on fire behavior.

2. calculate the heat produced as the released compounds later react with oxygen and combust.

3. provide a basis for the calculation of pollutants and smoke formation.

While information on the yields of pyrolysis products and their composition would improve physics-based fire models, most models still utilize simple inputs when considering pyrolysis during fires (Linn et al., 2002; Mell et al., 2010).

Empirical fire models are developed based on statistical or observational data collected during past fires. While these models describe fire behavior under similar conditions well, their dependence on historical fire data may compromise their validity if fire conditions are novel (Sullivan, 2007, 2009a; Hoffman et al., 2016; Cruz et al., 2021).

Quasi-Physical (Hybrid) models combine empirical data with some physical principles to balance accuracy and computational efficiency. They offer better predictive capability than empirical models but are less

complex than full physical models. They are simpler and computationally efficient but limited to the conditions for which they were developed (Sullivan, 2009a, b; Mell et al., 2010; Prince et al., 2017).

WFDS has first been developed to model the behavior of wildland fires as they encounter urban structures. WFDS utilizes pyrolysis data, including tar formation, compounds released during pyrolysis and the kinetics of pyrolysis equations. There are some examples of using pyrolysis data to improve predictions of WFDS in the current literature. Mell et. al (2009) estimated the temperature of the fuel bed during fires by numerically solving a set of equations that accounted for pyrolysis on the surface of solid biomass. Shotorban and Mahalingam (2015) focused on enhancing WFDS to better predict the behavior of firebrands - embers travelling from the fire that if encounter dry vegetation may ignite spot fires distant from the main fire front. Since the firebrands go through pyrolysis, their mass loss due to thermal decomposition is accounted for. By including solid particle tracking capabilities into WFDS, researchers can describe firebrand dynamics, including their generation, travel, and descend more accurately, improving fire spread predictions. There are some examples of using pyrolysis data to improve predictions of WFDS in the current literature.

GPyro simulates material decomposition as they go through pyrolysis. This model is used for describing the chemical and thermal behavior of the solid material as the solid temperature increases due to exposure to fire (Stoliarov and Ding, 2023). The data provided by GPyro is sometimes used as input for CFD-based models such as FDS or WFDS. Detailed data on the composition of the volatiles released during pyrolysis, such as compounds and their concentration, improves the understanding of the reactions happening inside the pores and in general the understanding of what happens during pyrolysis on a molecular level.

FIRETEC accounts for turbulence and coupled atmosphere-fire interactions by simulating how fire affects the local wind and weather and their subsequent influence on fire growth. There is some research on incorporating pyrolysis data into the model to improve it. For example, Colman et al. (2007) have studied pyrolysis and combustion as two distinct yet dynamically linked processes which influence each other. By modeling pyrolysis separate from combustion, FIRETEC could simulate delayed ignition, the formation of volatile-rich areas ahead of the flame front, non-uniform combustion intensity, and dynamic behaviors such as spotting and flare ups which are often influenced by the generation and release of volatiles (Colman and Linn, 2007). It has been shown that model predictions of the rate of spread of wildland fires are particularly sensitive to windspeed and the thermal decomposition temperature of the burning vegetative fuel (McGrattan, 2017). Unfortunately, despite this sensitivity,

comprehensive data on thermal decomposition of burning vegetation are not available for many common vegetative fuels; Moreover, the fuel properties that are available from such experiments can exhibit high variability (Gollner et al., 2015). Sporri et al. (2022) used FDS to study charring properties of timber during its pyrolysis. Their study demonstrated that accurate simulation of timber pyrolysis using FDS requires careful specification of both the physical properties of the fuel such as density (essential to calculate mass loss and heat transfer rate), moisture content, specific heat capacity and detailed pyrolysis parameters such as reaction scheme which defines the number of reactions and their respective products (e.g., volatiles, char, ash). Leventon et al. (2023) measured thermal decomposition behavior of several U.S. plant samples. Incorporating species-specific thermal properties into wildfire simulations using the FDS showed that predicted fire spread rates varied between 0.50 m/s and 1.09 m/s. This highlights the sensitivity of fire spread predictions to the thermal decomposition characteristics of different fuels.

These examples show efforts to incorporate detailed pyrolysis reactions and chemical processes, including tar production and volatile compounds, into various physics-based models to improve present understanding of fires and predict the behavior of complex fires more precisely. Although previous studies provide an advanced understanding of biomass pyrolysis and its ignition behavior, most of the existing data focus on simplified biomass surrogates or study their pyrolysis at low heating rate conditions which are different from conditions in wildland fires. This leaves unanswered questions regarding pyrolysis of live vegetation during wildfires and the contribution of released volatiles to wildfire propagation. Current fire models often oversimplify the effect of pyrolysis of vegetation on fire propagation despite clear evidence that fuel characteristics such as their moisture content, chemical composition, and physiological state strongly affect their ignition and combustion behavior. Moreover, the lack of quantitative and fuel-specific characterization of volatiles generated during their pyrolysis limits the ability of physics-based wildfire models to predict heat release and fire propagation.

2.6 Previous Research on Pyrolysis of Live Vegetation

Safdari and Amini (Safdari, 2018; Safdari et al., 2018; Amini, 2020) investigated slow and fast pyrolysis of 14 plant species from southeastern U.S. under heating rates and temperatures representative of wildland fires. The slow pyrolysis experiments were conducted using a pyrolyzer apparatus while fast pyrolysis experiments were performed using a flat flame burner. They studied the effects of pyrolysis temperature, heating rates, and fuel conditions (whether the samples were dead or alive) on the yields and composition of pyrolysis products. Their results showed that

pyrolysis temperature, heating rate and fuel type significantly affected the yields and the composition of both tar and light gases. However, fuel conditions (whether the samples were dead or alive) imposed moderate effects on pyrolysis products. Their experiments revealed that the yield of light gases and tar depended on pyrolysis temperature and heating rates and as the pyrolysis temperature increased, the yield of light gases and tar increased. The effect of heating rate on the yields of slow pyrolysis products was investigated as heating rate varied from 5 to 30 °C/min and the temperature was set at 500 °C. They observed that increasing heating rate from 5 to 30 °C/min would increase tar yield and decrease char yield. The effect of temperature on pyrolysis product yields was investigated as temperature was raised from 400 to 500 °C at heating rate of 30 °C/min. The results showed that tar yield increased while char yield decreased as temperature increased from 400 to 500 °C. They concluded that the increase in the yield of tar due to increase in temperature or heating rate may be due to increase in the rate of bond breakage during primary pyrolysis reactions or secondary pyrolysis reactions.

Smith (2005) investigated the effects of moisture on combustion of live California and Utah chapparal. They observed that ignition temperature depended on the thickness of the foliage. The temperature range during which the moisture content of the foliage dropped varied between various species. Time to ignition(t_{ig}) depended on the thickness of the foliage and mass of moisture per mass of each sample (m_{H_2O}). However, there was no clear correlation between T_{ig} (ignition temperature) and m_{H_2O} for the individual samples.

Prince et al. (2014) studied differences in burning behavior of live and dead manzanita vegetation (*Arctostaphylos glandulosa*). They observed that combustion behavior of live and dead fuels varies even when the two fuels have similar nominal moisture contents. When exposed to high temperatures, live foliage experienced longer, and flatter temperature plateaus due to higher moisture contents compared to dead foliage. Dead foliage ignited faster and lost mass in a higher rate compared to live foliage. They suggested that wildfire models must integrate non-uniform leaf temperature distributions and water release patterns and consider differences in the effect of moisture on ignition temperature to accurately predict fuel ignition and combustion. Gallacher et al. (2016) studied the effect of season on ignition and burning behavior of ten live fuel from southern California, southeastern U.S. and northern Utah. They report that the main factors affecting ignition and flame behavior are moisture content, mass of the fuel and physical characteristics of the foliage such as apparent density and surface area (for broad-leaf species), and sample width (for needle species).

McAllister et al. (2012) studied ignition of live lodgepole pine and Douglas-fir needles to explore how live foliage ignites under piloted ignition conditions. They investigated whether existing empirical correlations between ignition time and moisture content (mainly developed for dead fuels) would be applicable to live fuels. Their results showed that while higher moisture content in live fuels led to longer ignition delay times, the correlation between moisture content and ignition delay times in live fuels was weaker than for dead fuels. They reported that including chemical composition of live foliage (for the Douglas-fir needle dataset) resulted in improved predictions of their ignition behavior as ignition behavior of live fuels vary significantly from dead fuels. McAllister and Weise (2017) investigated the effect of season (i.e., changes in physiological state, moisture content, biochemical content of live vegetation over the year) on ignition characteristics (ignition delay, mass loss rate at ignition) of live wildland fuels. They reported a large variation between species in how moisture content affected ignition delay and mass loss rate. They suggested that other factors such as chemical composition of the fuel may affect ignition behavior of live fuels. Their findings highlight the need for more detailed understanding of live fuel ignition and combustion behavior that incorporates physical state and chemical composition of the vegetation.

Collectively, these studies show that while fuel moisture content is a key factor affecting ignition and pyrolysis behavior of biomass, there are other characteristics of the fuel and process that have an influence on the combustion dynamics of live vegetation. The combined effects of heating rate, temperature, fuel morphology, chemical composition, and seasonal physiological should be considered when predicting the onset and progression of thermal degradation and ignition. Therefore, improving wildfire and pyrolysis models requires incorporating process-based understanding of live-fuel behavior as they are exposed to high temperatures—one that couples thermal, chemical, and physical processes involved during pyrolysis and combustion of living vegetation.

This dissertation addresses these gaps by providing experimental characterization of pyrolysis products from live vegetation collected from multiple U.S. regions under heating rates and temperatures observed during wildfires. By quantifying the yields of volatiles (tar and light gases), and their chemical composition, and consequently, estimating the energy content (HHV) of pyrolysis products, this work provides a detailed and relevant data set needed to improve wildfire models such as WFDS, FDS, and GPyro. Ultimately, these results aim to narrow the existing gap between experimental data on pyrolysis of vegetation and large-scale fire modeling, improving the prediction of wildfire spread.

3 Objectives and Tasks

The objective of this project was to study the pyrolysis behavior of a variety of leaves and foliage from species native to the wildlands of western United States, including northern Utah and southern California.
This objective included the following tasks:

1. Analysis of the major products generated during pyrolysis of samples from 8 western shrub species, including condensable and non-condensable volatiles released in the form of tar and light gases.
2. Analysis of tar species collected at different heights in flames from a pine needle bed to have a better understanding of how the composition of gases in the interior of the flame changes due to temperature and residence time in the flame.
3. Analysis of heavy molecular weight tar species generated during pyrolysis of plant species.
4. Analysis of synergetic effects of co-pyrolysis of samples from two plant species on the yields and chemical composition of tar and light gases.

This project is related to previous studies on pyrolysis of species from southeastern U.S. performed by Safdari (2018) and Amini (2020). It is also related to the previous studies on combustion of individual leaves from Western U.S. performed at BYU (Smith, 2005; Gallacher, 2016). The experiments provide crucial information on the yields and compositions of pyrolysis products for a variety of plant species and discuss how simultaneous pyrolysis of various biomass species affect pyrolysis products. Each task will be discussed separately.

4.1 Task 1. Pyrolysis of Western U.S. Plant Species

Pyrolysis of four plant species native to southern California (scrub oak, Eastwood's manzanita, chamise and hoaryleaf ceanothus), and four other species native to the woods of northern Utah (big sagebrush, Utah juniper, Gambel oak and bigtooth maple) were studied at conditions mimicking wildfires.

This work utilized: (1) a flat-flame burner (FFB) apparatus to study pyrolysis of various fuels at high heating rates; (2) two gas chromatograph (GC) instruments each equipped with either a mass spectrometer (MS) or thermal conductivity detector (TCD) to analyze condensable and non-condensable pyrolysis products respectively; (3) a high performance liquid

chromatography (HPLC) device to analyze the heavy molecular weight portion of tar to provide better understanding about pyrolysis products.

4.2 Task 2. Analysis of Tars from a Flame Above a Moving Pine Needle Bed

The main goal of this part of the project was to investigate the differences in chemical compounds and their relative ratios at various heights in a flame. Studying the effect of flame height on types of chemical compounds and the changes in their relative ratios released into flame at various flame heights provides more information about the chemical reactions and probable pyrolysis mechanisms responsible for release of these compounds.

Flames above a pine needle bed were studied as a joint project with several Forest Service personnel in the burn building at the USDA Forest Service Pacific Southwest Research Station in Riverside, California. The Riverside laboratory was equipped with a wind tunnel, ca. 3 m long and 1 m wide. The fuel bed consisted of dead longleaf pine needles (*Pinus palustris* Mill). Pine needles were selected as the fuel in this study to imitate forest floors and burned under no-wind conditions. Tar samples from the burns were collected at three different heights to investigate the differences in the concentrations of major tar components. Other investigators obtained gas samples at the same locations in the flame.

4.3 Task 3. Analysis of Heavy Tar Species Generated During Pyrolysis of Plant Species

The GC/MS system could only measure compounds with molecular weights lower than about 300 amu. An HPLC system was used to analyze heavy molecular weight fraction of tar. The HPLC instrument was in the Chromatography facility in the BYU Chemistry Department. This part of the project only used longleaf pine litter (since large amounts of this sample were already in the lab remaining from previous studies) and Utah juniper due to ease of access.

4.4 Task 4. Analysis of Synergetic Effects of Co-pyrolysis of Samples from Two Plant Samples

To investigate the synergetic effect of co-pyrolysis of two plant samples, first, samples from individual plant species were pyrolyzed, and the yields and composition of tar and light gases were studied. A sample consisting of two different plant species was then pyrolyzed. Volatiles yields were measured along with the pyrolysis products. Chamise and scrub oak were selected as fuel. The effect of simultaneous pyrolysis on various

compounds of tar and light gases was investigated. The co-pyrolysis effects were of particular interest to the Forest Service. The data collected in this part will help understand wildland fires better since forest floors are always covered with litter from shrubs and trees or with grass species.

4 Description of Experiments

4.1 Plants Tested

The plant species tested in this research are native to the wildlands of southern California and northern Utah. Longleaf pine litter used during heavy molecular weight tar analysis is native to southeastern United States. These plants were selected as they are from regions of U.S. with frequent wildfires. The Utah juniper samples were obtained on Highway 6, one half-mile northeast of Eureka, Utah (approximately 39°58′02″ N 112°05′34″ W). All other northern Utah samples were taken at the Rock Canyon Trailhead in Provo, Utah (approximately 40°15′52″ N 111°37′51″ W). The Southern California samples were freshly cut from the North Mountain Experimental Area, adjacent to the San Bernardino National Forest (approximately 33°50′20″ N 116°55′36″ W). The Southern California plant samples were put in zip lock bags to maintain their moisture and were express mailed to the lab located in Brigham Young University, Provo, Utah. The pyrolysis of southeastern plant species was conducted by Safdari (2018). Samples of southeastern plants were cultivated in a nursery in Florida. Live potted plants were shipped to the lab location in Provo, Utah. Upon arrival, these plants were kept under well-lit conditions and were watered regularly to make sure they remained alive during experiments. Table 4.1 contains the names and the location of the plant species used for the pyrolysis experiments. The images of each of the plants is provided in Figure 4.1.

Table 4.1: Species used during pyrolysis experiments of U.S. plant species. (S.E. U.S. stands for southeastern United States and S.CA stands for southern California. N. Utah represents northern Utah.)

Common name	Scientific name	Location
Longleaf pine	*Pinus palustris Mill.*	S.E. U.S.
Sparkleberry	*Vaccinium arboreum* Marshall	S.E. U.S.
Chamise	*Adenostoma fasciculatum* Hook. and Arn.	S. CA
Eastwood's manzanita	*Arctostaphylos glandulosa* Eastw.	S. CA
Scrub oak	*Quercus berberidifolia* Liebm.	S. CA
Hoaryleaf ceanothus	*Ceanothus crassifolius* Torr.	S. CA
Big sagebrush	*Artemisia tridentata* Nutt.	N. Utah
Utah juniper	*Juniperus osteosperma* (Torr.) Little	N. Utah
Gambel oak	*Quercus gambelii* Nutt.	N Utah
Bigtooth maple	*Acer grandidentatum* Nutt.	N. Utah

(a) Longleaf pine

(b) Sparkleberry (c) Chamise (d) Eastwood's manzanita

(e) Scrub oak (f) Hoaryleaf ceanothus (g) Big sagebrush

(h) Utah juniper (i) Gambel oak (j) Bigtooth maple

Figure 4.1: (a) from (Willis et al., 2026), (b) from (Tirmenstein, 1991), (c) photo taken by Bryant Baker, via (ForestWatch), (d) photo taken by Daniel Fitzgerald, via (Mount Diablo Interpretive Association), (e) from (City of Glendale), (f) Photo by Juan Avise from (UC Irvine – Natural History of Orange County, 2009), (g) photo taken by Tom Lebsack, via (Lady Bird Johnson Wildflower Center, 2019), (h) Image courtesy of Utah State University Extension (n.d.). Used for academic purposes (Utah State University Extension), (i) Reproduced from (Olsen et al., 2021), Utah State University Extension, Used for academic purposes. (j) Photo taken by Lee Page, taken on June 13, 2018, at the Lady Bird Johnson Wildflower Center, Austin, Texas. Courtesy of the Wildflower Center Digital Library (Lady Bird Johnson Wildflower Center, 2018).

4.2 Moisture Content Measurements

For each of the species studied, the moisture content was measured twice daily (at the beginning and the end of the day) by a Computrac MAX 1000 moisture analyzer (manufactured by Arizona Instrument, L.L.C., Chandler, AZ, U.S.). The average of these two values was reported as the moisture content for each of the samples used that day. Moisture content here was defined on a dry basis (mH2O/mdry) as commonly used in forestry research.

4.3 Ash Content Measurements

The chemical compositions of the plant samples were primarily comprised of carbon, oxygen, hydrogen and nitrogen, with trace amounts of elements such as heavy metals and alkali metals (Di Blasi, 2008; Shen et al., 2016). These metals contribute to the ash content of the sample. Ultimate and proximate analyses for species studied here are provided in the Appendix (Table A1). To determine the ash content, the sample was placed in a crucible and was heated in an oven from 105 to 500 °C over the course of one hour. Then, its temperature increased to 750 °C over the next hour. The sample remained in the oven for almost 24 h. Eventually, the residual mass in the crucible was reported as the ash content of the original sample. The ash content for the plant species used in these experiments varied between 1.84 and 5% (See Table 4.2).

Table 4.2: Ash content of the plant species studied.

Plant species	wt% Ash (moisture-free basis)
Longleaf pine litter	1.65%
Big sagebrush	4.00%
Utah juniper	4.20%
Gambel oak	2.80%
Bigtooth maple	3.30%
Chamise twigs with foliage	3.10%
Chamise twigs w/o foliage	3.70%
Eastwood's manzanita foliage	2.50%
Eastwood's manzanita twigs	3.40%
Scrub oak	4.80%
Hoaryleaf ceanothus	2.70%

4.4 Experimental Setup

To mimic high temperatures and heating rates observed during the pyrolysis of plants in wildland fires, the experiments were conducted using a flat-flame burner (FFB) apparatus which was set to maintain a sample heating rate of 180 °C/s and gas temperature of 725 °C. These conditions were carefully selected to mimic those of wildland fires. Butler et al. (2004) reported temperatures between 800 °C and 1000 °C during the wildland fires.

4.4.1 Description of the Flat-flame Burner

The flat-flame burner apparatus consisted of a 20 cm × 27 cm perforated metal base, surrounded by ceramic glass windows. The ceramic (Neoceram) windows were 30.5 cm high. The gaps between the burner and glass walls were filled with zirconia felt to prevent oxygen from entering the system. One of the glass windows featured a 5 cm diameter circular opening to insert the foliage samples. Samples were placed in an alligator clip connected to a metal rod to enter the high temperature zone. Upon entering the high temperature and high heating rate zone, the samples were positioned parallel to the surface of the metal base. A balance weighed the metal rod apparatus and the weight vs. time was recorded. Flame conditions were set to be fuel rich (equivalence ratio of 1.13) to support an oxygen-free, high-temperature environment for the pyrolysis of samples. The fuel mixture feeding the pre-mixed flame was made up of hydrogen and methane. The flow rates of CH_4 and H_2 were 26.5 L/min and 16.6 L/min, respectively. This fuel mixture would mix with atmospheric air with a flow rate of 258.8 L/min. The gas temperature at the location of the sample was 725 °C during pyrolysis of southern California and northern Utah species. When the flame was set to burn at fuel rich conditions, a flat blue flame appeared a few millimeters above the surface of the burner, followed by a secondary flame at the top of the glass chamber. There was no O_2 present at the region between these two flames, providing a high temperature and high heating rate zone for pyrolysis of samples. The FFB structure was set on a conveyor belt which enabled the burner structure to be moved. After loading the sample, the burner was pulled into position to stop under the sample. The vertical distance between the burner and the sample was 26 cm. The temperature within the flame at the level at which the samples were loaded was measured by an Omega K-type thermocouple (wire diameter of 0.38 mm, response time of 0.8 s, and maximum working temperature of 871°C). The FFB utilized a cooling water recirculation system to prevent overheating and potential damage to the surface of the metal base. This cooling system kept the temperature of

the burner surface low enough that radiation from the metal surface to the sample could be considered negligible.

Figure 4.1 shows the schematic of the flat-flame burner, cooling bath and sample collection system during pyrolysis experiments. Pyrolysis products were collected through a funnel positioned on the top of the high-temperature area. The mouth diameter of the funnel was 12.5 cm and the distance between the sample and the funnel mouth was 10 cm. Figure 4.2 shows a photo of the flat-flame burner, foliage sample and funnel. The pyrolyzed foliage sample is glowing slightly red in this photo. The funnel was attached to a line that was heated to 300 °C (to prevent tar compounds from condensing in the tube), leading to a vacuum pump. The velocity of the gases at sample location was about 1 m/s. Pyrolysis products went through the cooling system consisting of test tubes, sitting in an ice bath. Tar compounds and moisture condensed as their temperature decreased and became trapped in the glass wool inside the test tubes. The light gases generated during pyrolysis were collected in 1 L Tedlar® bags (manufactured by CEL Scientific, Cerritos, California, U.S.) and were later analyzed.

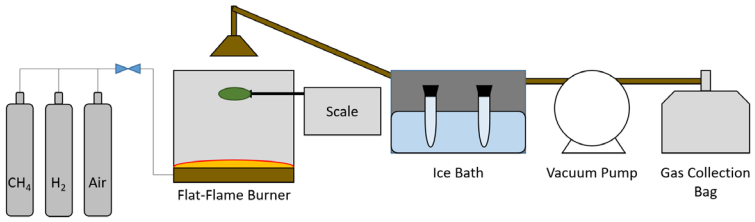

Figure 4.2: Schematic of the pyrolysis gas collection system (from (Alizadeh et al., 2024))

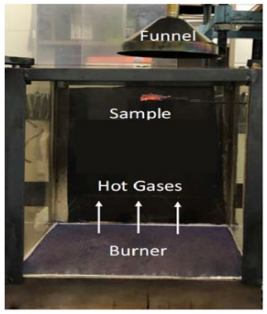

Figure 4.3: Photo of the flat-flame burner system. The fuel-rich flame is blue (barely visible) and only a few millimeters from the surface of the burner (from (Safdari, 2018)).

4.4.2 Description of setup used to study compounds at various flame heights

Flames above a pine needle bed were studied as a joint project with several Forest Service personnel in the burn building at the USDA Forest Service Pacific Southwest Research Station in Riverside, California. The bed consisted of dead longleaf pine needles (*Pinus palustris* Mill.) with average moisture content of 8.53% on a dry fuel basis. Elemental composition of the longleaf pine needles was analyzed previously by Matt et al. (2020).

The fuel bed consisted of 1.2 kg of pine needles placed on the surface of a conveyer belt which consisted of a non-combustible fabric. The fuel bed was 160 cm long, 51 cm wide, and 10 cm deep, for a mass load of 1.5 kg/m^3. Fuel beds were ignited in a line across the conveyor belt, resulting in a line fire that spanned the width of the fuel bed (see Fig. 4.3). Fuel moisture content and mass loading, ambient temperature, and relative humidity in the tunnel were measured between each experiment. Average room temperature was 27.7±0.5°C with an average relative humidity of 12.8±0.7%, where the deviation is the 95% confidence interval.

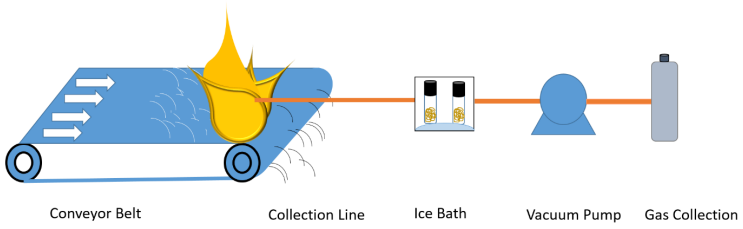

Figure 4.4 : Schematic of experiments conducted to analyze compounds at various flame heights.

Probes consisting of ¼ inch diameter stainless steel tubes were placed at a specified height above the conveyor belt (see Table 4.3). Only one sampling location was used for each experiment. Probe lines were heated at 300°C to prevent condensation of heavy hydrocarbons released during pyrolysis. The conveyor belt was operated manually to keep the flame in the same location relative to the probe as the flame spread through the pine needle bed. A pump sucked gases through the probe into glass tubes filled with glass wool that were placed in an ice bath to condense the tar (See Fig. 4.3). Additional probes at the same location sampled light gases in stainless steel vessels for subsequent analysis by other groups. After each experiment, the test tubes were capped and sealed with parafilm for later analysis. Tar deposited on the glass wool and sides of the test tube was extracted using dichloromethane (CH_2Cl_2). The extracted tar was analyzed using a GC/MS system.

Table 4.3: Probe Locations, where z represents the distance above the top of the fuel bed.

Flame Region	z (cm)	# of experiments
Flame base	20	11
Intermittent flame	64	9
Plume	128	4

4.4.3 Tar Extraction

As the pyrolysis products passed through the ice bath, their temperature decreased, leading to condensation of moisture and tar. The condensable products were captured in the test tubes. After the experiment, CH_2Cl_2 was added to the test tubes to dissolve tar. To remove moisture, approximately 2 grams of Anhydrous $CaSO_4$ were added to the tar-CH_2Cl_2 mixture. After a few minutes, phase separation transpired inside the test tubes, with tar being in the liquid phase and moisture being adsorbed by the $CaSO_4$ and turning into a solid.

4.4.4 Tar Yield

Tar yield is defined as the weight percentage of condensable pyrolysis products, aside from moisture, released per mass of the initial sample. Tar yield is reported on a dry, ash-free basis. The difference between the mass of the test tubes before and after the experiments was used to estimate the moisture and tar generation during experiments.

Moisture in this experiment originated from three sources: (a) the inherent moisture in each sample; (b) the water produced by combustion of the FFB gas mixture (H_2, CH_4); and (c) the water produced by the pyrolysis of the foliage sample. Moisture contribution from the flame was estimated through control experiments in the FFB with no foliage sample.

4.4.5 Char Yield

Char yield was calculated as the weight percentage of solid pyrolysis products relative to the mass of the initial sample, calculated on a dry, ash-free basis. Following each experiment, the mass of the residue on the alligator clip represented the combined char and ash for that experiment. Sudden changes in mass indicated detachment of portions of the sample occurring occasionally, and hence, those data were not used in the determination of char yield.

4.4.6 Gas Yield

Gas yield was defined as the weight percentage of non-condensable light gas products generated relative to the mass of the initial sample, on a dry, ash-free basis. Tar and char yields were measured separately, following

pyrolysis experiments; the gas yield was calculated by difference using Equation (4.1).

$$\text{Yield}_{\text{tar}} + \text{Yield}_{\text{light gas}} + \text{Yield}_{\text{Char}} = 1 \quad (4.1)$$

4.4.7 Description of GC/MS

Tar was analyzed using a 1310 Thermo Fisher® gas chromatography mass spectrometry (GC/MS) system (Manufactured by Thermo Fisher Scientific, Waltham, MA, U.S.) equipped with a Rxi-1 ms capillary column (60 m × 0.25 mm × 1 μm, manufactured by Restek, Bellefonte, PA, U.S.). After tar extraction, 1.0 μL of the CH_2Cl_2–tar mixture was injected into the GC/MS system. The oven temperature was adjusted, based on a pre-established program. The temperature of the injected mixture was held at 50 °C for 5 min, then was raised to 250 °C at a rate of 10 °C/min and subsequently was maintained at 250 °C for 5 min.

Ultra-high purity (UHP) helium was used as a carrier gas in the GC/MS system. Each test was performed three times to ensure reproducibility, and the average of the measured values was reported, along with the 95 percent confidence interval. Identification of tar compounds was achieved by comparing the mass spectra of the detected compounds with the NIST23 spectral database (NIST, 2023). Analysis of tar samples revealed that many tar compounds were present in low concentrations, resulting in a low signal-to-noise ratio, below the detection limit. This complicated the identification of some of these tar compounds. Concentrations of identified tar compounds were reported as mole fractions. To calculate the mole fraction of a specific tar compound, the area under the GC peak associated with that specific compound was divided by the sum of areas under all detected and identified GC peaks.

4.4.8 Description of GC/TCD

Post-pyrolysis gases were collected in 1 L Tedlar® gas bags and were immediately analyzed using a gas chromatograph (Agilent Technologies 7890A, manufactured by Agilent Technologies Inc., Santa Clara, CA, U.S. equipped with a Supelco Carboxen 1004 packed column (2 m × 1.5 mm), manufactured by Merck, Darmstadt, Germany) and a thermal conductivity detector (GC/TCD). Ultra-high purity (UHP) helium was used as a carrier gas. Analysis of the gases showed that the four major species present in light gases from pyrolysis were CO, CO_2, CH_4 and H_2 on a wt% daf basis. After each experiment, 1 mL of the gas sample from the gas bag was injected into GC/TCD manually. The oven temperature was adjusted to start at 50 °C and was held at this value for 5 min, then increased to 225 °C at 20 °C/min. The temperature was then maintained at 225 °C for 6.5 min; the total run time was 21 min.

Using Tedlar bags to collect and measure hydrogen (H_2) was challenging due to the physical properties of both the gas and the sampling bags. Hydrogen is an extremely small molecule and is highly diffusive. Hydrogen molecules will diffuse rapidly through the polyvinyl fluoride (PVF) film of Tedlar® bags and escape through their seams and valves, resulting in significant decrease in its concentration in a short period of time. In addition, weak adsorption and desorption interactions between H_2 and the PVF film of the bag can change the measured concentrations of the hydrogen gas in the samples, especially when the concentration of hydrogen in the samples are already at low levels. These issues resulted in significant variations in H_2 concentrations during collection, reducing the accuracy of the measurements and leading to poor reproducibility. To tackle these issues, the gas samples were injected into the GC/TCD system as soon as they were collected. This significantly reduced the time available for H_2 molecules to diffuse away from the surface of the Tedlar® bags.

4.4.9 Description of HPLC

Tar extraction with the purpose of analyzing the collected tar with HPLC was achieved differently than the one used when it was subsequently analyzed by GC/MS. In the case of tar analysis with HPLC, acetonitrile was used to dissolve tar.

The analysis of samples with HPLC was done in the Department of Chemistry and Biochemistry at Brigham Young University, Provo, Utah. The instrument was a Shimadzu LC-20AT high performance liquid chromatograph (HPLC) with a Shimadzu SPD-M20A UV/Vis photodiode array detector and LabSolutions software. The column used was a 25 cm long bonded-phase C18 with 5 μm packing, pore size of 10 nm, and the internal diameter of 4.6 mm.

The mobile phase consisted of two solvents; A: water and B: acetonitrile. The flow rate was 1 mL/min. The gradient was increased linearly from 5% acetonitrile to 95% acetonitrile over 20 minutes, then held at 95% acetonitrile for 5 minutes before returning to initial settings.

4.5 Statistical Analysis

All concentrations reported in this dissertation are averages of at least three experiments. The error bars for the reported values are ±95% confidence intervals for at least three experiments. Data analysis and graphing were performed using Microsoft® Excel® for Microsoft 365 MSO (Version 2510, Build 16.0.19328.20178), 64-bit edition. Analysis of variance (ANOVA) was used to test whether the means of independent groups are significantly different from one another. The null hypothesis is that the means of the studied groups are in the same range and are not statistically different from each other. If the calculated *p*-value is less than 0.05, then null hypothesis

is rejected and there is a significant difference between the means of the investigated groups. The ANOVA test was done using Microsoft Excel to calculate p-values.

5 Gas and Tar Species Evolved during Rapid Pyrolysis of Southern California Chaparral

5.1 Introduction

Southern California is one of the regions in U.S. with frequent wildland fires. The overall area in this region affected annually by wildland fires was an average of 373,000 acres (National Interagency Fire Center). Studying pyrolysis of plant samples from this region is necessary to improve fire modeling and firefighting efforts (Weise et al., 2024).

This chapter investigates the yields and chemical composition of pyrolysis products (tar and light gases) released during thermal degradation of selected southern California chaparral plants. The results here have been published (Alizadeh et al., 2024). The freshly cut stems of scrub oak, Eastwood's manzanita, chamise and hoaryleaf ceanothus were shipped to Brigham Young University (in Provo, Utah) and were stored in sealed bags to reduce moisture loss. They were pyrolyzed in a flat flame burner at high temperatures and heating rates (725 °C and 180 °C/s respectively) and the pyrolysis products were collected and subsequently analyzed. The goal of these experiments was to provide insight into the chemical composition of the pyrolysis products of these plants which will subsequently improve our understanding of plant combustion and hence wildland fires.

5.2 Results and Discussion

5.2.1 Yield of Tar, Light Gases and Char

Figure 5.1 and Table 5.1 show the yields of tar, char and light gases released from the four California species on a dry ash-free (daf) basis. The total yield of volatiles is defined as combined yield of tar and light gases released during pyrolysis of each sample. As mentioned in Chapter 4, operating conditions during pyrolysis of southern California samples were 725°C and the heating rate of 180 °C/s.

Table 5.1: The yield of pyrolysis products, tar, light gases, and char released from common California species (All reported numbers are wt% and on a dry and ash-free basis.).

Plant species	Tar yield	Light gas yield	Char yield	Total yield of volatiles
Scrub oak	56	24	20	80
Eastwood's manzanita twigs w/o foliage	48	27	25	75
Eastwood's manzanita foliage	50	28	22	78
Chamise twigs w/o foliage	57	23	20	80
Chamise twigs with foliage	59	23	18	82
Hoaryleaf ceanothus	51	31	18	82

The total yield of volatiles ranged from 75 wt% (daf) for the Eastwood's manzanita twigs to 82 wt% (daf) for hoaryleaf ceanothus and chamise. The total yield of volatiles generated from the foliage was compared to the yield from the twigs to investigate any possible variations in the pyrolysis behavior of two different parts of one plant. The comparison of the volatiles yields from foliage to that from the twigs showed no significant difference.

The tar yield varied between 48% daf (Eastwood's manzanita twigs) to 59% daf (chamise), with a corresponding change in the yield of light gases.

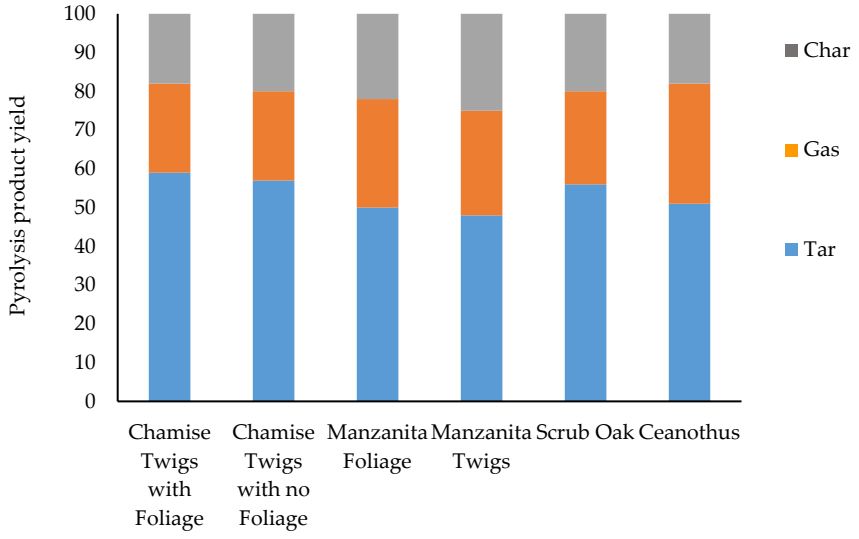

Figure 5.1: Yield of pyrolysis products for common California chaparral (wt%, daf basis).

5.2.2 Compounds Present in Tar

Tar analysis was conducted to investigate the chemical species and their concentration generated during pyrolysis of various plants. Table A2 (provided in the Appendix) contains the complete list of tar compounds, their chemical class, molecular formula, and molecular weight. Concentration of compounds from pyrolysis of California chaparral is provided in Table A3 (See Appendix). Compounds were classified as aromatic or non-aromatic to help understand possible mechanisms involved in thermal degradation of samples. Aromatics in tar from southern California plants were classified into three major subgroups: benzenoid aromatics (aromatic compounds containing only one benzene ring), heterocyclic aromatics and poly aromatic hydrocarbons (PAHs). Phenol, 1-ethyl, 3-methyl benzene, 2-methyl phenol, 3-methyl phenol, and 4-ethyl-2-methoxy phenol were all classified as benzenoid aromatics. However, these compounds are sometimes referred to as "phenolic compounds" to help compare the data to existing literature. Non-aromatic compounds present in tar from California plants were divided into cycloalkanes, cycloalkenes, alcohols, and heterocyclics. Heterocyclic compounds are cyclic non-aromatic compounds with at least one hetero atom (nitrogen, sulfur, oxygen, etc.) in their ring structure. Table 5.2 shows detailed classification of species present in tar from pyrolyzed samples. With the exception of Eastwood's manzanita, aromatic compounds are the major constituents of tar. Among aromatics, benzenoids, especially phenol, were the most abundant tar compound. Overall concentration of benzenoids in tar varied from 16.78 mole% in Eastwood's manzanita to 74.62 mole% in chamise. The other primary tar compounds were 2-methyl phenol, 3-methyl phenol, 4-ethyl-2-methoxy phenol (4-ethyl guaiacol), 2,3-dihydro benzofuran, and 9,10-dihydro-11,12-diacetyl- 9,10-ethanoanthracene. Variations in concentrations of phenolic compounds in tar may be due to several factors. Phenolic compounds are mainly formed due to lignin degradation. When lignin is exposed to high temperatures, exceeding 300°C, the C-C bonds between its monomer units start to break, releasing compounds with structures close to its monomer constituents. Since various plant species have different ratios of lignin to cellulose and hemicellulose, mole percentage of phenolic compounds in tar from various plants will be different. Also, physical differences between various samples affect their inner temperature profile. These samples (foliage and twigs) are not thermally thin, which means there is a temperature profile inside the samples affecting the heating rate.

Table 5.2: Major classification of tar compounds (All numbers are based on mole%. ''Ar'' stands for aromatic and ''non-Ar'' represents non-aromatics.)

Major classification of tar compounds	Chamise twigs with foliage	Chamise twigs w/o foliage	Eastwood's manzanita foliage	Eastwood's manzanita twigs	Scrub oak	Hoaryleaf ceanothus
Benzenoid Ar	74.61	63.00	16.79	33.53	70.87	65.82
PAHs	15.40	20.66	20.63	16.98	13.37	19.10
Heterocyclic Ar	2.08	0.00	0.00	0.00	2.46	0.00
Cyclo alkane	2.21	1.76	4.58	2.46	1.37	2.00
Cyclo alkene	3.32	11.12	48.12	35.67	7.67	4.34
Alcohols	0.00	1.45	6.94	5.52	4.25	7.37
Heterocyclic non-Ar	2.36	2.01	2.95	5.84	0.00	0.00

The abundance of single-ring aromatic compounds (benzenoids) seems to indicate the dominance of primary pyrolysis reactions. If the pyrolysis temperature is high enough for further polymerization reactions to occur, a portion of the single-ring aromatics polymerize and form poly aromatic hydrocarbons (PAHs). Pathways and mechanisms responsible for formation of PAHs depend on the chemical structure of the intermediates. Catechols (1,2-benzenediols) and pyrogallols (1,2,3-benzenetriol) are intermediates generating biphenyl, naphthalenes and phenanthrene more preferentially, while cresols and xylenols are more likely to transform into xanthene and anthracene. Catechols and its derivatives are not among natural components of lignin and are generated via secondary decomposition of guaiacols (Brebu and Vasile, 2010). Figure 5.2 shows a simplified version of the main reactions and intermediate compounds formed during pyrolysis of lignin as temperature increases.

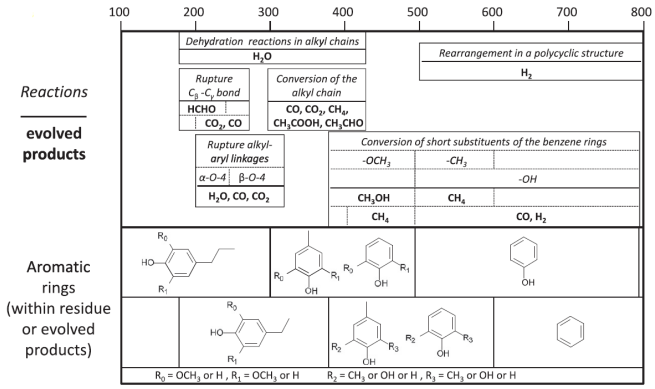

Figure 5.2: Main reactions and compounds released as temperature increases during pyrolysis of lignin (Collard and Blin, 2014).

The majority of PAHs in tar from southern California samples, with the exception of Eastwood's manzanita, have small alkyl attachments. Fluoranthene is the only PAH compound with no alkyl attachments present in tar from southern California. Concentration of PAHs in tar from southern California species varied from 13.4 mol% in scrub oak to 20.7 mol% in chamise twigs. As the distribution of tar compounds from various samples was examined, it was observed that as the concentration of benzenoids decreased, concentration of PAHs increased. There were only two samples that did not follow this pattern: Eastwood's manzanita foliage and its twigs. The higher concentration of heavy molecular weight aromatics such as PAHs may be attributed to prevalence of secondary pyrolysis reactions during the thermal degradation of these species. Disparities in temperature profile inside the biomass, which occur due to their different physical characteristics, may affect the chemical reactions occurring during biomass degradation. If the pyrolysis temperatures are

low, primary tar reactions will be more prevalent compared to secondary reactions. As the temperatures continue to rise, single-ring aromatics, such as phenolic compounds, polymerize and form benzenoid compounds with higher molecular weight substitutes and PAHs.

Concentration of non-aromatic compounds in tar from southern California samples varied from 7.9 mol% (chamise) to 62.6 mol% (Eastwood's manzanita). Cycloalkenes were the most abundant tar constituents for Eastwood's manzanita and its twigs. Their concentration in tar from Eastwood's manzanita was 48.1 mol% while tar from its twigs contained 35.7 mol%. Tar from other species contained between 3.3 mol% (chamise) to 7.7 mol% (scrub oak). Phorbol is the primary cycloalkene found in tar from Eastwood's manzanita and its twigs. Tar from manzanita twigs contained significantly lower concentrations of phorbol compared to tar from manzanita foliage (16.4 mol% and 34.1 mol% respectively).

2,3-dihydro-benzofuran is a furan detected in tar from all four southern California species with its concentration ranging from 3.1 mol% in Eastwood's manzanita to 6.5 mol% in tar from chamise. While one suggested pathway for furan formation in tar is cellulose degradation involving levoglucosan decomposition, Maggi and Delmon proposed that the presence of furans (and their derivatives such as 2,3-dihydro-benzofuran) in tar may be due to hemicellulose degradation (Maggi and Delmon, 1994; Ku and Mun, 2006). This suggests that some compounds such as 2,3-dihydro-benzofura, might be generated through more than one pathway during pyrolysis. 2,3-dihydro-benzofuran may be formed as a result of cellulose degradation or due to hemicellulose decomposition. Distinguishing which pathway is more involved in formation of a specific compound needs detection of potential intermediate compounds that may have been responsible for its generation. Due to short lifetime of most of these intermediate compounds, this was not pursued.

Hydroquinone, also known as 1,4-benzenediol, is a phenolic compound detected in tar from southern California plants. P-benzoquinone is a cycloalkene that is an oxidized derivative of hydroquinone seen in tar from chamise twigs (2.2 mol%). Based on the similar chemical structure of hydroquinone and p-benzoquinone, it is highly possible that these two compounds originated from the same intermediate. This shows that some of the differences observed in the species present in tar from the two sources may be due to secondary reactions these compounds get involved.

The presence of nitrogenated compounds in tar from biomass pyrolysis is expected since the biomass source contains small amounts of nitrogen. Therefore, when exposed to higher temperatures, the chemical structure of biomass including proteins starts to degrade releasing linear amines, amides, imines, imides and other nitrogen containing structures during

primary pyrolysis reactions (Debono and Villot, 2015). A positive correlation between the protein content of biomass and the overall concentration of nitrogenated compounds in tar has been observed. These released compounds may later get involved in the secondary pyrolysis reactions and generate more complex nitrogen-containing chemicals. The yield and composition of nitrogenated compounds is profoundly affected by pyrolysis operating conditions (He et al., 2018).

Almost all nitrogen present in the nitrogenated compounds is in ring structures. Samples from southern California generated small concentrations of nitrogenated species. Some nitrogen containing compounds such as indoles are generated during primary decomposition of proteins in the biomass while pyridines are produced during primary and secondary gas-phase reactions. Quinoline, an aromatic compound extensively found in coal tar and its byproducts as well as in plants (Sainsbury, 1964; Cao et al., 2012), has also been detected in tar from pyrolysis of southern California species. While indole is not detected in tar from southern California plants, indolizine is present in tar from all southern California species except for Eastwood's manzanita and its twigs. Concentration of indolizine ranged from 2.0 mol% in chamise twigs to 5.8 mol% in Eastwood's manzanita twigs. Similar to indolizine, quinoline was detected in tar from all southern California species except for Eastwood's manzanita and its twigs. Quinoline concentration ranged from 2.5 mol% in chamise twigs to 6.2 mol% in ceanothus.

Tar composition from pyrolysis of chamise twigs with foliage was compared to its twigs with no foliage attached to investigate any possible disparities due to pyrolysis of various parts of the same plant. Figure 5.3 illustrates the aromatic content of tar from pyrolysis of chamise twigs with foliage versus that of the twigs without foliage. Tar analysis of chamise samples showed no significant differences in their aromatic content due to presence of foliage. Comparison of aromatic content of tar from manzanita foliage and that of the manzanita twigs is presented in Figure 5.4. There were no significant differences between the two sources of biomass (Eastwood's manzanita foliage and its twigs) due to presence of foliage.

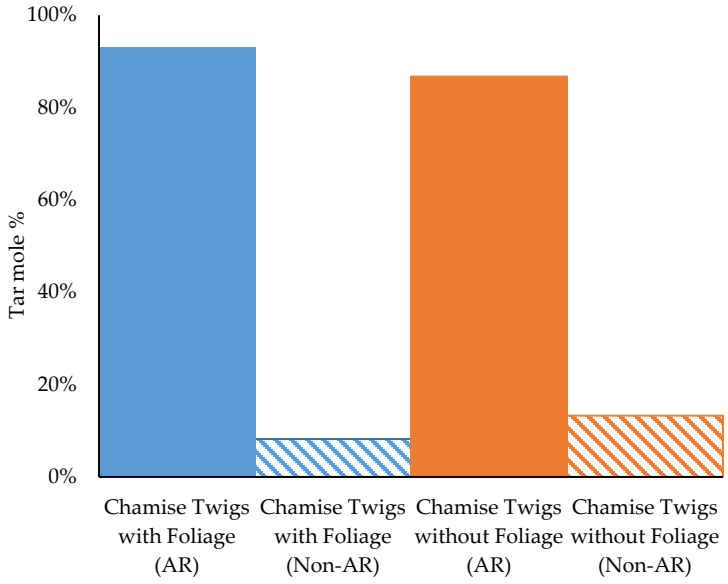

Figure 5.3: Aromatic content of chamise twigs with foliage and twigs without any foliage in tar. ''AR'' stands for aromatics and ''Non-AR'' stands for non-aromatics.

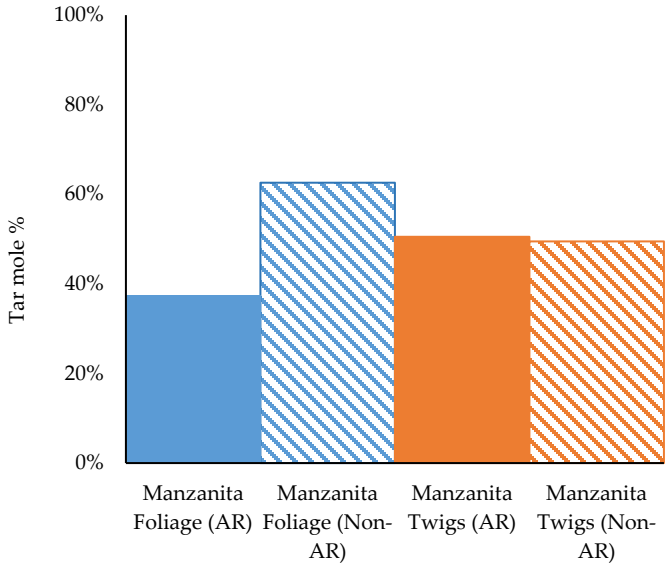

Figure 5.4: Aromatic content of Eastwood's manzanita twigs without foliage attached versus Eastwood's manzanita foliage. ''AR'' stands for aromatics while ''Non-AR'' stands for non-aromatics.

Figures 5.5- 5.6 provide information about tar compounds collected from pyrolysis of chamise twigs with foliage and chamise twigs without

any foliage. Phenol is the major tar constituent whether chamise samples contained leaves or not. The total concentration of benzenoids in tar from chamise twigs with foliage is close to 75%; while these compounds make up to approximately 63% of overall tar compounds collected from foliage-free twigs. This shows that presence of foliage on chamise twigs resulted in a moderate increase in concentration of benzenoids in tar. Tar obtained from foliage-free chamise twigs contained higher concentrations of cycloalkenes compared to that obtained from twigs with foliage. The differences in tar composition of chamise and that of foliage-free chamise twigs may have stemmed from the variations in ratios of major constituents, mainly cellulose, hemicellulose, lignin and extractives, of these two biomasses. As the plant grows, its lignin content increases since the woody material contains higher amounts of lignin compared to foliage; therefore, in most species, twigs contain higher lignin content compared to the leaves (Novaes et al., 2010; Abiven et al., 2011).

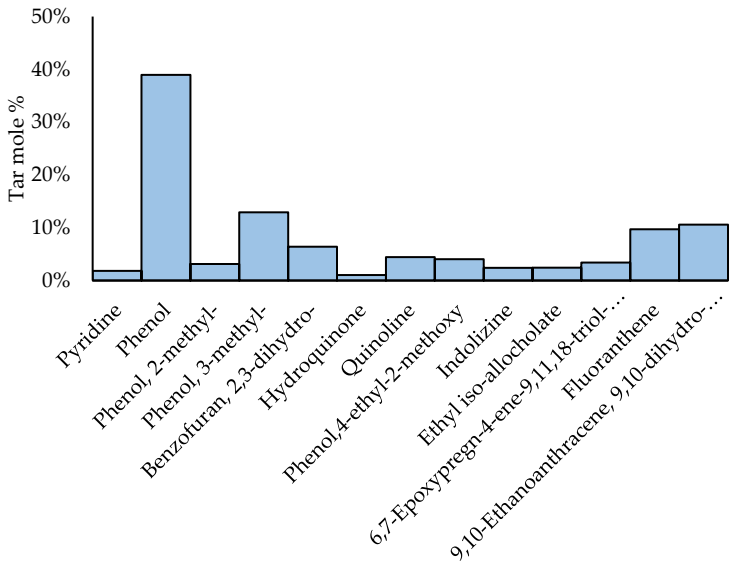

Figure 5.5: Detailed composition of tar derived from chamise twigs with foliage.

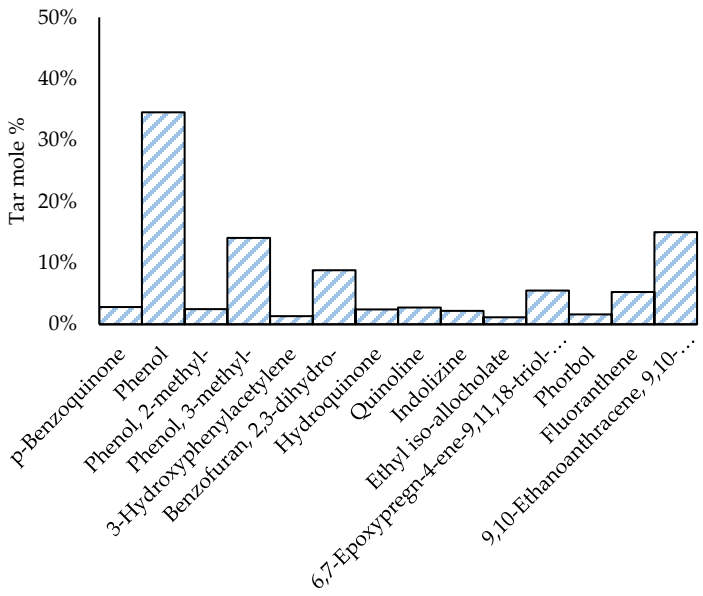

Figure 5.6: Detailed composition of tar derived from chamise twigs without foliage.

Detailed examination of compounds released into tar collected from pyrolysis of Eastwood's manzanita foliage and its foliage-free twigs showed some disparities (See Figures 5.7- 5.8). Contrary to chamise samples, Eastwood's manzanita twigs release higher concentrations of benzenoids than its foliage (33.54 mol% compared to 16.78 mol%). If lignin decomposition is considered as a major contributing factor to phenol generation, higher concentrations of phenol in tar from manzanita twigs compared to its foliage is due to the higher lignin content in twigs.

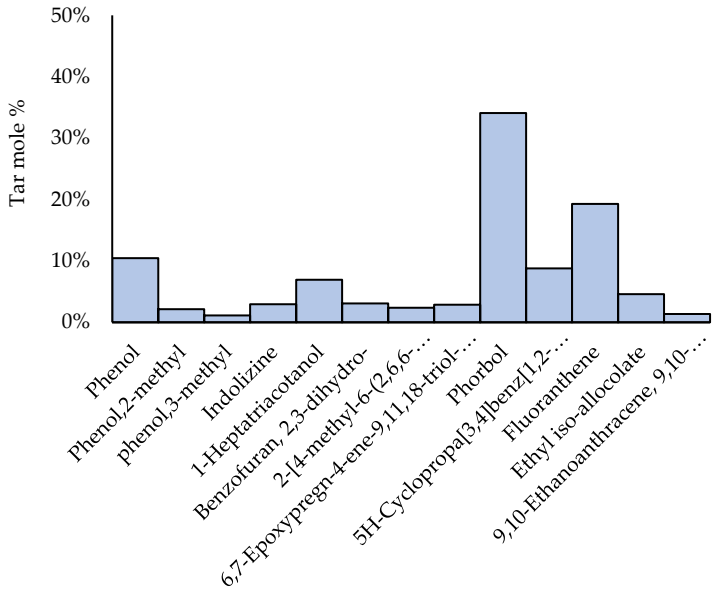

Figure 5.7: Detailed composition of tar from manzanita foliage.

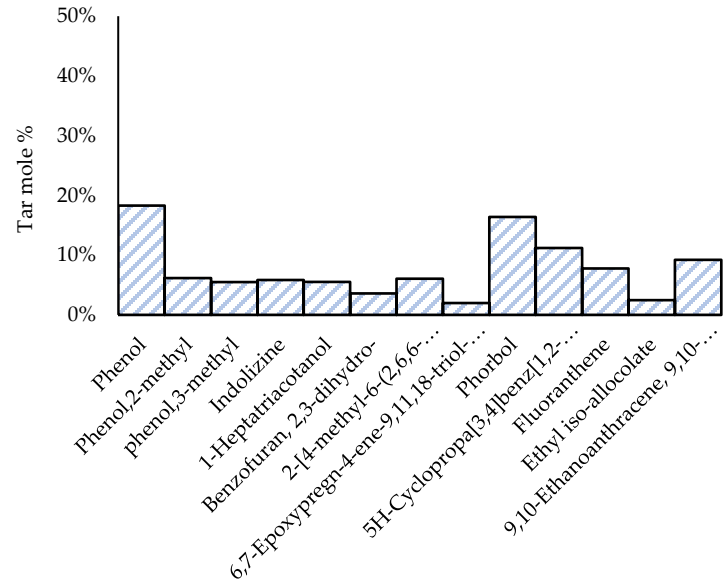

Figure 5.8: Detailed composition of tar from manzanita twigs.

5.2.3 Average Molecular Weight for Tar

Average molecular weight of tar is calculated as a weighted average of the mole percentage of each identified compound and its respective molecular weight. This value can provide some information on the distribution of heavy molecular weight compounds released into tar. Presence of heavy

molecular weight compounds in tar, which would increase the average molecular weight, may be due to the prevalence of secondary pyrolysis reactions.

All species in these experiments are exposed to similar conditions (temperature, pressure, resident time); meaning the only two factors that are affecting the molecular weight distribution are heating rate and inherent differences in composition of each species. The variations in physical characteristics of each plant, such as thickness of the leaves, affect the heating rate and temperature profile inside the leaves as they are exposed to elevated temperatures. This may lead to release of volatiles with different molecular weights.

Table 5.3 contains the average molecular weight for the species studied in this paper. Chamise generated tar with the lowest molecular weight compared to other species. Foliage-free chamise twigs resulted in a slightly heavier tar compared to chamise twigs with foliage. On the other hand, Eastwood's manzanita formed the heaviest tar among all species studied. Considering that the aromatic content of the tar generated by Eastwood's manzanita was the lowest among all pyrolyzed species, the non-aromatic portion of manzanita tar is actually responsible for increasing its average molecular weight.

Table 5.3: Elemental composition and average molecular weight (MW) of tar based on detected species in tar.

Species	Average elemental composition of tar	Average MW of tar
Chamise twigs w/foliage	$C_{9.59}H_{9.87}O_{1.37}N_{0.09}$	148.18
Chamise twigs w/o foliage	$C_{11.38}H_{12.25}O_{1.67}N_{0.05}$	176.23
Eastwood's manzanita	$C_{18.47}H_{24.66}O_{3.41}N_{0.03}$	301.16
Eastwood's manzanita twigs	$C_{16.07}H_{20.97}O_{20.69}$	256.85
Scrub oak	$C_{11.05}H_{12.97}O_{1.43}N_{0.07}$	169.43
Hoaryleaf ceanothus	$C_{12.1}H_{14.96}O_{1.22}N_{0.06}$	180.52

5.2.4 Light Gases

The four major components of pyrolysis gases were CO, CO_2, CH_4, and H_2. Other unspecified peaks were occasionally detected. However, since their concentration was below the detection limit, they were not identified. Carbon monoxide was the main component in the light gases on a wt% dry basis, followed by CO_2, CH_4, and H_2 for all studied plant species. Figure 5.9 illustrates concentration (wt% of light gas) of major gas components generated during pyrolysis of each studied biomass. The detailed composition of gas phase is available in Table 5.4.

Table 5.4: Detailed composition of pyrolysis gases from southern California chaparral.

Species	H_2	CO	CO_2	CH_4
Chamise twigs with foliage	1.53±0.15	54.97±1.41	34.78±2.11	8.72±2.05
Chamise twigs w/o foliage	1.61±0.17	57.07±2.28	33.41±1.67	7.92±1.25
Eastwood's manzanita foliage	1.34±0.11	58.31±1.36	31.00±1.54	9.35±1.86
Eastwood's manzanita twigs w/o foliage	1.38±0.10	59.42±1.64	32.06±1.50	7.15±1.64
Scrub oak	1.62±0.12	62.08±2.02	29.36±1.43	6.95±1.19
Hoaryleaf ceanothus	1.50±0.11	56.75±1.89	32.54±1.45	9.22±1.25

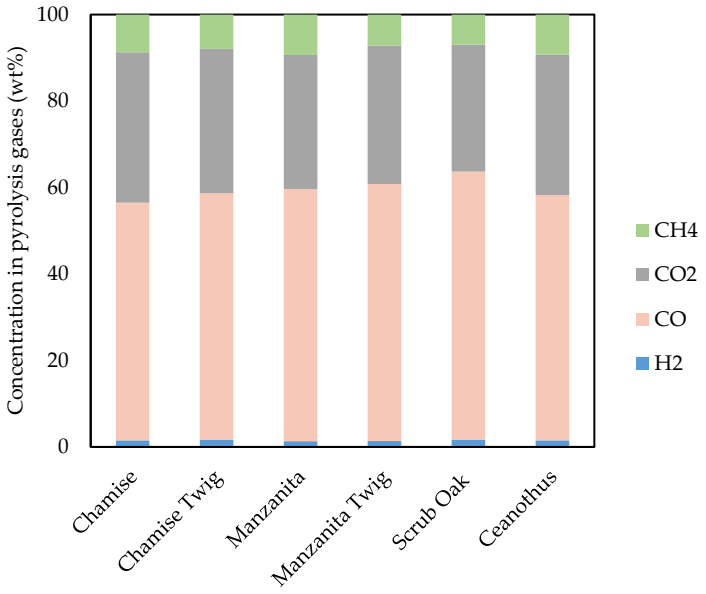

Figure 5.9: Average concentration of major gas components from each studied plant.

Statistical analysis showed there was a significant difference in concentration of CO released into light gases from various pyrolyzed species (p= 2.38×10^{-6}). Presence of foliage on chamise twigs did not affect concentration of CO in light gases (p= 0.09). Analysis of light gases from Eastwood's manzanita twigs and its foliage showed there was no significant difference in the concentration of CO in light gases due to the presence of foliage (p=0.30). Among the species studied, chamise generated

lowest concentration of CO (54.97 wt%) and scrub oak released highest amount of CO (62.08 wt%) into gases.

There is a statistically significant difference in concentration of CO_2 between species native to southern California (p=8.24 $\times 10^{-5}$). Statistical analysis showed there was no difference between chamise twigs with foliage and the ones without foliage in the concentration of CO_2 generated during pyrolysis of chamise samples (p=0.26). Analysis of fluctuations in concentration of CO_2 in pyrolysis gases from manzanita foliage and its twigs revealed there was no disparity between these two parts of the plant in generation of CO_2 (p=0.31).

Statistical evaluation of variations in concentration of CH_4 in pyrolysis gases of southern California samples shows there was a slight variation in the amount of generated CH_4 due to fuel type (p=0.08). Experiments conducted on chamise samples showed that presence of foliage did not cause any variations in the amount of CH_4 in pyrolysis gases (p=0.46). Similar to chamise, pyrolysis of Eastwood's manzanita samples, whether twigs or foliage, showed no difference in the amount of generated CH_4 (p=0.07).

Statistical analysis on variations in concentration of H_2 generated during pyrolysis of southern California species showed there was a significant difference in concentration of H_2 attributed to species type (p=0.003). There was no significant difference in concentration of H_2 resulting from presence of foliage during pyrolysis of chamise samples (p=0.42). Analysis of concentration of H_2 in pyrolysis gases from manzanita and manzanita twigs showed there was no detectable difference in concentration of H_2 between these two samples (p=0.59).

5.2.5 High Heating Value and Heat of Combustion

Table 5.5 contains high heating values for volatiles collected from pyrolysis of various species. The estimated values for HHV varied between approximately 19.37 to 23.01 MJ/kg of fuel. Volatiles from ceanothus had the highest HHV while that of manzanita twigs had the lowest. For chamise samples, the presence of foliage slightly increased the heat content of the resulting tar. A comparison between tar from Eastwood's manzanita foliage and its twigs showed that Eastwood's manzanita foliage generated tar with higher heat content compared to its twigs.

The findings on HHV align well with the existing literature. The experimental HHV analysis of the plants studied in this paper is not available. However, Matt et al. (2020) reported the high heating values for various plant species (Table 5.6). While the plants investigated in the two studies are different, their reported values were in the same range (Table 5.5 and Table 5.6).

Table 5.5: High heating values for southern California samples.

Sample Type	Overall tar HHV (MJ/kg of tar)	Overall gas HHV (MJ/kg of light gases)	Volatiles HHV (MJ/kg of volatiles)
chamise twigs with no foliage	33.76	12.51	22.12
chamise twigs with foliage	33.54	12.62	22.69
Eastwood's manzanita foliage	33.24	13.04	20.27
Eastwood's manzanita twigs	33.61	12.00	19.37
scrub oak	35.20	12.50	22.71
Hoary leaf ceanothus	37.19	13.04	23.01

Table 5.6: High Heating Value for various samples reported by Matt et al. (2020).

Sample Type	HHV(kJ/kg) (daf)
Saw palmetto	20.40
Dwarf palmetto	20.53
Swamp bay	21.88
Yaupon	21.83
Inkberry	22.32
Wax myrtle	20.28
Fetterbush	21.11
Live oak	19.89
Water oak	19.48
Longleaf pine	20.10
Wire grass	19.44
Little bluestem	19.75

5.3 Conclusion

In this chapter, pyrolysis of plant samples from southern California was studied. The effect of species type on characteristics of pyrolysis products, tar and light gases, was investigated. The main findings are:

Analysis of tar samples from southern California species showed, with the exception of Eastwood's manzanita, aromatics were the main tar constituents. Cycloalkenes were the major constituents of tar for Eastwood's manzanita. Among aromatics, benzenoids, especially phenol,

were the most abundant tar compound. Overall concentration of benzenoids in tar varied from 16.8 mole% in Eastwood's manzanita to 74.6 mole% in chamise. The other primary tar compounds were 2-methyl phenol, 3-methyl phenol, 4-ethyl-2-methoxy phenol (4-ethyl guaiacol), 2,3-dihydro benzofuran, and 9,10-dihydro-11,12-diacetyl- 9,10-ethanoanthracene. Concentration of PAHs in tar from southern California species varied from 13.4 mol% in scrub oak to 20.7 mol% in chamise twigs. As the concentration of benzenoids decreased, concentration of PAHs increased. Variations in concentration of benzenoids and PAHs in tar were more likely due to differences in the ratios of major biopolymers (cellulose, hemicellulose, and lignin) in biomass and the physical differences between various samples which may affect their inner temperature profile. Variations in inner temperature profile between different plant species may lead to different pyrolysis temperature and heating rate. Pyrolysis temperature along with heating rate are the two main factors affecting pyrolysis of biomass.

The potential effect of foliage on pyrolysis of chamise samples was studied to investigate possible disparities in tar compounds and their concentration due to the presence of leaves. The ratios of major constituents of biomass (cellulose, hemicellulose and lignin) vary between various parts of a specific plant. The possible effect of these differences on pyrolysis behavior of chamise and manzanita was examined. No significant differences were observed in the aromatic content of tar collected from chamise samples due to presence of foliage. Similar results were obtained from pyrolysis of Eastwood's manzanita foliage and twigs.

Gases released during pyrolysis of these species were collected and further analyzed by GC/TCD. It was determined that CO, CO_2, CH_4 and H_2 were the major components of pyrolysis gases on a wt% dry, ash-free basis. CO was the main constituent of the pyrolysis gases followed by CO_2, CH_4 and H_2 on a wt% dry, ash-free basis. Concentration of CO, CO_2 and H_2 in light gases from pyrolysis of various plant samples depended on the species type while there was no statistically significant difference in the concentration of CH_4 in light gases from southern California plants. Comparison of the pyrolysis behavior of foliage and twigs was conducted using manzanita and chamise samples. There was no difference in the concentration of major components of light gases between foliage and twigs of Eastwood's manzanita. For chamise samples, there was no difference in the composition of gases due to presence of foliage. This could be explained due to small differences in the ratios of major biopolymers composition of twigs and foliage belonging to the same plant species.

High heating values (HHV) for tar, light gases, and total volatiles released during pyrolysis of southern California samples were calculated for each plant species. The estimated values for HHV varied between

approximately 19.37 to 22.32 kJ/kg of dry volatiles. This range of HHV for volatiles is consistent with HHV data from other biomass species, including HHVs from live plants reported by Matt et al. (2020). Tar contribution to high heating value of volatiles was calculated and it was estimated that tar accounted between 81.99% (Eastwood's manzanita foliage) to 87.2% (chamise foliage) to HHV of volatiles. This shows the importance of tar analysis as better understanding of tar composition would lead to more precise estimations of its HHV and tar contribution to wildfires.

6 Gas and Tar Species Evolved during Rapid Pyrolysis of northern Utah Shrubs

6.1 Introduction

This chapter focuses on pyrolysis of selected Utah foliage and the role of released volatiles in the propagation of wildland fires. The results in this chapter were published previously (Alizadeh and Fletcher, 2025). Utah has a semi-arid climate with flammable vegetation making it prone to recurring wildfires. The total area in Utah affected by wildfires in 2024 exceeded one million acres. The huge area affected by fires, along with the rising population in Utah, increases the wildland-urban interfaces (WUI), increasing the chance of human exposure and property losses during fires.

Four species native to northern Utah (big sagebrush, Utah juniper, Gambel oak and bigtooth maple) were pyrolyzed in a flat-flame burner system at 725°C with a heating rate of approximately 180 °C/s, close to conditions measured during wildland fires. Pyrolysis yield and characteristics of its products are studied to investigate whether they are influenced by biomass type. Most of the previous studies on pyrolysis of biomass have focused on optimizing the operating conditions with the purpose of increasing the yield of one specific pyrolysis product (mainly tar to later be used as fuel) and decreasing char production. These studies have used controlled setups such as reactors and operating conditions different from wildland fires (Miller and Bellan, 1997; Yu et al., 1997; Dufour et al., 2009). The studies on the effect of biomass type on pyrolysis products at wildland fire conditions are scarce.

This chapter describes the chemical composition of tar and light gases released during pyrolysis of selected northern Utah plant species. The freshly cut stems were collected and brought back to Brigham Young University (in Provo, Utah) and were stored in sealed bags to reduce moisture loss. The goal of these experiments was to provide insight into the chemical composition of the pyrolysis products of these plants which will subsequently improve understanding of plant combustion and hence wildland fires.

6.2 Materials and Methods

The experimental setup used for pyrolysis of biomass and the products' collection systems, including flat flame burner, ice bath, tar, and light gas

collection systems, and analysis instruments have been extensively explained in Chapter 4.

6.3 Results and Discussion

6.3.1 Tar, Gas, and Char Yields

Table 6.1 lists the yields of pyrolysis products collected during pyrolysis of the selected northern Utah plant species. The total yield of volatiles varied from 80 wt % daf for Utah juniper to 82 wt % daf for the big sagebrush and Gambel oak. The average tar yield ranged from 53 wt % daf (Gambel oak) to 58 wt % daf (bigtooth maple), while the average yield of light gases changed respectively. The average yield of light gases released during pyrolysis of Utah samples varied from 25 wt% (Utah juniper) to 29 wt% (Gambel oak). The disparities in the yields of tar and light gases may be due to inherent chemical and physical differences between various plant species.

Table 6.1: Pyrolysis product yields for various northern Utah species (all numbers are wt % and on a dry and ash-free basis).

Pyrolysis Products	Big sagebrush	Utah juniper	Gambel oak	Bigtooth maple
Tar	54.0 ± 6.6	55.0 ± 2.5	53.0 ± 5.0	58.0 ± 6.6
Gas	28.0 ± 5.0	25.0 ± 2.5	29.0 ± 2.5	31.1 ± 5.0
Char	18.0 ± 2.5	20.0 ± 5.0	18.0 ± 6.6	19.0± 10.8
Total yield of volatiles	82.0 ± 11.5	80.0 ± 5.0	82.0 ± 7.5	81.0 ± 11.5

6.3.2 Compounds Present in Tar

Tar collected during pyrolysis of various plant species was analyzed offline using a GC/MS system to study the various volatile compounds and disparities in their concentrations. Compounds were classified as aromatic or non-aromatic. Aromatic compounds are divided into subgroups of benzenoid aromatics, non-benzenoid aromatics, heterocyclic aromatics, and poly aromatic hydrocarbons (PAHs). Compounds such as 2-methylare pyrimidine and 2-furan methanol which are aromatic and contain at least one hetero atom (N or O) in their ring structure are classified as heterocyclic aromatics.

Non-aromatic compounds are divided into amines, cyclo-alkenes, cyclo-esters, acids and ketones. In the case of ketones, cyclic compounds are sometimes referred to as a separate sub-group of cyclic ketones for

discussion purposes. Mole percentages of each of these major sub-groups in tar from various Utah species is shown in Table 6.2. Detailed description of tar compounds and their concentration from pyrolysis of northern Utah species are reported in Table 6.3.

Table 6.2: Major classification of tar compounds (tar mole %). (''AR'' stands for aromatic.)

Compound Type	Big sagebrush	Utah juniper	Gambel oak	Bigtooth maple
Benzenoid AR	24.23	55.69	37.96	43.89
Non-benzenoid AR	0.00	2.98	6.07	6.59
Heterocyclic AR	0.00	0.39	0.00	0.00
PAHs	63.33	19.61	46.44	32.55
Amine	0.00	0.00	0.00	5.77
Acid	12.44	18.50	9.54	10.14
Ketone	0.00	0.11	0.00	0.00
Cyclic ketone	0.00	1.70	0.00	0.00
Cyclo-alkene	0.00	0.16	0.00	1.06
Cyclo-ester	0.00	0.74	0.00	0.00

Table 6.3: Detailed composition of tar collected from pyrolysis of selected northern Utah samples.

No.	Compounds detected in tar	AR/Non-AR	Compound Type	Molecular Structure	MW (g/mol)	Big Sagebrush (mol%)	Utah Juniper (mol%)	Gambel Oak (mol%)	Bigtooth maple (mol%)
1	Triethylamine	Non-AR	Amine	$C_6H_{15}N$	101	0.00	0.00	0.00	5.77
2	1,3-Diazine	AR	Non-Benz. AR	$C_4H_4N_2$	80	0.00	0.01	0.00	0.00
3	1-Hydroxy-2-butanone	Non-AR	Ketone	$C_4H_8O_2$	88	0.00	0.11	0.00	0.00
4	Pyrimidine,2-methyl	AR	Hetrocyclic AR	$C_5H_6N_2$	94	0.00	0.13	0.00	0.00
5	2- cyclo- penten-1- one	Non-AR	Cyclic Ketone	C_5H_6O	82	0.00	0.57	0.00	0.00
6	2- Furanmethanol	AR	Hetrocyclic AR	$C_5H_6O_2$	98	0.00	0.38	0.00	0.00
7	Butyrolactone	Non-AR	Cyclo-Ester	$C_4H_6O_2$	86	0.00	0.74	0.00	0.00
8	2-cyclopenten-1- one, 2-methyl	Non-AR	Cyclic Ketone	C_6H_8O	96	0.00	0.21	0.00	0.00
9	2-cyclopenten-1- one, 3-methyl	Non-AR	Cyclic Ketone	C_6H_8O	96	0.00	0.92	0.00	0.00
10	Phenol	AR	Benzenoid AR	C_6H_6O	94	2.10	13.81	2.35	3.66
11	3- pyridine carbonitrile	Non-AR	Cyclo-alkene	$C_6H_4N_2$	104	0.00	0.15	0.00	1.06
12	Benzyl Alcohol (α-cresol)	AR	Benzenoid AR	C_7H_8O	108	0.00	1.11	0.00	0.00

Table 6.3 continued.

No	Compounds detected in tar	AR/Non-AR	Compound Type	Molecular structure	MW (g/mol)	Big Sagebrush (mol%)	Utah Juniper (mol%)	Gambel Oak (mol%)	Bigtooth maple (mol%)
13	Hexanoic acid, 4-methyl	Non-AR	Acid	$C_7H_{14}O_2$	130	0.00	0.32	0.00	2.13
14	6- Heptenoic acid	Non-AR	Acid	$C_7H_{12}O_2$	128	4.84	1.64	0.00	0.00
15	Phenol, 2- methyl	AR	Benzenoid AR	C_7H_8O	108	0.00	3.70	1.61	0.00
16	Phenol, 3-methyl	AR	Benzenoid AR	C_7H_8O	108	2.42	22.71	0.00	2.59
17	Benzyl nitrile	Non-AR	Cyclo-alkene	C_8H_7N	117	0.00	0.01	0.00	0.00
18	Phenol, 2,4-dimethyl (m-Xylenol)	AR	Benzenoid AR	$C_8H_{10}O$	122	0.00	1.92	2.13	0.00
19	7- octenoic acid	Non-AR	Acid	$C_8H_{14}O_2$	142	0.00	1.83	0.00	0.00
20	Benzoic acid	AR	Acid	$C_7H_6O_2$	122	0.00	0.00	0.00	3.99
21	Phenol, 3-ethyl	AR	Benzenoid AR	$C_8H_{10}O$	122	0.00	2.35	2.25	1.95
22	3-Hydroxy phenyl acetylene	AR	Benzenoid AR	C_8H_6O	118	0.00	1.48	0.00	2.44
23	Benzofuran, 2,3-dihydro	AR	Benzenoid AR	C_8H_8O	120	0.00	4.83	0.00	0.00
24	8- Nonenoic acid	Non-AR	Acid	$C_9H_{16}O_2$	156	0.00	1.83	0.00	0.10
25	Quinoline	AR	Benzenoid AR	C_9H_7N	129	5.77	0.60	4.26	5.89
26	Indole	AR	Benzenoid AR	C_8H_7N	117	0.00	0.00	0.00	1.43

Table 6.3 continued.

No	Compounds detected in tar	AR/Non-AR	Compound Type	Molecular structure	MW (g/mol)	Big Sagebrush (mol%)	Utah Juniper (mol%)	Gambel Oak (mol%)	Bigtooth maple (mol%)
27	2,2'- Bifuran	AR	Non-Benz. AR	$C_8 H_6 O_2$	134	0.00	2.97	6.07	6.59
28	1H-Indenol	AR	Benzenoid AR	$C_9 H_8 O$	132	1.74	1.57	7.53	0.99
29	Coumarin	AR	Benzenoid AR	$C_9 H_6 O_2$	146	10.03	0.00	4.85	16.50
30	Acenaphthylene	AR	PAH	$C_{12} H_8$	152	10.18	1.09	7.80	3.04
31	Naphthalene, 2-phenyl	AR	PAH	$C_{16} H_{12}$	204	12.54	3.57	9.66	0.00
32	Dodecanoic acid, 3-hydroxy	Non-AR	Acid	$C_{12} H_{24} O_3$	216	1.75	6.28	7.00	0.00
33	Dodecanoic acid	Non-AR	Acid	$C_{12} H_{24} O_2$	200	5.85	6.59	2.54	3.93
34	Fluorene	AR	PAH	$C_{13} H_{10}$	166	0.00	0.98	4.47	0.00
35	3-Hydroxy Biphenyl	AR	Benzenoid AR	$C_{12} H_{10} O$	170	2.16	1.62	12.98	8.44
36	9H Fluorene- 9 - one	AR	PAH	$C_{13} H_8 O$	180	3.07	2.79	0.29	5.57
37	Fluoranthene	AR	PAH	$C_{16} H_{10}$	202	32.38	7.55	7.30	9.32
38	Anthracene	AR	PAH	$C_{14} H_{10}$	178	5.16	3.63	16.92	14.62

Figure 6.1 contains the distribution of aromatic compounds versus the non-aromatic ones detected in tar from Utah samples studied. Aromatics were the major constituents of chemicals released into tar. As shown in Table 6.4, concentration of aromatics in tar varied from approximately 78.8 mol% in Utah juniper to 90.5 mol% in Gambel oak. The concentration of benzenoids in tar from Utah species varied from 24.2 mol% (big sagebrush) to around 56 mol% (Utah juniper). Among Utah species, tar from big sagebrush and Gambel oak contained higher concentrations of PAHs than benzenoids.

There was a significant disparity in concentration of phenolic compounds in tar from Utah samples. While phenolic compounds made up to 45 mol% of Utah juniper tar, their overall concentration varied between almost 5 mol% to 8.3 mol% for the rest of the plants studied. This shows that majority of the benzenoids in Utah juniper tar are phenolic compounds. As the distribution of tar compounds from Utah samples was examined, it was observed that as the concentration of phenolic compounds decreased, concentration of benzenoids with higher molecular weight substitutes (compounds such as quinoline, 2,3-dihydro benzofuran, indole, 1H-indenol, coumarin, 3-hydroxy biphenyl, etc.) and PAHs increased.

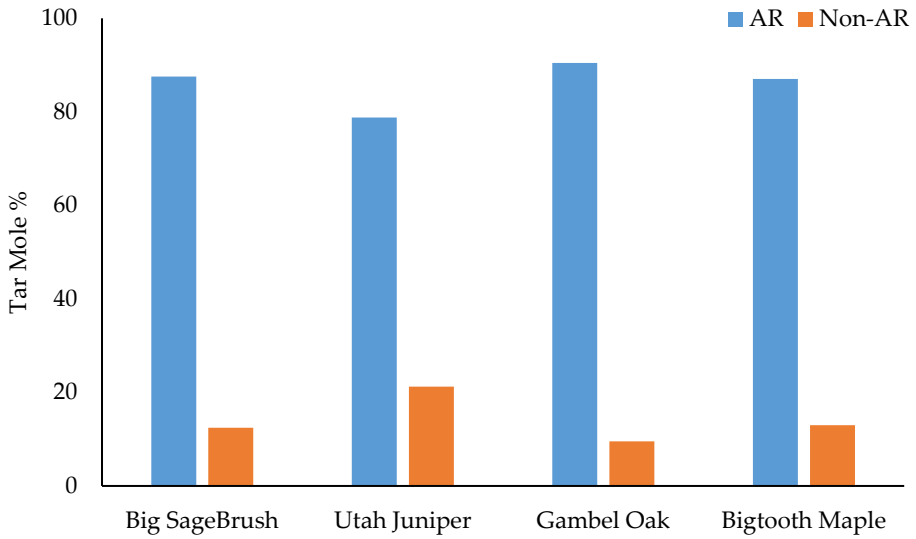

Figure 6.1: Distribution of aromatic compounds versus non aromatics in selected Utah samples. ''AR'' stands for aromatics while ''Non-AR'' represents non-aromatics.

Table 6.4: Aromatic content in various Utah species (All reported numbers are mole percentage of tar.)

	Big sagebrush	Utah juniper	Gambel oak	Bigtooth maple
Aromatic	87.56	78.78	90.46	87.02
Non-Aromatic	12.44	21.22	9.54	12.98

Although the relative ratio of lignin, cellulose and hemicellulose in the plant species was not measured, it is suggested variations in concentrations of tar compounds may have stemmed from differences in biomass composition. Also, the physical differences between various foliage affects the inner temperature profile affecting pyrolysis reactions.

PAHs made up from 19.6 mol% (Utah juniper) to 63.3 mol% (big sagebrush) of overall compounds detected in tar from Utah species. Acenaphthylene, 2-phenyl naphthalene, fluorene and anthracene were among the PAHs detected in tar from Utah species. With the exception of anthracene that constituted 3.6 mol% (Utah juniper) to 17 mol% (Gambel oak) of tar, all other PAHs were 2-ring poly aromatics.

The majority of PAHs detected in tar from Utah species had no substitutes. 2-phenyl naphthalene was the only PAH compound with an attachment (a phenyl ring) present in tar from Utah species. Prevalence of secondary reactions would result in PAH compounds with fewer substitutes or no substitutes.

Majority of non-aromatic compounds were classified as cyclo alkenes, cyclo-esters, cyclic ketones, ketones, acids, and amines with acidic compounds making up the majority of non-aromatics.

Compounds such as 2-furan methanol, 2,3-dihyro benzofuran and 2,2'-bifuran were classified as furans in tar. Tar from big sagebrush did not contain any furans while other samples contained between 5.2 to 6.1 mol%.

6.3.3 Average Molecular Weight for Tar

Table 6.5 lists average molecular weight and estimated elemental composition of tar for each plant species. As seen in Table 6.4, among Utah species, tar from big sagebrush had highest molecular weight while Utah juniper generated tar with the lowest value. A deeper look into the aromatic content of tar in each of the plant species showed big sagebrush had the lowest content of single-ring aromatics (benzenoids) among Utah species followed by Gambel oak, bigtooth maple and Utah juniper. It was observed that as the concentration of high molecular weight compounds (such as PAHs) increased, the average molecular weight of tar increased. The variations in concentrations of PAHs in tar may be due to differences in chemical composition of the plant species since pyrolysis conditions

(heating rate and temperature) were the same during all pyrolysis experiments.

Table 6.5: Average molecular weight (MW) and elemental composition for tar from Utah species.

Utah species	Ave MW of tar (g/mol)	Ave elemental composition of tar
Big sagebrush	175.51	$C_{13.0}H_{10.4}O_{0.6}N_{0.06}$
Utah juniper	140.01	$C_{9.30}H_{10.4}ON_{1.2}$
Gambel oak	166.56	$C_{12.0}H_{10.5}O_{0.7}N_{0.04}$
Bigtooth maple	151.41	$C_{11.0}H_{9.0}ON_{0.15}$

6.3.4 Light Gases

After each experiment, light gases were collected and analyzed following the methods explained in chapter 4. Similar to what was observed during pyrolysis of southern California species, CO, CO_2, CH_4 and H_2 were the major gas components (wt%) generated during pyrolysis of Utah samples. Occasionally peaks related to other gas species were observed in gas samples but due to their low concentration, further detection and quantification of these gas components were not feasible. Concentration of each of the major gas components obtained in mole percentage and converted to wt%.

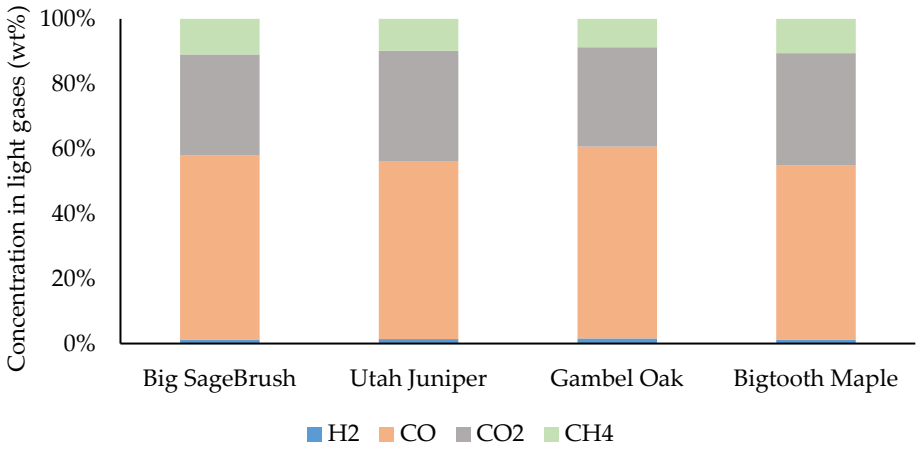

Figure 6.2: Concentrations of all major components of light gases from pyrolysis of northern Utah samples.

As seen in Figure 6.2, CO was the most abundant compound in light gases from pyrolysis of Utah species. Its average concentration varied from 53.8 wt% (bigtooth maple) to 56.8 wt% (big sagebrush). Statistical analysis on

fluctuations in concentration of CO showed that biomass type affected its concentration (p=0.003). Statistical evaluations on variations in concentration of CO_2 in pyrolysis gases from Utah samples showed moderate changes due to biomass type (p=0.06). Statistical analysis showed there was a significant difference in the concentration of H_2 released into light gases during pyrolysis of various types of Utah biomass (p=0.01). Concentration of CH_4 in pyrolysis gases of Utah samples changed significantly due to biomass type (p=0.03). The concentrations of all major components of the gas phase are presented in Table 6.6 along with the 95 % confidence intervals.

Table 6.6: concentration of major gas components generated from pyrolysis of northern Utah species (wt % of light gas).

species	H_2	CO	CO_2	CH_4
Big sagebrush	1.2±0.3	56.8±4.0	31.0±4.6	11.0±1.0
Utah juniper	1.4±0.3	54.8±1.5	34.0±3.1	9.8±2.5
Gambel oak	1.6±0.4	59.1±2.1	30.6±3.9	8.7±1.5
Bigtooth maple	1.1±0.4	53.8±3.7	34.5±6.0	10.5±2.1

6.3.5 High Heating Value of Tar and Light Gases

Estimated values for high heating values of tar and light gases generated during pyrolysis of selected Utah samples are reported in Table 6.7. HHV of tar varied between 34.67 (MJ/kg of tar) for bigtooth maple to 36.80 (MJ/kg of tar) for big sagebrush. These values are in the same range as the reported HHV values for bio-oil in the literature which is between 20 to 35 (MJ/kg of tar).

HHVs of light gases from northern Utah species were estimated to be from 12.93 (MJ/kg of light gases) for bigtooth maple to 13.60 (MJ/kg of light gases) for big sagebrush. The HHV of volatiles from northern Utah samples ranged between 22.798 to 23.680 (MJ/kg of volatiles).

Table 6.7: HHV of tar, light gases and volatiles released from pyrolysis of selected northern Utah samples.

Sample	HHV of tar (MJ/kg of tar)	Tar yield	HHV of gas (MJ/kg of light gases)	Light gas yield	HHV of volatiles (MJ/kg of volatiles)
Big sagebrush	36.801	0.54	13.599	0.28	23.680
Utah juniper	35.534	0.55	13.019	0.25	22.798
Gambel oak	36.542	0.53	13.117	0.29	23.171
Bigtooth maple	34.671	0.58	12.928	0.23	23.083

6.4 Conclusion

In this chapter, pyrolysis of selected Utah species was investigated. The effect of species type on characteristics of pyrolysis products (tar and light gases) was investigated.

The primary outcomes of this research are:

- No differences were observed in the yield of volatiles generated during pyrolysis of Utah samples.
- Majority of tar compounds are aromatic. This is similar to what was observed during pyrolysis of southern California species. The most abundant tar compounds in Utah samples are fluoranthene, 2-phenyl naphthalene, 3-methyl phenol, phenol, anthracene, and coumarin. The primary compounds of tar, with the exception of Utah juniper, are PAHs. Since operating conditions were the same during pyrolysis of all Utah samples, the differences observed in tar composition may have stemmed from variations in biomass composition.
- Concentration of PAHs produced during pyrolysis of Utah samples is higher than that of southern California species. This could be due to variations in biochemical composition of biomass from Utah and southern California. Also, proximity of lab location to sample collection spots during Utah experiments made it easier to pyrolyze higher amounts of biomass which increases the concentration of compounds released into tar that are otherwise generated in lower concentrations.
- The major constituents of pyrolysis gases on a wt % dry, ash-free basis were CO, CO_2, CH_4 and H_2. CO was the main component of the light gases succeeded by CO_2, CH_4 and H_2 on a wt % dry, ash-free basis. Concentrations of CO, CH_4 and H_2 varied significantly due to species type. CO_2 was the only gas component with moderate changes in its concentration due to species type.
- High heating values (HHV) for tar, light gases, and total volatiles generated during pyrolysis of selected Utah samples were estimated. HHV of volatiles varied between 22.798 to 23.680 (MJ/kg of volatiles). Volatiles from big sagebrush had the highest heating value while those from Utah juniper had the lowest. Tar contributes from 83 to 87% to the HHV of volatiles. This shows the importance of analyzing tar from pyrolysis of biomass as it has a huge effect on overall heating value of volatiles.

7 A comprehensive analysis of pyrolysis of selected plant species in U.S. to suggest components for physics-based wildland fire models

7.1 Introduction

This chapter focuses on analysis of pyrolysis of 25 various samples of foliage from three U.S. regions with frequent wildland fires, southeastern U.S., northern Utah, and southern California. Pyrolysis data for southeastern U.S. foliage samples were reported by Safdari (Safdari, 2018; Safdari et al., 2018) Pyrolysis data for northern Utah foliage were given in Chapter 6 and for southern California species in Chapter 5.
The purpose of this chapter is to compare the pyrolysis data from all three regions of the U.S. with the goal to identify differences and recommend average properties for simulation purposes. The analysis here was published by Alizadeh and Fletcher (Zhang et al., 2010; Alizadeh et al., 2024).

7.2 Experimental Setup

The experimental setup used for pyrolysis of biomass and the products' collection systems, including flat flame burner, ice bath, tar, and gas collection systems, and analysis instruments are explained in Chapter 4. The only difference between pyrolysis experiments of southeastern U.S. samples and the pyrolysis experiments of northern Utah and southern California samples was temperature. During pyrolysis of southeastern U.S. samples, the foliage was pyrolyzed at 765°C while northern Utah and southern California samples were pyrolyzed at 725°C.

7.2.1 Plants Studied

Table 7.1 contains names and regions of species studied here. These plant species are all involved in wildland fires in the United States.

Table 7.1: Species studied in this research.(S.E. U.S. stands for southeastern United states while N. Utah and S.CA represent northern Utah and southern California respectively.)

Region	Common name	Scientific name
S.E. U.S.	Darrow's blueberry	*Vaccinium Darrowii*
S.E. U.S.	Fetterbush	*Lyonia lucida*
S.E. U.S.	Dwarf Palmetto	*Sable minor*
S.E. U.S.	Inkberry	*Ilex glabra*
S.E. U.S.	Live oak	*Quercus virginiana*
S.E. U.S.	Little bluestem	*Schizachyrium scoparium*
S.E. U.S.	Saw palmetto	*Serenoa repens*
S.E. U.S.	Sparkleberry	*Vaccinium arboreum Marshall*
S.E. U.S.	Swamp bay	*Persea palustris*
S.E. U.S.	Water oak	*Quercus nigra*
S.E. U.S.	Wax myrtle	*Morella cerifera*
S.E. U.S.	Pineland threeawn	*Aristida stricta*
S.E. U.S.	Yaupon	*Ilex vomitoria*
S.E. U.S.	Longleaf pine Foliage	*Pinus palustris*
N. Utah	Big sagebrush	*Artemisia tridentate*

Table 7.1 continued.

Region	Common name	Scientific name
N. Utah	Bigtooth maple	*Acer grandidentatum*
N. Utah	Utah juniper	*Juniperus osteosperma*
N. Utah	Gambel oak	*Quercus gambelii*
S. CA	Chamise	*Adenostoma fasciculatum* Hook & Am
S. CA	Eastwood's manzanita	*Arctostaphylos parryana*
S. CA	Scrub oak	*Quercus berberidifolia*
S. CA	Hoaryleaf ceanothus	*Ceanothus crassifolius*

7.3 Results and Discussion

7.3.1 Yields of Tar, Gas, and Char

Table 7.2 shows the yields of pyrolysis products - tar, light gases, and char- generated from thermal degradation of plants originating from three regions of U.S.: southeastern U.S., northern Utah, and southern California.

The total yield of volatiles from all three regions is shown in Figure 7.1. Total yield of volatiles released from selected southeastern U.S. samples ranged from 78.0 ± 5.0 wt% (daf) in wax myrtle to 83.0 ± 6.6 wt% (daf) in yaupon. Northern Utah plants yielded between 80.0 ± 5.0 wt% (daf) to 82.0 ± 11.5 wt% (daf) of volatile compounds while southern California samples generated between 75.0 to 82.0 wt% (daf). Comparing the total yields of volatile compounds from pyrolysis of southeastern U.S., northern Utah and southern California samples shows only a slight variation in volatiles yield with pyrolysis temperature, ranging from 75 to approximately 84 wt% (daf) of the initial foliage.

Yield of tar obtained from all three regions, southeastern U.S., northern Utah, and southern California, is shown in Figure 7.2. Tar yield from southeastern U.S. samples varied from 53.0 ± 2.5 wt% (saw palmetto) to 62.0 ± 5.0 wt% (dwarf palmetto) while the yield of light gases changed respectively. Tar yield ranged from 53.0 ± 5.0 wt% (Gambel oak) to 58.0 ± 6.6 wt% (Bigtooth maple) for northern Utah samples while southern California samples exposed to similar pyrolysis conditions yielded between 48 wt% (manzanita twigs) to 59 wt% (chamise twigs with leaves) tar. The slight disparities in the tar yield of plants from different U.S. regions (southeastern U.S., northern Utah, and southern California) is likely due to inherent chemical and physical differences between various plant species. Tar from pyrolysis of plants during wildfires can be estimated to be between 48 wt% to 62 wt% of the plant.

Table 7.2: Yields of pyrolysis products collected from various plant species. For southeastern U.S. species and northern Utah species, averages along with 95% confidence intervals are provided. (All data provided on a dry ash-free basis. S.E. U.S. stands for southeastern U.S. while N. Utah and S. CA represent northern Utah and southern California.)

Region	Plant Species	Tar	Gas	Char	Total yield of volatiles
S.E. U.S.	Darrow's blueberry	57±2.5	22±2.5	21±4.3	79±5.0
S.E. U.S.	Dwarf palmetto	62±5.0	18±5.0	20±5.0	80±10.0
S.E. U.S.	Fetterbush	54±6.6	24.3±1.4	21.7±5.7	78.3±8.0
S.E. U.S.	Inkberry	59±5.0	22±2.5	19±4.3	81±7.5
S.E U.S.	Live oak	56±5.0	23±2.5	21±6.6	79±7.5
S.E. U.S.	Little bluestem	61±2.5	20±6.6	19±7.5	81±9.1
S.E. U.S.	Saw palmetto	53±2.5	25±5.0	22±6.6	78±7.5
S.E. U.S.	Sparkleberry	55±2.5	23±5.0	22±6.6	78±7.5
S.E. U.S.	Swamp bay	58±5.0	22±2.5	20±7.5	80±7.5
S.E. U.S.	Water oak	56.7±3.8	23±2.5	20±3.3	79.7±6.3
S.E. U.S.	Live oak	56±5.0	23±2.5	21±6.6	79±7.5
S.E. U.S.	Wax myrtle	55±2.5	23±2.5	22±5.0	78±5.0
S.E. U.S.	Pineland threeawn	59±2.5	23±2.5	18±5.0	82±5.0
S.E. U.S.	Yaupon	61±2.5	22±5.0	17±6.6	83±7.5
S.E. U.S.	Longleaf pine foliage	57±5.0	23±2.5	20±6.6	80±7.5

Table 7.2 continued.

Region	Plant Species	Tar	Gas	Char	Total yield of volatiles
N. Utah	Big sagebrush	54±6.6	28±5.0	18±2.5	82±11.6
N. Utah	Utah juniper	55±2.5	25±2.5	20±5.0	80±5.0
N. Utah	Gambel oak	53±5.0	29±2.5	18±6.6	82±7.5
N. Utah	bigtooth maple	58±6.6	23±5.0	19±10.8	82±11.6
S. CA	Chamise	59	23	18	82
S. CA	Chamise twig	57	23	20	80
S. CA	Eastwood's manzanita	50	28	22	78
S. CA	Eastwood's manzanita twig	48	27	25	75
S. CA	Scrub oak	56	24	20	80
S. CA	Hoaryleaf ceanothus	51	31	18	82

*Error bars for the southern California species were not available due to the limited supply of fresh samples.

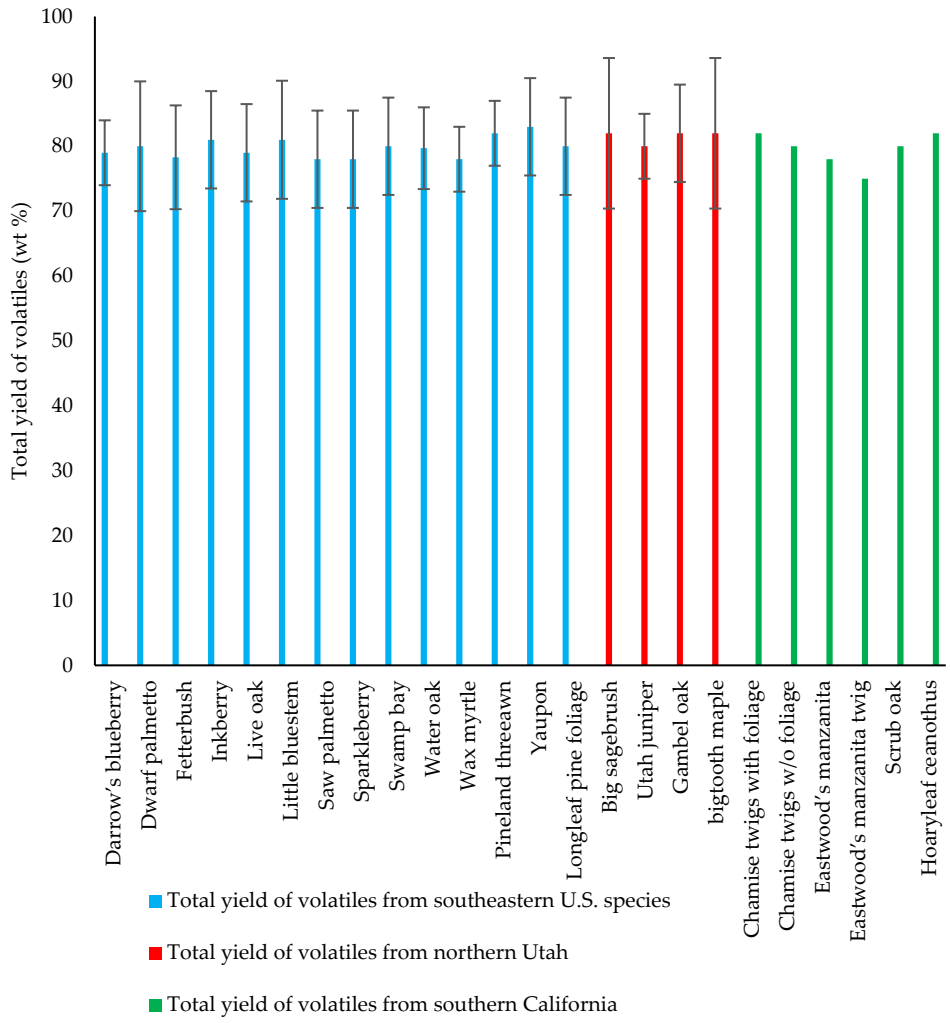

Figure 7.1: Total yields of total volatiles by region

The yield of permanent gases released during pyrolysis of various samples is shown in Figure 7.3. Light gases released from southeastern U.S. samples ranged from 18.0 ± 5.0 wt% (dwarf palmetto) to 25.0 ± 5.0 wt% (saw palmetto) while the range of light gases from northern Utah species varied from 23.0 ± 5.0 wt% (bigtooth maple) to 29.0 ± 2.5 wt% (Gambel oak). Southern California samples generated approximately 23 wt% (chamise twig) to 31 wt% (hoaryleaf ceanothus). The overall yield of light gases from pyrolysis of plants in these experiments ranged from 18 wt% to 31 wt% of the plant.

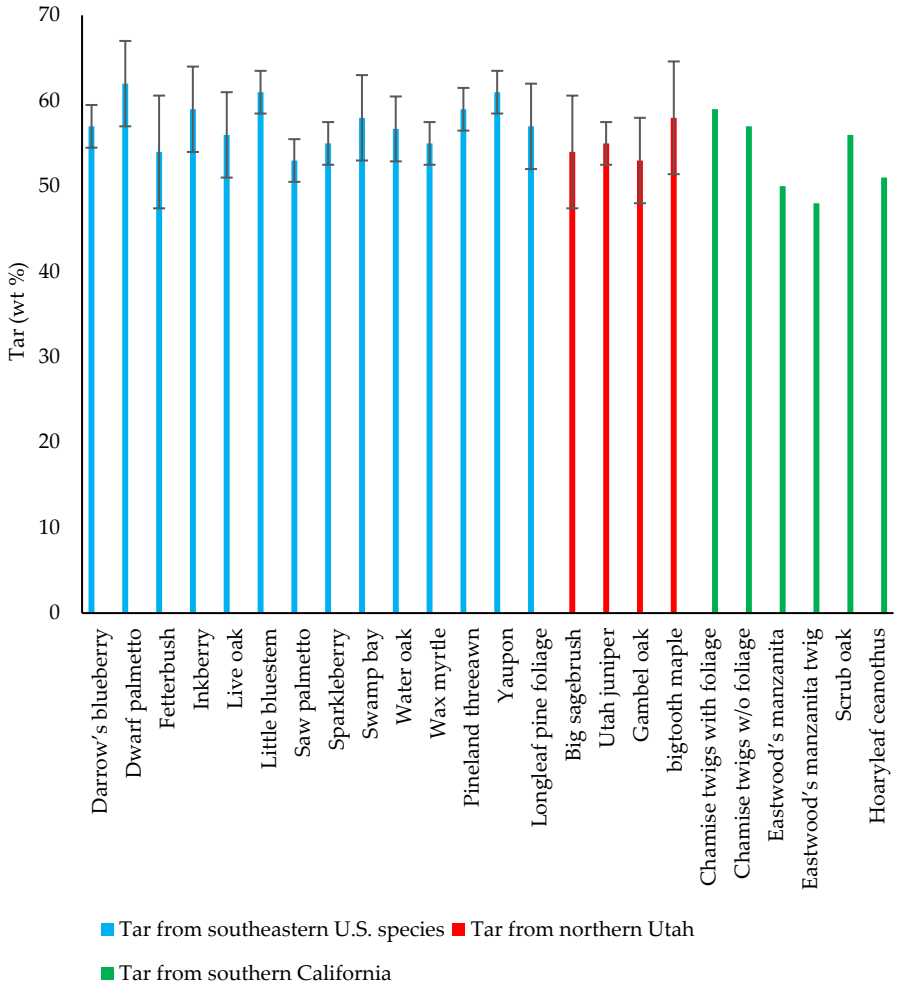

Figure 7.2: Tar yields by region

7.3.2 Compounds Present in Tar

Tables 6.3, A3, A4a, and A4b (See Appendix) contain the complete list of compounds and their concentrations in tar from pyrolysis of the various plant species. Compounds were classified as aromatic or non-aromatic. Aromatic compounds were divided into subgroups of benzenoid aromatics, heterocyclic aromatics, and polyaromatic hydrocarbons (PAHs). Compounds such as 2-methyl pyrimidine and 2-furan methanol which are aromatic and contain at least one hetero atom (N or O) in their ring structure were classified as heterocyclic aromatics.

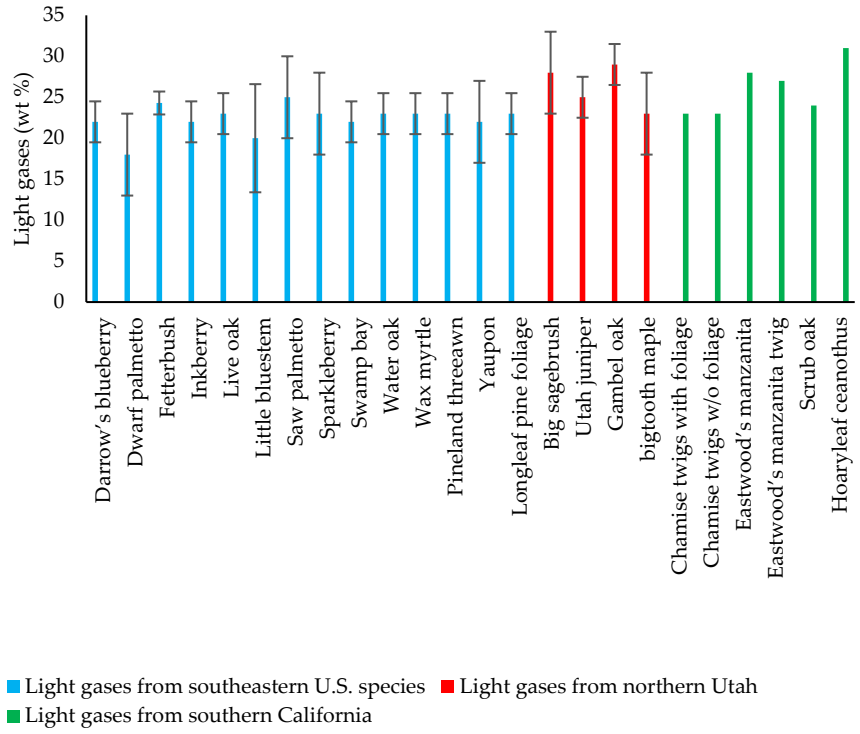

Figure 7.3: Light gas yields by region

Non-aromatic compounds were divided into cycloalkanes, cycloalkenes, cyclo esters, cyclic ketones, ketones, acids, amines, alcohols, and heterocyclics.

Table 7.3 contains the distribution of aromatic versus non - aromatic compounds in tar from the various plant species. Aromatics are the major constituents of chemicals released as tar. Southeastern U.S. plant species generated tar with highest overall concentration of aromatics compared to northern Utah and southern California samples. Overall concentration of aromatics in tar from southeastern U.S. plant species varied from 97.8 mol% (dwarf palmetto) to 100 mol% (inkberry, live oak, little bluestem, saw palmetto, sparkleberry, swamp bay, water oak, wax myrtle and pineland threeawn). The total concentration of aromatics in tar from the northern Utah plant species ranged from 78.8 mol% (Utah juniper) to 90.5 mol% (Gambel oak). Two of the samples from the southern California plant species produced significantly lower amounts of aromatics compared to other examined plant species; Eastwood's manzanita tar contained 37.4 mol% aromatics whereas tar derived from its twigs (no foliage attached) had 50.5 mol%. The rest of the tar samples from southern California contained higher contents of aromatics, ranging from 83.7 mol% (chamise twigs) to 92.1 mol% (chamise). The aromatic content of tar from sparkleberry is reported 100 mol% by Safdari (2018) whereas tar from the

same plant contained 90.9 mol% when examined by (Alizadeh et al., 2024) The disparities in the concentration of aromatics released into tar may be due to slight differences in operating conditions; the pyrolysis temperature during experiments conducted by Safdari reached 765°C while the temperature during experiments performed by Alizadeh (2024) was maintained slightly lower at 725 °C. If the pyrolysis temperatures are low, primary tar reactions will be more prevalent compared to secondary reactions. As the temperatures continue to rise, long chain aliphatic compounds, cycloalkenes, and single-ring aromatics polymerize and form benzenoid compounds with higher molecular weight substitutes and PAHs.

As the distribution of tar compounds from various samples from all three U.S. regions (southeastern U.S., northern Utah, and southern California) was examined, it was observed that as the concentration of benzenoids decreased, concentration of PAHs increased. There were only two samples that do not follow this pattern: Eastwood's manzanita foliage and its twigs. These two samples had significantly higher concentration of cycloalkenes in their tar compared to others.

Table 7.3 : Tar aromatic content for the plant species studied (mol%)

Region	Plant Species	Aromatic	Non-Aromatic
S.E. U.S.	Darrow's blueberry	99.9	0.1
S.E. U.S.	Dwarf palmetto	97.8	2.2
S.E. U.S.	Wax myrtle	100	0.0
S.E. U.S.	Pineland threeawn	100	0.0
S.E. U.S.	Yaupon	98.9	1.1
S.E. U.S.	Longleaf pine foliage	100	0.0
S.E. U.S.	Fetterbush	99.9	0.1
S.E. U.S.	Inkberry	100	0.0

Table 7.3 continued.

Region	Plant Species	Aromatic	Non-Aromatic
S.E. U.S.	Live oak	100	0.0
S.E. U.S.	Little bluestem	100	0.0
S.E. U.S.	Saw palmetto	100	0.0
S.E. U.S.	Sparkleberry	100	0.0
S.E. U.S.	Swamp bay	100	0.0
S.E. U.S.	Water oak	100	0.0
N. Utah	Big Sagebrush	87.6	12.4
N. Utah	Utah juniper	78.8	21.2
N. Utah	Gambel oak	90.5	9.5
N. Utah	Bigtooth maple	87.0	13.0
S. CA	Eastwood's manzanita	37.4	62.6
S. CA	Eastwood's manzanita twig	50.5	49.5
S. CA	Scrub oak	86.7	13.3
S. CA	Hoaryleaf ceanothus	84.9	15.1

The higher concentration of heavy molecular weight aromatics such as PAHs may be attributed to prevalence of secondary pyrolysis reactions during the thermal degradation of these species. Disparities in temperature

profile inside the biomass, which occur due to their different physical characteristics, also affect the chemical reactions occurring during biomass degradation. If the pyrolysis temperatures are low, primary tar reactions will be more prevalent compared to secondary reactions. As the temperatures continue to rise, single-ring aromatics, such as phenolic compounds, polymerize and form benzenoid compounds with higher molecular weight substitutes and PAHs.

Comparisons between some of the compounds detected in tar from southeastern U.S., northern Utah, and southern California species revealed similarities in the functional groups and main ring structures of some of these compounds suggesting they may have originated from the same intermediates. For example, tar collected from southeastern U.S. and northern Utah species contained anthracene while tar from southern California species contained 11,12-diacetyl- 9,10-Ethanoanthracene.

1H-Indenol, indolizine and indole are all compounds with similar structures (See Figure 7.4) detected in tar from northern Utah samples, southeastern U.S. and southern California species.

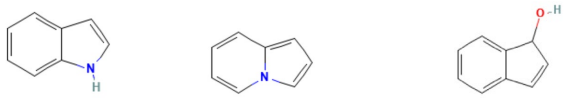

(a) Indole (b) Indolizine (c) 1H-indenol

Figure 7.4: Structure of indole, Indolizine, and 1H-indenol (Raveendran and Ganesh, 1996).

Most non-aromatic tar compounds were classified as cycloalkanes, cycloalkenes, amines, ketones, esters and acids. Tar from southeastern U.S. species contained few non-aromatic compounds. However, this was not the case for tar from northern Utah and southern California species. Acidic compounds were the major contributors to non-aromatic composition of tar from northern Utah species with their concentration varying from approximately 6.2 mol% (bigtooth maple) to 18.5 mol% (Utah juniper). The main portion of acidic compounds in tar had straight chain structure, except for benzoic acid. Contrary to northern Utah samples, tar from southern California and southeastern U.S. samples contained no acidic compounds.

No cycloalkenes were detected in tar from southeastern U.S. samples. Among northern Utah samples, bigtooth maple was the only one containing small concentrations of cycloalkenes (1.1 mol%) in its tar. However, cycloalkenes were the major constituents of non-aromatics in tar from southern California species. Tar collected from Eastwood's manzanita foliage, and its twigs had the highest overall concentration of cycloalkenes (48.1 mol% and 35.7 mol% respectively).

2H-1-benzopyran-2-one, is one of over 300 compounds found in plants known collectively as coumarins. It was detected in tar from northern Utah species except for juniper. Its concentration varied from 4.9 mol % in Gambel oak to 16.5 mol % in bigtooth maple. The presence of 2H-1-benzopyran-2-one in tar from these species may have resulted from their condensation after evaporating and releasing from the complex structure of the plant as they were exposed to high temperatures. Lack of 2H-1-benzopyran-2-one in tar from pyrolysis of southeastern U.S. species and southern California plants may be due to several factors. The chemical makeup of southeastern U.S. and southern California species may contain very small concentrations or no amounts of coumarins. This will result in either very small concentration of these compounds which will be below the detection limit of the GC/MS system used or no detectable compounds at all.

The highest concentration of quinoline detected in tar from southeastern U.S. samples was 3.2 mol% in live oak. Analysis of tar from all northern Utah samples showed quinoline was present in tar. Tar from Utah juniper contained the lowest concentration of quinoline (0.6 mol%) while bigtooth maple generated highest (5.9 mol%). Southern California species, except for Eastwood's manzanita, contained quinoline with its concentration ranging from 2.5 mol% (chamise branches with foliage) to 6.2 mol% (hoaryleaf ceanothus).

In summary, the differences in biochemical composition of various plant species and the differences in their physical characteristics may contribute to the variations in the yields of pyrolysis products and the composition of chemicals detected in tar. While the yields of tar and light gases from different plants vary, the total volatiles and char yields show only minor variations. Tar from all species (except for Eastwood's manzanita) is primarily comprised of aromatic components. Single-ring aromatics (i.e., benzenoids such as phenol, 2-methyl phenol, 3-methyl phenol) followed by PAHs (such as fluoranthene, pyrene, anthracene, benzofluorene, and phenanthrene) are the prevalent aromatics in tar from all species except for Eastwood's manzanita. The higher ratio of PAHs compared to benzenoids in tar may be due to prevalence of secondary pyrolysis reactions during their thermal degradation. Despite similarities in the functional groups of some of the tar compounds, the differences in the chemical composition of biomass may lead to the presence of different compounds in tar. For instance, while phenol is a compound that is detected in tar from all species, anthracene, 9,10-ethanoanthracene, 9,10-dihydro-11,12-diacetyl-, and benz(a)anthracene are only detected in tar from some of the plant species. Considering the structural similarities of these compounds, it is highly probable that they shared common intermediates at some point during their formation. This shows that

despite similarities of tar from various species, it is necessary to collect and analyze tar from any specific biomass to have a better understanding of its chemical composition.

7.3.3 Average Molecular Weight for Tar

Table 7.4 lists the average molecular weight and elemental composition of tar collected from each plant. As seen in Table 7.4, among southeastern U.S. plants, live oak released tar with lowest molecular weight (143.3 g/mol) while little bluestem yielded tar with the highest value (180.2 g/mol). For northern Utah species, tar from Utah juniper had lowest molecular weight (140.0 g/mol) whereas tar from big sagebrush exhibited the highest value (175.5 g/mol). Average molecular weight for tar from southern California species varied from 148.3 g/mol (chamise) to 310.2 g/mol (Eastwood's manzanita).

A deeper look into the chemical makeup of tar from each plant shows that tar from species producing lower molecular weight tar contained relatively lower concentrations of PAHs and heavy molecular weight cycloalkenes, but higher proportions of benzenoids, when compared to tar from species generating heavier tar. Live oak from southern U.S. had significantly higher concentrations of single ring aromatics and much lower concentrations of PAHs in its tar compared to little bluestem. Tar from northern Utah species followed the same trend as southeastern U.S. plants. Big sagebrush had the lowest content of single-ring aromatics among northern Utah species followed by gambel oak, bigtooth maple and Utah juniper. Among southern California samples, chamise had the lightest tar (148.3 g/mol) whereas Eastwood's manzanita generated one with the heaviest value (310.2 g/mol). Tar from Eastwood's manzanita contained high concentrations of phorbol, (34.1 mol%), whereas other southern California species contained much lower concentrations (ranging from 0 to 3.6 mol%). As the concentration of PAHs and heavier compounds in tar increased, the average molecular weight of tar increased. The variations in concentrations of PAHs and heavy cycloalkenes in tar may be due to differences in the chemical composition of the plant species since pyrolysis conditions (heating rate and temperature) were the same during southern California and northern Utah experiments.

Table 7.4: Average molecular weight (MW) and elemental composition for tar from various species.

Region	Plant Species	Average MW for tar (g/mol)	Average elemental composition of tar
S.E. U.S.	Darrow's blueberry	144.0	$C_{9.85}H_{8.4}O_{1.04}N_{0.02}$

Table 7.4 continued.

Region	Plant Species	Average MW for tar (g/mol)	Average elemental composition of tar
S.E. U.S.	Dwarf palmetto	146.2	$C_{10.41}H_{8.51}O_{0.7}N_{0.05}$
S.E. U.S.	Fetterbush	159.6	$C_{11.74}H_{8.97}O_{0.54}N_{0.3}$
S.E. U.S.	Inkberry	167.6	$C_{12.37}H_{9.17}O_{0.59}N_{0.02}$
S.E. U.S.	Live oak	143.3	$C_{10.03}H_{8.46}O_{0.78}N_{0.07}$
S.E. U.S.	Little bluestem	180.2	$C_{13.66}H_{10.50}O_{0.17}$
S.E. U.S.	Saw palmetto	151.5	$C_{11}H_{8.65}O_{0.58}N_{0.04}$
S.E. U.S.	Sparkleberry	154.2	$C_{10.88}H_{8.79}O_{0.88}N_{0.01}$
S.E. U.S.	Swamp bay	154.4	$C_{11.07}H_{8.82}O_{0.7}N_{0.03}$
S.E. U.S.	Water oak	147.5	$C_{10.52}H_{8.52}O_{0.7}N_{0.05}$
S.E. U.S.	Wax myrtle	146.4	$C_{10.33}H_{8.30}O_{0.8}N_{0.02}$
S.E. U.S.	Pineland threeawn	175.6	$C_{13}H_{10.16}O_{0.46}$
S.E. U.S.	Yaupon	164.5	$C_{12.1}H_{9.33}O_{0.55}N_{0.03}$
S.E. U.S.	Longleaf pine foliage	172.2	$C_{12.76}H_{10.10}O_{0.41}$
N. Utah	Big sage brush	175.5	$C_{12.91}H_{10.4}O_{0.5}N_{0.06}$
N. Utah	Utah juniper	140.0	$C_{9.29}H_{10.49}O_{1.1}N_{0.01}$
N. Utah	Gambel oak	166.6	$C_{11.93}H_{10.53}O_{0.77}N_{0.04}$
N. Utah	Bigtooth maple	151.4	$C_{10.46}H_{9.08}O_{0.92}N_{0.15}$
S. CA	Chamise	148.3	$C_{9.61}H_{9.95}O_{1.37}N_{0.09}$
S. CA	Chamise twig	176.4	$C_{11.39}H_{12.32}O_{1.68}N_{0.05}$
S. CA	Eastwood's manzanita	310.2	$C_{18.86}H_{25.19}O_{3.67}N_{0.03}$
S. CA	Eastwood's manzanita twig	269.0	$C_{16.55}H_{21.52}O_{3.02}N_{0.06}$
S. CA	Scrub oak	169.5	$C_{11.06}H_{13.02}O_{1.43}N_{0.07}$
S. CA	Hoaryleaf ceanothus	180.6	$C_{12.11}H_{15.04}O_{1.22}N_{0.06}$

7.3.4 Light Gases

CO, CO_2, CH_4 and H_2 were the major gas components observed for all plant species. Mass concentrations of all major components in the gas phase are presented in Table 7.5 along with the 95 % confidence intervals.

CO was the dominant light gas species in these experiments. Figure 7.5 represents concentration of CO in light gases from pyrolysis of various plant species. Southeastern U.S. samples generated between 53.4 wt% (swamp bay) to 63.0 wt% (saw palmetto) carbon monoxide in their light gases. The concentration of CO in light gases from northern Utah species

ranged between 53.8 wt% (bigtooth maple) to 59.1 wt% (Gambel oak) whereas southern California samples produced between 55.0 wt% (chamise) to 62.1 wt% (scrub oak). The average concentration of carbon monoxide in light gases from pyrolysis of foliage can be estimated to be between 53.4 wt% (daf) to 63.0 wt% (daf).

Table 7.5: Concentration of major gas components generated from pyrolysis of the plant species studied (wt% of light gas).

Region	Species	CO	CO_2	CH_4	H_2
S.E.U.S.	Darrow's blueberry	62.1±6.9	25.0±3.4	10.9±3.8	2.1±0.3
S.E.U.S.	Dwarf palmetto	59.7±2.5	31.2±1.8	7.6±1.3	1.5±0.5
S.E.U.S.	Fetterbush	59.1±7.5	30.9±8.3	7.9±1.3	2.1±0.0
S.E.U.S.	Inkberry	59.8±10.7	29.3±7.8	9.0±3.6	1.9±0.1
S.E.U.S.	Live oak	60.5±6.2	29.8±5.2	8.1±1.6	1.7±0.1
S.E.U.S.	Little bluestem	62.1±4.3	28.6±6.8	8.0±2.3	1.4±0.4
S.E.U.S.	Saw palmetto	63.0±3.3	29.1±2.9	6.3±0.9	1.6±0.5
S.E.U.S.	Sparkleberry	61.7±6.2	26.2±3.8	10.3±3.2	1.8±0.5
S.E.U.S.	Swamp bay	53.4±9.5	34.7±5.1	9.8±4.6	2.1±0.2
S.E.U.S.	Water oak	59.2±6.0	30.7±4.3	8.4±1.2	1.7±0.6
S.E.U.S.	Wax myrtle	61.4±7.2	26.7±5.1	10.2±2.2	1.8±0.1
S.E.U.S.	Pineland threeawn	56.7±11.2	32.9±8.2	9.1±2.8	1.3±0.3
S.E.U.S.	Yaupon	57.9±4.6	29.7±3.0	10.6±3.8	1.8±0.2
S.E.U.S.	Longleaf pine foliage	60.6±5.7	28.9±4.7	9.2±1.7	1.4±0.1
N. Utah	Big sagebrush	54±6.6	28±5.0	18±2.5	82±11.6
N. Utah	Utah juniper	55±2.5	25±2.5	20±5.0	80±5.0
N. Utah	Gambel oak	53±5.0	29±2.5	18±6.6	82±7.5
N. Utah	Bigtooth maple	53.8±3.7	34.5±6.0	10.6±2.1	1.1±0.4
S. CA	Chamise	55.0±1.4	34.8±2.1	8.7±2.1	1.5±0.0
S. CA	Chamise twig	57.1±2.3	33.4±1.7	7.9±1.3	1.6±1.2
S. CA	Eastwood's manzanita	58.3±1.4	31.0±1.5	9.4±1.9	1.3±0.1
S. CA	Hoaryleaf ceanothus	56.8±1.9	32.5±1.5	9.2±1.3	1.5±0.1
S. CA	Scrub oak	62.1±2.0	29.4±1.4	7.0±1.2	1.6±0.1

Table 7.5 continued.

Region	Species	CO	CO_2	CH_4	H_2
S. CA	Eastwood's manzanita twig	59.4±1.9	32.1±1.7	7.2±1.9	1.4±0.1

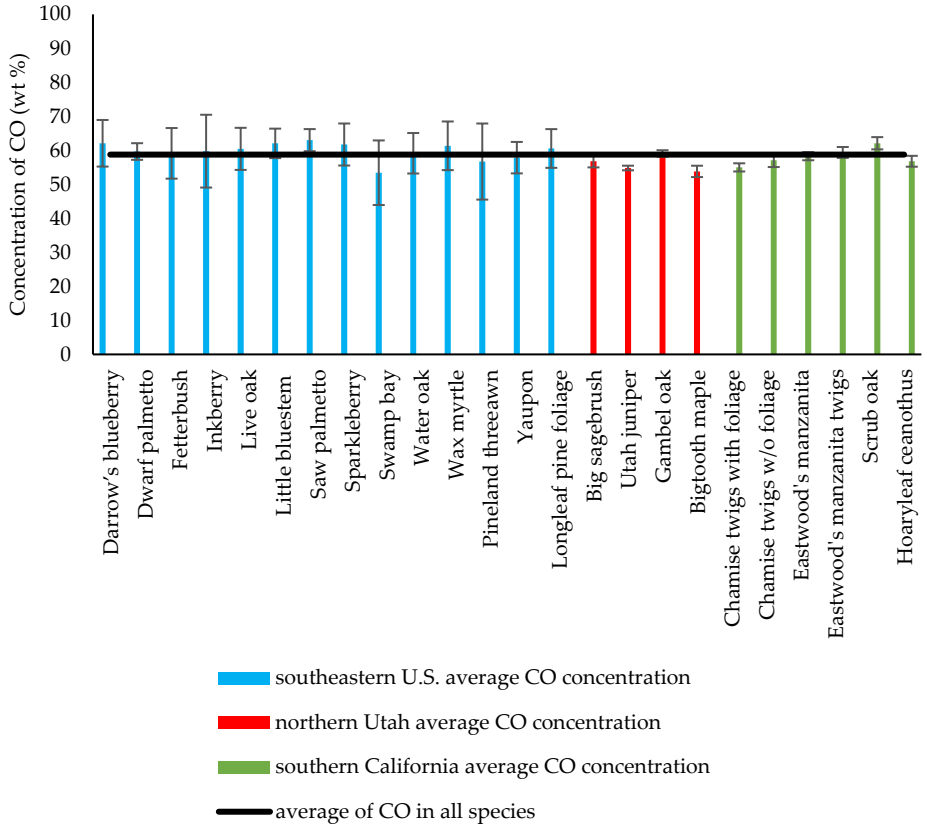

Figure 7.5: Concentration of CO in light gases from pyrolysis of various samples. All concentrations are in weight percentage of light gas.

Statistical analysis on fluctuations in concentration of CO in light gases from pyrolysis of southeastern U.S. samples showed changes in concentration due to the species type were statistically significant (p=0.025). Statistical evaluations on northern Utah species showed that biomass type affects concentration of CO (p=0.003). Comparing the results obtained from analysis of light gases from southern California species showed that, similar to what was observed during pyrolysis of southeastern U.S. and northern Utah species, changes in concentration of

CO in light gases from southern California species due to fuel type were statistically significant ($p = 2.37\times 10^{-6}$).

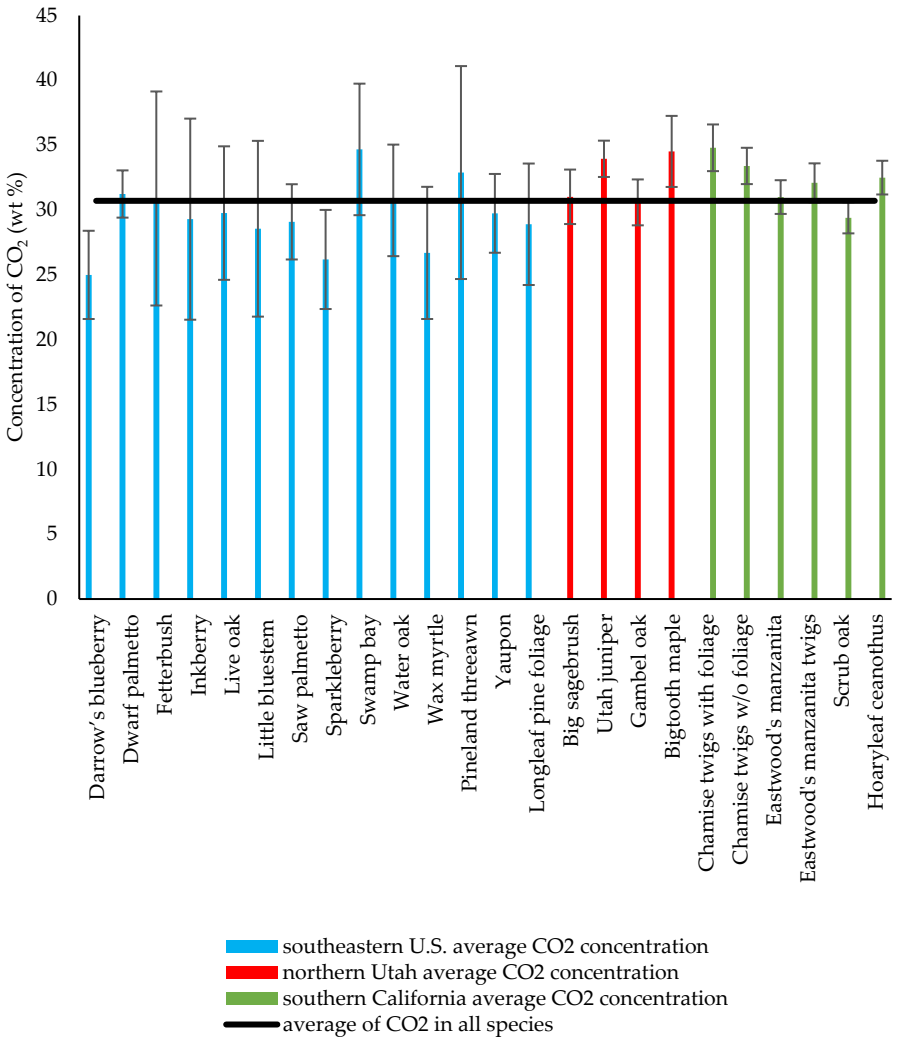

Figure 7.6: Concentration of CO_2 in light gases from pyrolysis of various samples. All concentrations are in weight percentage of light gas.

Figure 7.6 illustrates concentration of CO_2 in light gases from pyrolysis of various plant species. The concentration of CO_2 generated during pyrolysis of southeastern U.S. species ranged from 25.0 wt% (Darrow's blueberry) to 34.7 wt% (swamp bay). Northern Utah species yielded between 30.6 wt% (Gambel oak) to 34.5 wt% (bigtooth maple) whereas light gases from southern California samples contained between 29.4 wt% (scrub oak) to 34.8 wt% (chamise). The average concentration of carbon dioxide in light gases from pyrolysis of foliage can be estimated to be approximately between 25 wt% (daf) to 35 wt% (daf).

Statistical evaluations on variations in concentration of CO_2 in pyrolysis gases from southeastern U.S. samples showed statistically significant changes due to biomass type (p=0.0007). However, concentration of CO_2 in northern Utah samples changed moderately due to biomass type (p=0.06). Similar to what was observed from southeastern U.S. samples, a statistically profound difference was observed in concentration of CO_2 between southern California species (p=0.00008). Since operating conditions (pyrolysis temperature and heating rate) were the same during southern California and northern Utah experiments, this contradictory result was likely due to differences in the biomass composition.

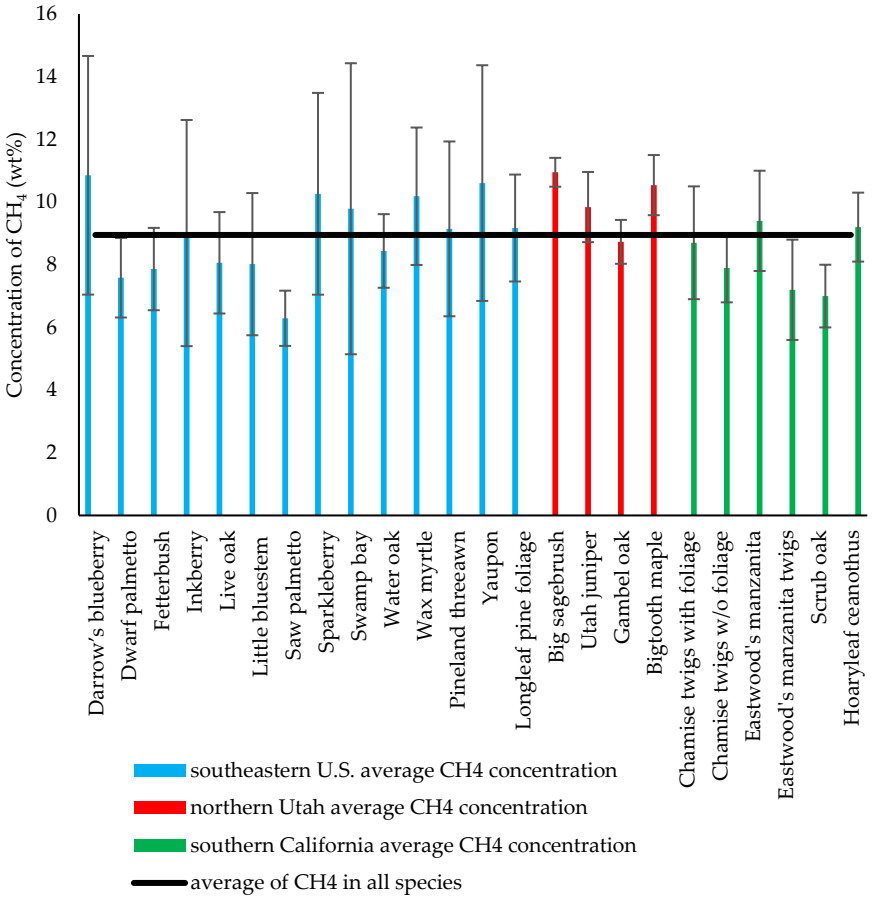

Figure 7.7: Concentration of CH_4 in light gases from pyrolysis of various samples. All concentrations are in weight percentage of light gas.

Concentration of CH_4 produced from pyrolysis of various samples is shown in Figure 7.7. Concentration of CH_4 generated from southeastern U.S. samples varied from 6.3 wt% (saw palmetto) to 10.9 wt% (Darrow's

blueberry). Northern Utah samples yielded between 8.7 wt% (Gambel Oak) to 11.0 wt% (big sagebrush) whereas light gases from southern California samples contained between 7.0 wt% (scrub oak) to 9.4 wt% (Eastwood's manzanita). The average concentration of methane in light gases from pyrolysis of foliage can be estimated to be between 6.3 wt% (daf) to 11 wt% (daf). Analysis of gases from southeastern U.S. samples showed that concentration of CH_4 in pyrolysis gases changed due to species type were statistically significant (p=0.0005). Similar to southeastern U.S. samples, changes in the concentration of CH_4 in pyrolysis gases of northern Utah samples due to biomass type were statistically significant (p=0.03). However, statistical analysis of fluctuations in wt % of CH_4 generated during pyrolysis of southern California species showed that plant type affected concentration of CH_4 slightly (p=0.08). The differences in behavior of northern Utah samples and southern California samples in whether a correlation exists between wt% of CH_4 and biomass type were due to differences in composition of biomass.

Figure 7.8 shows concentration of H_2 (wt %) in light gases from pyrolysis of various plant samples. Pyrolysis light gases from southeastern U.S. samples contained between 1.3 wt% (pineland three awn) to 2.1 wt% (swamp bay) H_2. The average concentration of H_2 in light gases from northern Utah species varied between 1.1 wt% (bigtooth maple) to 1.6 wt% (Gambel oak) whereas southern California samples yielded between 1.3 wt% (Eastwood's manzanita) to 1.6 wt% (scrub oak). The average concentration of hydrogen in light gases from pyrolysis of foliage can be estimated to be between 1.1 wt% (daf) to 2.1 wt% (daf).

Statistical analysis showed that there was a statistically significant variation in the concentration of H_2 released into light gases during pyrolysis of various types of northern Utah biomass (p=0.01). This is consistent with the results obtained during pyrolysis of southern California and southeastern U.S. species. Analysis of gases from pyrolysis of southern California and southeastern U.S. species showed statistically significant changes in the concentration of H_2 in light gases due to plant species (p=0.003, and p=1.57$\times 10^{-8}$ respectively). However, the released H_2 represented only a small percentage of the mass of the original biomass.

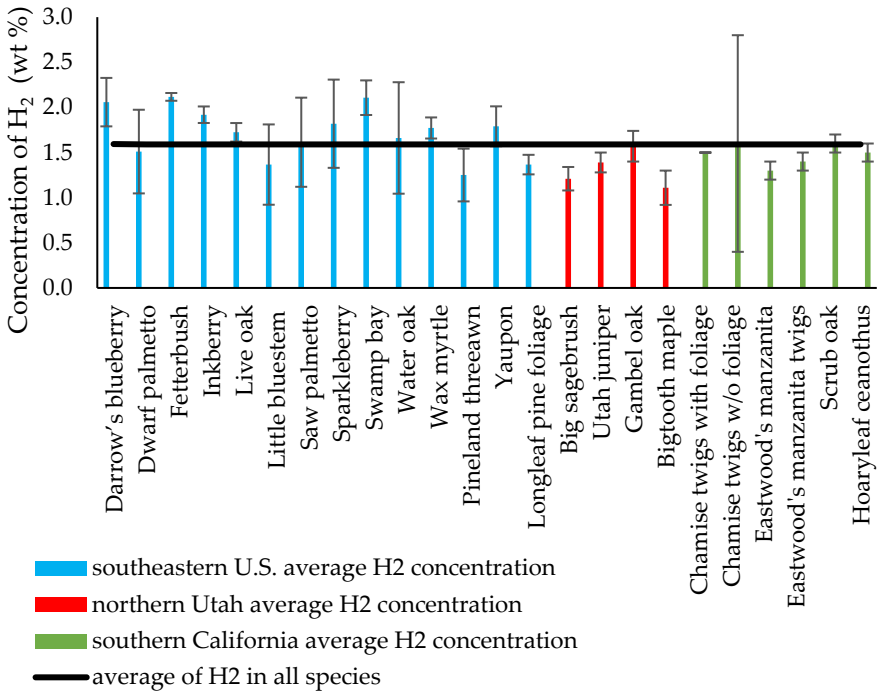

Figure 7.8: Concentration of H_2 in light gases from pyrolysis of various samples. All concentrations are in weight percentage of light gas.

7.3.5 High Heating Value

Since the purpose of this chapter is to study the volatiles released during pyrolysis of selected U.S. species to better understand their possible contribution to the propagation of wildland fires, high heating values of the volatiles generated during pyrolysis were estimated.

High heating values for tar and light gases generated during pyrolysis of selected U.S. samples are reported in Table 7.6. High heating value of tar from southeastern U.S. samples was estimated to be between 34.12 (MJ/kg of tar) for Darrow's blueberry to 38.80 (MJ/kg of tar) for little bluestem. The HHV of tar from northern Utah samples varied between 34.68 (MJ/kg of tar) for bigtooth maple to 36.81 (MJ/kg of tar) for big sagebrush. For southern California samples, HHV of tar was estimated to be between 33.24 (MJ/kg of tar) for Eastwood's manzanita and 37.19 (MJ/kg of tar) for hoaryleaf ceanothus. The high heating value for tar generated during pyrolysis of plant samples examined here range between 33.24 (MJ/kg of tar) and 38.80 (MJ/kg of tar). These values are slightly higher than the reported HHV values for bio-oil in the literature which are between 20 and 35 (MJ/kg of tar). There is a large amount of published research on high heating value of bio-oil from various sources of biomass due to its potential as fuel (Raveendran and Ganesh, 1996; Yang et al., 2017; Nunes et al., 2020).

Composition of bio-oil varies due to several factors such as operating conditions, reactor type, and the composition of parent biomass. Variations in bio-oil composition eventually contribute to variations in the bio-oil HHV. HHVs of light gases generated during pyrolysis of southeastern U.S. samples varied from 12.20 (MJ/kg of light gases) for saw palmetto to 15.29 (MJ/kg of light gases) for Darrow's blueberry. HHVs of light gases from northern Utah species were estimated to be from 12.92 (MJ/kg of light gases) for bigtooth maple to 13.60 (MJ/kg of light gases) for big sagebrush. HHVs of southern California species varied from 12.00 (MJ/kg of light gases) for Eastwood's manzanita twig to 13.04 (MJ/kg of light gases) for hoaryleaf ceanothus. HHV values for total volatiles from selected southeastern U.S. samples fluctuated between 22.49 (MJ/kg of volatiles) for wax myrtle to 26.21 (MJ/kg of volatiles) for little bluestem. The total HHV of total volatiles from northern Utah samples ranged between 22.83 to 23.68 (MJ/kg of volatiles), which were in the same range as the values for southern California samples reported by (Alizadeh et al., 2024). HHV of total volatiles for selected southern California species varied between 19.37 to 23.01 (MJ/kg of volatiles).

Based on these results, the HHV of total volatiles generated during pyrolysis of foliage can be estimated to be between 19.37 to 26.21 (MJ/kg of volatiles). The contribution of tar and light gases to the HHV of the total HHV from volatiles is illustrated in Figure 7.9. The contribution of tar to the HHV of volatiles was 82 to 92% which shows the importance of tar identification to estimate the impact of pyrolysis of biomass prior to combustion of foliage.

Table 7.6: High heating values of tar, light gases, and volatiles released from pyrolysis of selected U.S. plant species.

Region	Species	HHV of tar (MJ/kg of tar)	HHV of gas (MJ/kg of gas)	HHV of volatiles (MJ/kg of volatiles)
S.E. U.S.	Darrow's Blueberry	34.13±2.35	15.29±2.16	22.82±4.53
S.E. U.S.	Dwarf palmetto	35.53±2.75	12.44±1.10	24.27±7.4
S.E. U.S.	Fetterbush	36.60±2.89	13.40±1.05	23.02±4.03
S.E. U.S.	Inkberry	36.47±2.89	13.83±2.19	24.56±5.55
S.E. U.S.	Live oak	35.37±3.05	13.08±1.14	22.82±4.24
S.E. U.S.	Little bluestem	38.80±3.06	12.73±1.58	26.21±9.50
S.E. U.S.	Saw palmetto	36.46±2.62	12.20±1.28	22.51±5.20
S.E. U.S.	Sparkleberry	35.08±2.86	14.58±2.11	22.65±6.26

Table 7.6 continued.

Region	Species	HHV of tar (MJ/kg of tar)	HHV of gas (MJ/kg of gas)	HHV of volatiles (MJ/kg of volatiles)
S.E. U.S.	Swamp bay	35.87±2.82	13.90±2.64	23.86±5.90
S.E. U.S.	Water oak	35.70±2.91	13.08±1.46	23.25±4.36
S.E. U.S.	Wax myrtle	34.85±2.90	14.43±1.44	22.49±3.93
S.E. U.S.	Pineland threeawn	37.50±3.11	12.63±2.11	25.03±5.50
S.E. U.S.	Yaupon	36.76±3.00	14.33±1.95	25.58±7.14
S.E. U.S.	Longleaf pine foliage	37.96±1.33	13.21±1.14	24.67±2.76
N. Utah	Big sagebrush	36.81	13.60±6.27	23.68
N. Utah	Utah juniper	35.59	13.03±8.50	22.83
N. Utah	Gambel oak	36. 55	13.11±7.29	23.17
N. Utah	Bigtooth maple	34.68	12.92±9.75	23.09
S. CA	Chamise	33.54	12.62±1.17	22.69
S. CA	Chamise twig	33.76	12.51±1.02	22.12
S. CA	Eastwood's manzanita	33.24	13.04±1.14	15.27
S. CA	Eastwood's manzanita twig	33.61	11.99±1.22	19.37
S. CA	Scrub oak	35.20	12.49±0.91	22.71
S. CA	Hoaryleaf ceanothus	37.19	13.04±0.90	23.01

It is interesting to compare the high heating values determined here with the results published by Susott (1982) who used both evolved gas analysis (EGA) at a low heating rate of 20 °C to 500 °C and conventional bomb calorimetry on forest fuels. Many of the fuels studied by Susott were from trees, but he did study chamise, manzanita, big sagebrush and Utah juniper. It was not clear from the publication if the reported values were the high heating value (HHV) or the low heating value (LHV). The yields of volatiles reported by Susott for the four species in common ranged from 66.6 to 69.4 wt% daf compared to 78 to 82 wt% daf for the same samples reported here from experiments at higher heating rates and temperatures. The heating values for total volatiles reported by Susott for these four common species ranged from 11.8 to 15.8 MJ/kg (daf) which are lower than the HHV range of 15.3 to 23.7 MJ/kg (daf) in these experiments. Manzanita volatiles have the lowest heating value in both studies. The total fuel heating values for these four species reported by Susott (which includes

combustion of volatiles and char) ranged from 21.7 to 23.28 MJ/kg, which are close to the HHV values for total volatiles for most species reported here. The higher yield of volatiles at higher heating rates seems to transfer energy from the char to the volatiles, resulting in higher HHV values of the volatiles. This finding emphasizes the need to perform experiments at realistic temperatures and heating rates to provide meaningful information to direct simulations.

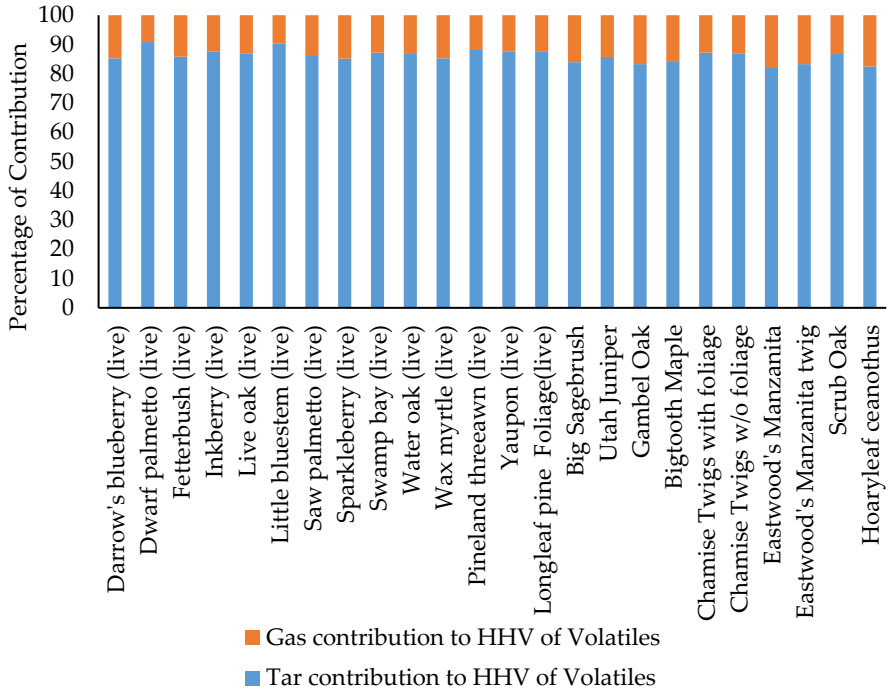

Figure 7.9: Contribution of tar and light gases to HHV of total volatiles.

7.4 Summary and Conclusions

In this chapter, pyrolysis products' yields and compounds released from 24 foliage samples originating from three U.S. regions were studied. The operating conditions for pyrolysis of samples during experiments were selected to mitigate the heating rate and temperature of wildland fires. Ranges of yields of tar and gas products were compared. Major components of tar and light gases were identified and differences in their concentrations were investigated. The average molecular weights of the tar were estimated for each plant species. The high heating values (HHVs) of the tar, light gases, and total volatiles (tar and light gases combined) were

estimated and compared. The average values of yields and heating values from the 24 plant species are presented in Table 7.7 for convenience.

Table 7.7: Average yields and heating values for the 24 plant species studied

Pyrolysis products' yield (wt%, daf)			Light gas composition (wt% dry)				Total HHV of volatiles (MJ/kg dry)
Tar	Light gases	Total volatiles	CO	CO_2	CH_4	H_2	
56.0	24.0	80.0	58.8	32.5	9.2	1.5	23.19

The primary conclusions of this research are:

- The total yields of volatiles were similar for all plant species at the temperatures and heating rates studies, ranging from 75 wt% to 83 wt%.
- Tar was the principal pyrolysis product, ranging from 48 wt% to 62 wt% of the dry ash free plant samples and 57 to 70% of the volatiles released.
- Tar from all species, except for Eastwood's manzanita, was mainly composed of aromatics. Southeastern U.S. samples produced tar with highest overall concentration of aromatics compared to northern Utah and southern California samples. The concentration of aromatics in tar from southeastern U.S. species ranged from 97.8 mol% to 100 mol%. The concentration of aromatics in Eastwood's manzanita tar was 37.4 mol% while tar from other southern California species contained between 83.7 mol% to 92.1 mol% aromatics. Northern Utah species generated tar with 78.8 to 90.5 mol% aromatics. These disparities in the concentration of aromatics in tar from various species show that biomass type affects the overall concentration of aromatics released into tar. Excluding Eastwood's manzanita as an outlier, the overall concentration of aromatics in tar varied from 78 to 100 mol%.
- Comparisons among tar samples from southeastern U.S., northern Utah, and southern California revealed some similarities and differences in the key components and their concentration. The primary compounds of tar from all southeastern U.S. samples, excluding little bluestem, were benzenoids: phenol, 1,2- benzenediol, 1,4- benzenediol, and 2,6-dimethoxy phenol. Tar from little bluestem was abundant in PAHs such as fluorene and pyrene. Tar from southern California species, excluding Eastwood's manzanita, were

mainly composed of phenol and phenol, 3-methyl. Tar from northern Utah species had a composition different from southeastern U.S. and southern California ones. Big sagebrush and Gambel oak yielded tar abundant in PAHs such as fluoranthene, 2-phenyl naphthalene, and anthracene. Tar from Utah juniper was primarily made up of phenol and phenol 3-methyl. Bigtooth maple, on the other hand, generated tar that was abundant in coumarin, anthracene and fluoranthene. This shows that while in most cases tar from pyrolysis of biomass is mainly made up of aromatics, the detailed composition of tar depends on the biomass type, and therefore detailed analysis of tar is needed to predict what compounds are released during wildland fires.

- Concentration of PAHs in tar from southeastern U.S. samples ranged from 39.2 mol% to 89 mol%. Tar from southern California samples contained much lower concentrations of PAHs, ranging from 13.4 mol% to 20.7 mol%, compared to one obtained from southeastern U.S. samples. Northern Utah samples generated tar that contained between 19.6 mol% to 63.3 mol% PAHs. The differences in the concentration of PAHs in tar could be due to variations in biochemical composition of the plants.
- Light gases generated during pyrolysis of all species were collected and analyzed by GC/TCD. CO, CO_2, CH_4, and H_2 were the major constituents of pyrolysis gases on a wt % basis. CO was the main component of the light gases succeeded by CO_2, CH_4, and H_2 on a wt % basis. The CO concentration ranged from 53.4 wt% to 63 wt%. CO_2 ranged between 25 wt% and 35 wt% of light gases while CH_4 comprised 6.3 wt% to 11 wt% of the light gases. Concentration of H_2 was between 1.1 wt% and 2.1 wt%.
- Concentration differences of CO and H_2 due to species type were statistically significant, although the concentration of H_2 was always quite low. Concentration of CO_2 in light gases from pyrolysis of northern Utah samples changed moderately due to plant species type. However, its concentration in light gases from southern California and southeastern U.S. samples depended on the species type. Concentration of CH_4 in light gases from southern California samples changed moderately due to species type; however, its concentration in light gases from northern Utah and southeastern U.S. samples changed significantly due to species type.

- The high heating value (HHV) of volatiles generated during pyrolysis of foliage were estimated to be between 19.37 to 26.21 (MJ/kg of volatiles), with the lowest value from Eastwood's manzanita. The HHV of tar ranged from 33.24 to 38.80 MJ/kg of tar, representing between 82% to 91% of the heating value of the volatiles. The large contribution of tar to the heating value of the volatiles implies that tar cannot be overlooked in combustion simulations.

This work was limited to the plant species studied at the heating rates and temperatures pertaining to active fires. Different temperatures and heating rates would apply to smoldering. Intact foliage samples were used in all cases which may be part of any differences with data from TGA studies where small sections of foliage samples are used. The type and amount of large molecular weight tar species should be studied further using GC columns at higher temperatures. Tar HHVs were only calculations; actual measurement of tar HHVs would be more precise.

The data on yields, gas and tar species, and heating values obtained at relevant heating rates and temperatures should provide a basis for improving pyrolysis modeling and subsequent combustion modeling for wildland fire simulation.

8 Investigation of Co-pyrolysis of Biomass

8.1 Introduction

Investigating possible synergetic effects of two different types of biomass during pyrolysis broadens comprehension of wildland fires since the forest beds are heterogeneous environments always covered with more than one type of plant species. While studies on simultaneous pyrolysis of more than one type of biomass are scarce, co-pyrolysis of biomass and other types of fuel such as coal, and polymers (mostly as plastic waste) has been studied more extensively (Zhang et al., 2007; Paradela et al., 2009; Li et al., 2015; Burra and Gupta, 2018; Esso et al., 2022).

This chapter intends to investigate the possible synergetic interactions occurring during co-pyrolysis of two different types of plant species originating from southern California, chamise, and scrub oak. Clippings of these two plant species were put in ziplock bags to preserve their moisture and were express mailed to Brigham Young University. Various blends of chamise and scrub oak with different predefined mass ratios were pyrolyzed in a flat flame burner. The released pyrolysis products were analyzed to investigate the effects of simultaneous pyrolysis of the two plant species on product yields and chemical composition.

8.2 Experimental Setup

The experimental setup used for pyrolysis of biomass and the products' collection systems, including flat flame burner, ice bath, tar, and gas collection systems, and analysis instruments are explained in chapter 4.

8.3 Sample Preparation

Three ratios of chamise to scrub oak were selected; (chamise 1:1 scrub oak), (chamise 2.5: 1 scrub oak) and (chamise 1: 2.5 scrub oak). These ratios were easy to repeat and required minimal foliage cutting for sample preparation. Minimizing the tearing of the surface of the samples before each experiment reduced possible escaping of volatile compounds from samples. Mass fraction of chamise was defined as the ratio of the mass of chamise in the biomass blend to the combined mass of chamise and scrub oak prior to each experiment. β represents mass fraction of chamise during these experiments. The values for β were 0, 0.29, 0.5, 0.71 and 1. Both samples of chamise and scrub oak were put together in the alligator clip connected to the metal rod and entered the high-temperature zone. The

overall mass of the sample blend prior to pyrolysis was between 3 to 5 grams.

8.3.1 Ash Content

Ash content of each of biomass samples, chamise and scrub oak, and their blends were measured according to procedure described in chapter 4 as a consistency check. It was found that the ash content of the blends was a weighted average of the two species used. Table 8.1 contains ash content of chamise, scrub oak, and their various blends.

Table 8.1: Ash content of chamise and scrub oak, and their blends

Biomass combination	β	Ash content (wt%) (moisture-free basis)
Scrub oak	0	4.8
Chamise 1- Scrub oak 2.5	0.29	4.3
Chamise 1- Scrub oak 1	0.5	4.0
Chamise 2.5- Scrub oak 1	0.71	3.6
Chamise	1	3.1

8.4 Results and Discussions

In this section, co-pyrolysis of three various blends of chamise and scrub oak was studied. Tar and light gases generated during co-pyrolysis experiments were analyzed. The yield of pyrolysis products was measured, and possible synergistic effects on the yields of tar and light gases were investigated. Detailed analysis of tar and light gases collected from pyrolysis of each of the blends was studied followed by mechanisms responsible for observed synergistic effects.

8.4.1 Tar, Gas, and Char Yields

Table 8.2 shows the yields of pyrolysis products from chamise, scrub oak and various blends of the two species. Estimated values for yields of pyrolysis products were calculated as the weighted average of mass fraction of chamise and scrub oak and their respective yields if there were no synergetic effects during co-pyrolysis. Measured values for pyrolysis products show recorded values for tar, light gases, and char after each experiment. As seen in Table 8.2, deviations from estimated values were negligible. Since chamise generated higher yields of tar compared to scrub oak, it was expected that adding chamise to scrub oak and increasing its mass fraction in the biomass blend would enhance tar generation. As seen

in Table 8.2, a positive correlation between α and tar yield was observed. Measured values for tar during co-pyrolysis experiments were slightly higher than estimated values. The estimated values for tar ranged from 56 wt% to 59 wt% while the measured values were between 56 wt% to 60 wt%. This suggests that slight synergistic effects may have promoted tar generation during the co-pyrolysis of chamise and scrub oak. The yield of light gases from chamise was slightly lower than that of scrub oak. It was expected that adding chamise to the biomass blend may decrease production of light gases. As shown in Table 8.2, the yield of light gases exhibited a negative correlation to chamise mass fraction in biomass blend. Similar to tar, the differences between estimated and measured values of light gases from co-pyrolysis of the two biomasses were minimal; suggesting minor synergistic effects due to blending two types of biomass. The total yield of volatiles was not significantly affected due to co-pyrolysis of chamise and scrub oak. Overall, no significant synergetic effects from co-pyrolysis of chamise and scrub oak on pyrolysis product yields were observed.

Table 8.2: The yields of pyrolysis products (Tar, light gases and char) from chamise, scrub oak and various blends of the two species. EV stands for estimated values while MV represents measured value.

	Tar yield (wt.%) (daf)		Light gases yield (wt.%) (daf)		Total yield of volatiles (wt.%) (daf)		Char yield (wt.%) (daf)	
β	EV	MV	EV	MV	EV	MV	EV	MV
0	56	56	24	24	80	80	20	20
0.29	56.9	57	23.7	24	80.6	81	19.4	19
0.5	57.5	58.5	23.5	22.5	81	81	19	19
0.71	58.1	60	23.3	22	81.4	82	18.6	18
1	59	59	23	23	82	82	18	18

Hopa et al. (2019) tried to explain synergistic effects observed during co-pyrolysis of three different types of biomass: bagasse, poppy capsule pulp, and rice husk. They reported that an increase in the total ash content of the biomass blend would enhance char generation from pyrolysis of the

biomass blend. Due to higher ash content of scrub oak compared to chamise, it was anticipated that the yield of volatiles would increase as mass fraction of chamise (β) increased in the biomass blend. However, comparisons of total volatiles yield collected from experiments with values of β equaling 0.29 and 0.5 revealed no variations in the yield of volatiles despite higher proportions of scrub oak in biomass.

8.4.2 Effect of Co-pyrolysis of Biomass on Tar Composition

Extensive analysis of tar from pyrolysis of chamise and scrub oak was conducted previously (Alizadeh et al., 2024). Here, the possible changes to tar composition due to simultaneous pyrolysis of chamise and scrub oak were investigated in a similar manner. A complete list of compounds identified for each plant species is provided in Table A5 (Provided in the appendix). Tar compounds are classified according to the same criteria explained in 5.3.2. Tables 8.3 and 8.4 show detailed classification of species present in tar from the pyrolyzed plant samples. Similar to what was observed during pyrolysis of chamise and scrub oak, benzenoids and poly aromatic hydrocarbons (PAHs) are the main constituents of tar from co-pyrolysis of chamise and scrub oak blends. Tar from chamise contains higher concentrations of aromatics compared to scrub oak. It was observed that increasing β (mass fraction of chamise) in the biomass blend yielded tar with higher overall concentration of aromatics.

Pyridine, phenol, phenol 2-methyl, phenol 3-methyl, benzofuran 2,3-dihydro, quinoline, fluoranthene, and, 9,10-dihydro-11,12-diacetyl-ethanoanthracene are compounds present in tar collected from chamise, scrub oak and all biomass blends. Acenaphthylene and 3-hydroxy dodecanoic acid are compounds absent in tar from chamise and scrub oak; However, they are detected in tar from all three biomass blends. Hydroquinone, indolizine, 1-heptatriacotanol, and phorbol are compounds that are present in tar from either chamise or scrub oak but are not detected in tar from pyrolysis of their blends. Analysis of tar from biomass blends shows that while phorbol is detected in tar from all biomass blends, hydroquinone, indolizine and 1-heptatriacotanol may be absent in tar from one of the biomass blends. This shows that there are no specific rules on detailed composition of tar compounds from co-pyrolysis of two types of biomass. While tar from biomass blends were very similar to those from chamise and scrub oak, there were some variations in compounds and their concentrations. These variations were minor and were not significant enough to indicate the presence of synergistic effects during pyrolysis processes.

Table 8.3: Detailed classification of aromatic species present in tar from pyrolysis of individual plant samples and their blends (All numbers, with the exception of β, are tar mole %. β is unit-less. ''Ar ''stands for aromatics.)

β	Non-benzenoid Ar	Benzenoid Ar	PAH	Hetero-cyclic Ar
0	2.46%	66.34%	17.90%	0.00%
0.29	2.50%	67.00%	18.20%	0.00%
0.5	2.42%	66.77%	18.46%	1.53%
0.71	2.20%	69.20%	17.70%	1.10%
1	2.08 %	69.90%	20.11%	2.38%

Table 8.4: Detailed classification of non-aromatic species present in tar from pyrolysis of individual plant samples and their blends (All numbers, with the exception of β, are tar mole %. β is unit-less.

β	Cyclo-alkane	Cyclo-alkene	Acid	Alcohol
0	1.37%	7.67%	0.00%	4.25%
0.29	1.10%	7.00%	1.30%	2.90%
0.5	2.00%	6.50%	2.30%	0.00%
0.71	1.20%	6.10%	1.50%	1.00%
1	2.21%	3.32%	0.00%	0.00%

8.4.3 Average Molecular weight of Tar

Table 8.5 lists the average molecular weight of tar from pyrolysis of each plant species and their blends. It contains two columns: Estimated values for average molecular weight and measured values. Estimated values are calculated using equation 8.1, assuming there are no interactions between chamise and scrub oak during their simultaneous pyrolysis. On the other hand, measured values represent the weighted average of mole percentage of each compound detected in tar from biomass blends and their molecular weight. Due to variations in composition of tar due to co-pyrolysis effects, there are some discrepancies between estimated and measured values of molecular weight. However, more experiments need to be conducted to examine possible synergistic effects of co-pyrolysis on tar composition and subsequently, its average molecular weight.

$$1/MW_{blends} = \beta / MW_{chamise} + (1- \beta) /MW_{Scrub\ oak} \quad (8.1)$$

Table 8.5: Average molecular weight (MW) of tar collected from pyrolysis of chamise, scrub oak and their blends

β	MW (estimated)	MW (measured)
0	168.8	168.8
0.29	162.2	162. 8
0.5	157.8	151.52
0.71	153.6	143.4
1	148.1	148.1

8.4.4 Effect of Co-pyrolysis of Biomass on Light Gas Composition

The gas collection system and the analysis method used for light gases were explained more extensively in chapter 4. CO, CO_2, CH_4 and H_2 were the four major gas components generated during pyrolysis of biomass on a wt% daf basis. The concentrations of all major components of the gas phase are presented in Table 8.6 along with the 95% confidence intervals.

Table 8.6: Concentrations (wt%) of all major components of the gas phase collected from pyrolysis of chamise and scrub oak and their blends

β	CO	CO_2	CH_4	H_2
0	62.05 ± 2.03	29.36± 1.43	6.97 ± 1.21	1.62 ± 0.12
0.29	58.59 ± 1.87	31.87 ± 1.86	7.96 ± 2.15	1.58 ± 0.12
0.5	58.38 ± 2.45	31.70 ± 2.27	8.41 ± 1.77	1.51 ± 0.10
0.71	58.70 ± 2.60	31.55 ± 2.70	8.15 ± 2.08	1.60 ± 0.11
1	54.97 ± 1.41	34.78 ± 2.11	8.72 ± 2.05	1.53 ± 0.15

Analysis of light gases from pyrolysis of chamise and scrub oak showed that concentration of CO in light gases from pyrolysis of chamise was significantly different from concentration of CO in gases from scrub oak (p=4.3 × 10^{-6}). Adding chamise to scrub oak and pyrolyzing them simultaneously (β=0.29) resulted in significant variations in the concentration of CO in light gases compared to concentration of CO from pyrolysis of chamise (p=0.0026). Increasing mass of chamise in co-pyrolysis experiments, (β=0.5, β=0.7), yielded light gases with CO concentrations significantly different from that collected during pyrolysis of chamise (p=0.014 and p=0.03 respectively). In other words, since there was a significant difference between chamise and scrub oak in the concentrations of CO in their pyrolysis light gases, adding even small amounts of chamise

to scrub oak during pyrolysis would result in significant variations in the concentrations of CO in light gases from co-pyrolysis compared to CO in light gases from pyrolysis of chamise. The variations in concentration of CO due to changes in β is shown in Figure 8.1.

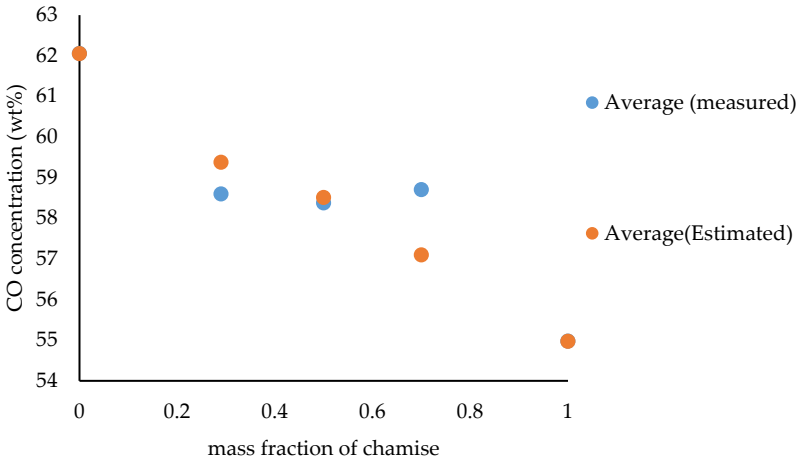

Figure 8.1: Average concentration of CO in gases from co-pyrolysis of chamise and scrub oak

Analysis of light gases from pyrolysis of chamise and scrub oak showed that concentration of CO_2 in light gases from pyrolysis of chamise was significantly different from concentration of CO_2 in gases from scrub oak (p=1.4 × 10^{-4}). Adding small amounts of chamise to scrub oak in the biomass blend (β=0.29) would yield pyrolysis gases with concentrations of CO_2 significantly different from that collected during pyrolysis of chamise (p=0.03). As concentration of chamise in the biomass blend increased, (β=0.5 and β=0.7), significant variations in the concentration of CO_2 in the pyrolysis gases were observed (p=0.04, p=0.047). However, increasing mass of chamise in the biomass blend caused p-value to increase. While there was a statistically significant difference between chamise and scrub oak in the concentration of CO_2 in their pyrolysis gases, adding chamise to the scrub oak would decrease the difference observed in the concentration of CO_2 in the gases from the blend.

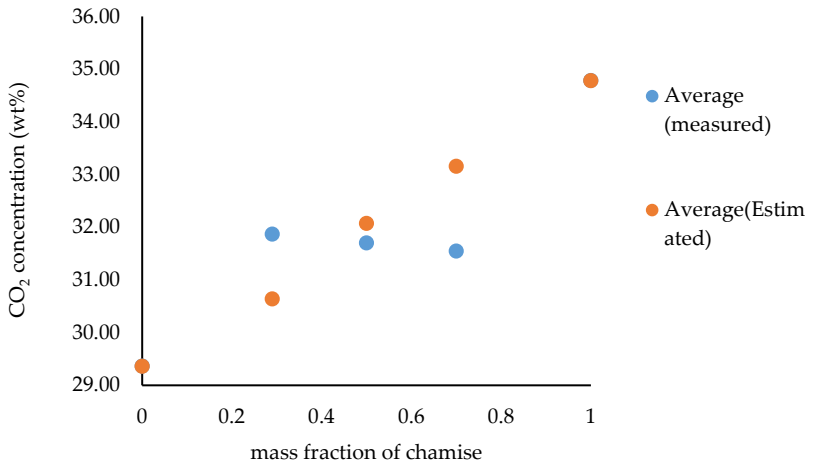

Figure 8.2: Average concentration of CO_2 in gases from co-pyrolysis of chamise and scrub oak

As shown in Figure 8.3, analysis of light gases collected from pyrolysis of chamise and scrub oak showed that there was not a significant difference in the concentration of methane (p=0.11). Adding small amounts chamise (β=0.29) to scrub oak yielded pyrolysis light gases with concentrations of CH_4 that were not significantly different from that released during pyrolysis of chamise (p=0.57). Increasing the amount of chamise in the blend during pyrolysis (β=0.5 and β=0.7) did not cause significant variations in the concentration of methane present in light gases (p= 0.8 and p=0.67 respectively).

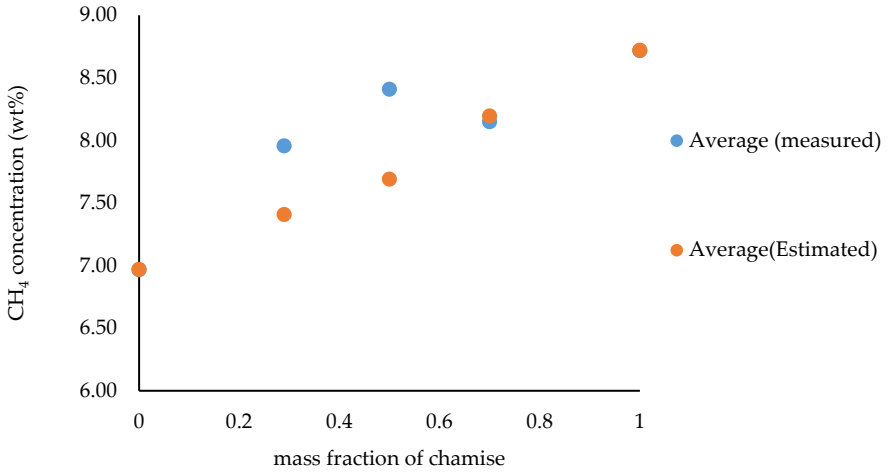

Figure 8.3: Average concentration of CH_4 in gases from co-pyrolysis of chamise and scrub oak

Analysis of light gases from pyrolysis of chamise and scrub oak showed that concentration of H_2 did not vary due to the species type and there was no significant difference in the concentration of H_2 in light gases from pyrolysis of chamise and scrub oak (p=0.29). Further analysis revealed that adding scrub oak to chamise did not cause any significant difference in the concentration of H_2 in light gases compared to the concentration of H_2 in gases from individual pyrolysis of chamise. As seen in Figure 8.4, during co-pyrolysis of chamise and scrub oak, adding smaller amounts of chamise to the blend, (β=0.29, β=0.5, β=0.7), did not result in any fluctuations in the concentration of H_2 (p=0.52, p=0.88, p=0.37 respectively).

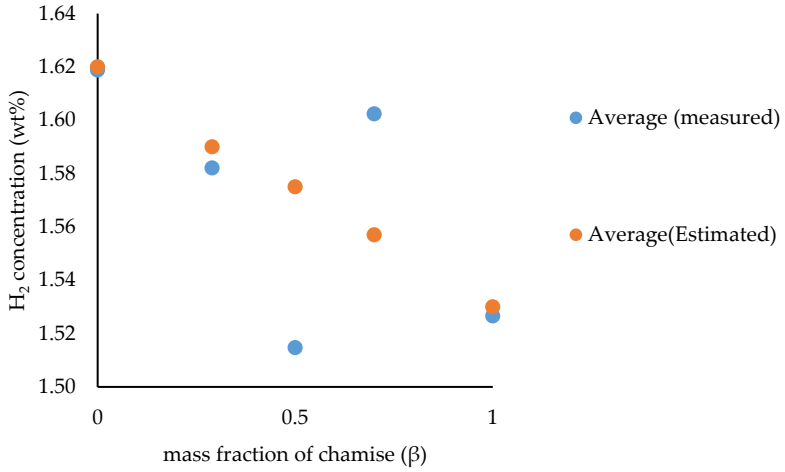

Figure 8.4: Average concentration of H_2 in gases from co-pyrolysis of chamise and scrub oak

8.4.5 Mechanism of Synergistic Effects

Synergistic effects during simultaneous pyrolysis of two (or more) types of biomass are observed when interactions between compounds (or intermediates) involved in pyrolysis mechanisms result in at least one of the following outcomes:

- Interactions during co-pyrolysis reactions may generate compounds which are not present in products of individual pyrolysis of each biomass or some of the compounds generated during individual pyrolysis of each biomass may be absent from the composition of co-pyrolysis products.
- Additive interactions during simultaneous pyrolysis of two or more types of biomass may result in final concentrations for some compounds that deviate from arithmetic average concentrations generated by the individual pyrolysis reactions.

If any of the above interactions occur during co-pyrolysis of two types of fuels, the yield of pyrolysis products (tar, light gases, and char) generated during co-pyrolysis of biomass blends would differ than the arithmetic average of the yields of products produced from individual pyrolysis of each biomass.

Synergistic effects observed during co-pyrolysis of two or more types of fuels may be due to several factors such as radical interactions, introduction of novel intermediates compounds from one of the fuel sources (such as water from biomass), and enhancement of other pathways and reactions that may have not been possible if the other type of fuel was not introduced (H donation by biomass to other types of fuel with lower concentrations of hydrogen in their structure) (Zhang et al., 2007; Johannes et al., 2013; Liu et al., 2013).

If the two types of fuel blending during co-pyrolysis are very different, such as coal and biomass or biomass and polymers, the synergistic effects will be more pronounced. This may be due to inherent differences in pathways, reactions and compounds involved in the pyrolysis of coal, biomass, and polymers. Pyrolysis of two similar fuels, such as two plant species or two polymers occurs through a series of similar reactions and pathways; however, when the two types of pyrolyzing fuels are very different, the reactions and compounds involved in their pyrolysis may be significantly different thus enhancing synergistic effects (Ren et al., 2009; Fei et al., 2012).

Hydrogen donation from biomass (due to higher ratios of H/C in biomass compared to some types of fuels) may cause synergistic effects during co-pyrolysis of biomass and other fuel types. Liu et al. (2013) studied the co-pyrolysis of fir sawdust and waste electrical and electronic equipment (WEEE) at 773 K. They reported a significant increase in the tar yield during the co-pyrolysis process which they attributed to hydrogen donation from biomass. Zhang et al. (2007) suggested that water, released in higher concentrations from biomass, may promote tar cracking during simultaneous pyrolysis of WEEE and biomass.

Another possible explanation for significant differences observed during co-pyrolysis of biomass and polymers compared to their individual pyrolysis may be different pathways and reactions through which each of these fuels decompose. Biomass pyrolysis occurs through a series of exothermic and endothermic reactions, whereas for polymers, radical mechanism (initiation, propagation, and termination) is usually responsible for pyrolysis (Abnisa and Daud, 2014). Jakab et al. (Jakab et al., 2000; Jakab et al., 2001) suggested that lower thermal stability of biomass may result in generation of radicals that promote thermal degradation of plastics. Sun et al. (2013) investigated the simultaneous pyrolysis of poplar wood and high-density polyethylene (HDPE) in a micro-scale reactor.

They came to similar conclusions as Jakab et al. (Jakab et al., 2000; Jakab et al., 2001) suggesting that free radicals formed during biomass pyrolysis facilitate plastic decomposition, generating lighter paraffins.

8.5 Conclusion

Simultaneous pyrolysis of chamise and scrub oak was studied in this chapter. Three blends of chamise and scrub oak were prepared and pyrolyzed in the flat flame burner. The possible effect of mixing two different types of foliage on the yields of pyrolysis products, tar and light gases, and their composition was investigated. The main findings are:

Tar yield collected from co-pyrolysis of chamise and scrub oak was slightly higher than the estimated values. Estimated values for tar yield were calculated based on the weighted averages of tar yields from individual pyrolysis of chamise and scrub oak. Since chamise had generated higher amounts of tar compared to scrub oak, it was expected that adding chamise to scrub oak would increase tar yield. While the recorded values for tar from co-pyrolysis of chamise and scrub oak were consistent with this theory, the deviations observed during co-pyrolysis experiments were not significant enough to suggest the presence of substantial synergistic effects.

The yields of light gases from co-pyrolysis of chamise and scrub oak were slightly lower than the estimated values. The estimated values for light gases from co-pyrolysis of chamise and scrub oak were calculated in the same manner as the estimated values for tar. Since chamise had lower gas yields compared to scrub oak, it was expected that adding chamise to scrub oak would lower gas yields. This was consistent with experiment results. However, the decrease in gas yields during co-pyrolysis experiments was not significant, suggesting slight synergistic effects.

The total yield of volatiles (tar and light gases combined) was not significantly affected due to co-pyrolysis of the two species. Overall, no synergetic effects from co-pyrolysis of chamise and scrub oak on pyrolysis product yields were reported.

Composition of tar from biomass blends was very similar to that collected from individual pyrolysis of chamise and scrub oak, with slight variations in compounds and their concentration in tar. Benzenoids and poly aromatic hydrocarbons (PAHs) were the main constituents of tar from co-pyrolysis of chamise and scrub oak blends. Tar from chamise contained higher concentrations of aromatics compared to scrub oak. Increasing β (mass fraction of chamise) in the biomass blend was associated with higher amounts of aromatics in tar. While majority of compounds detected in tar from blends were also present in tar from individual pyrolysis of each biomass, tar from blends contained compounds, such as acenaphthylene and 3-hydroxy dodecanoic acid, that were absent in tar from individual

pyrolysis of chamise and scrub oak. These variations are minor and are not significant enough to suggest the presence of synergistic effects during pyrolysis processes.

CO, CO_2, CH_4, and H_2 were the four major gas components generated during pyrolysis of biomass. This was consistent with observations from pyrolysis of individual samples of chamise and scrub oak. Analysis of light gases from pyrolysis of chamise, scrub oak and their blends revealed that in the cases of compounds such as H_2 and methane that there were no significant differences between the two species in the concentration of these two compounds in their light gases, no synergistic effect was observed during co-pyrolysis experiments. For compounds such as CO and CO_2, which there were significant differences between chamise and scrub oak, adding chamise to scrub oak would result in blends which still generate light gases that contain concentrations of CO and CO_2 that are statistically different from those released from pyrolysis of chamise or scrub oak. However, as mass fraction of chamise in the blend increased, the difference became less significant as *p*-value increased.

9 Analysis of Tars from a Flame above a Moving Pine Needle Bed

9.1 Introduction

This chapter describes the chemical composition of condensable compounds sampled from within and above flames resembling wildland fires. Samples were taken from three regions of a flame: (1) near the base of the flame, (2) in the intermittent pulsating flame region near the tip of the flame, and (3) in the flame-free plume region immediately above the fire. The goal of these experiments was to have a better understanding of how the composition of gases in the interior of the flame changes with temperature and residence time in the flame. This chapter describes the tar sampling portion of the experiments; sampling of light gases and temperature measurement were performed by colleagues and was reported separately (Weise et al., 2026).

9.2 Materials and Methods

The setup used during these experiments is described in Chapter 4.

9.3 Results and Discussions

Quantitative tar yields were not measured, although the largest amount of tar was collected at the flame base, followed by tar from the intermittent region. The amount of tar collected in the plume region was negligible.

The concentration of compounds in tar samples collected from the plume were so low that identification and further quantitative comparison of these compounds was not possible. Phenol was the only identifiable chemical present in the tar samples from the plume.

The full tar analysis for each sampling height in the flame is given in Tables A7-A8 in the Appendix. The fraction of aromatic species detected is shown in Figure 9.2 for the flame base and intermittent region. The tar from the flame base had 79.6% aromatic species as opposed to 29.0% for the intermittent region. In the absence of O_2 and as the gas temperature increases, one would expect the tar to either (a) polymerize to form higher molecular weight compounds, eventually forming soot, or (b) crack to form lower molecular weight compounds. However, in the intermittent region, it is likely that oxygen is in contact with the pyrolysis products, and oxidation of these pyrolysis products would occur. The lower aromatic

content of the tars from this analysis indicates that either the aromatic tars were cracked or oxidized preferentially to non-aromatic species, or that the tars formed aromatic species that were of higher molecular weight than could be analyzed in the GC/MS system.

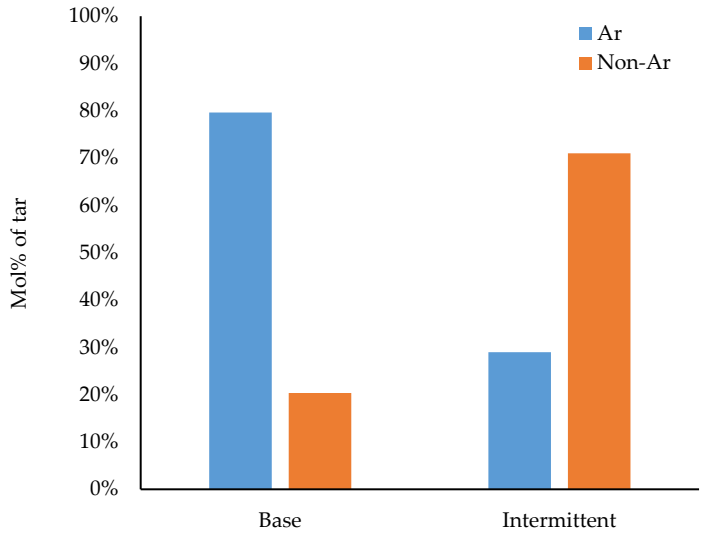

Figure 9.2: Percentage of aromatic compounds vs. non-aromatic compounds at different sample collection regions.

Figure 9.3 also shows the distribution of non-aromatic compounds detected in the tar. The major non-aromatic tar species detected at the flame base were cyclo-alkanes, cyclo-alkenes, and ketones. However, in the intermittent region alcohols, aldehydes, alkanes, cyclo-alkanes, cyclo-alkenes, and ketones were detected. These non-aromatic compounds had high molecular weights, as indicated in Tables A7-A8. (Tables A7 and A8 are provided in the Appendix). The long chains observed in the non-aromatic compounds were indicative of either large primary pyrolysis products or polymerization of pyrolysis products. The presence of these non-aromatic compounds in the intermittent region but not in the base region seems to indicate that these compounds were formed from secondary reactions of primary pyrolysis products. However, this argument would be stronger if actual tar yields were available.

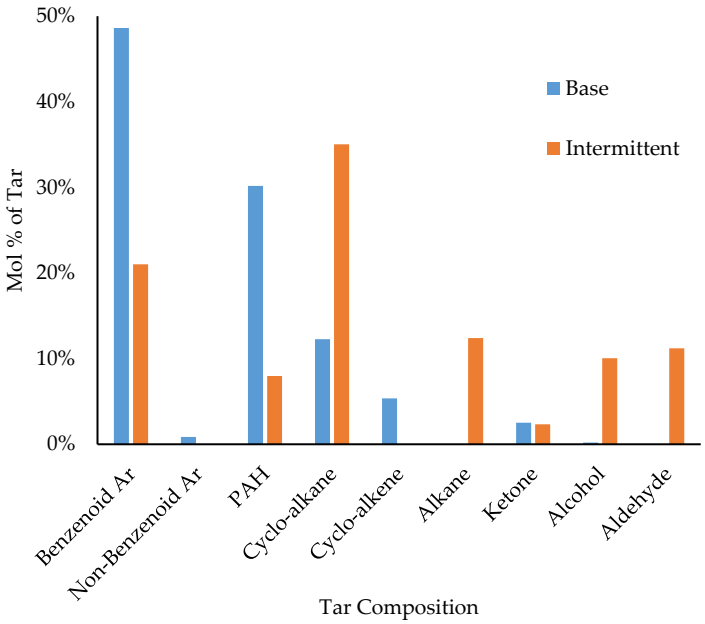

Figure 9.3: Distribution of functional groups in the tar samples obtained from the base and intermittent regions. "Ar" stands for aromatic.

Tar samples collected in the base region were rich in phenolic compounds. Following the general trend of decrease in concentration of aromatic compounds as sampling height increases, mole% of phenolic compounds decreased as the sampling height increased. Concentration of cyclic compounds (cyclo-alkanes and cyclo-alkenes) was higher in samples from the intermittent region compared to the base region. The increase in the concentration of cyclic compounds may be due to the oxidation of aromatic compounds. On the other hand, concentration of high molecular weight aldehydes, alkanes and alcohols was higher in samples from the intermittent region compared to the base samples. This could be due to the degradation of aromatics and cyclic compounds that may have been formed during pyrolysis reactions at the flame base.

Figure 9.4 shows that the concentration of 1-ring aromatic compounds is much higher in samples collected from the flame base compared to samples collected from intermittent region. A similar trend is seen for two-ring and three-ring aromatic compounds. This may be explained by degradation of aromatic compounds as height increases and the possibility of the presence of O_2 in the sampling region increases. Oxidation of aromatic compounds may result in ring-opening of multi-ring aromatic compounds and further production of single-ring aromatic compounds or non-aromatics.

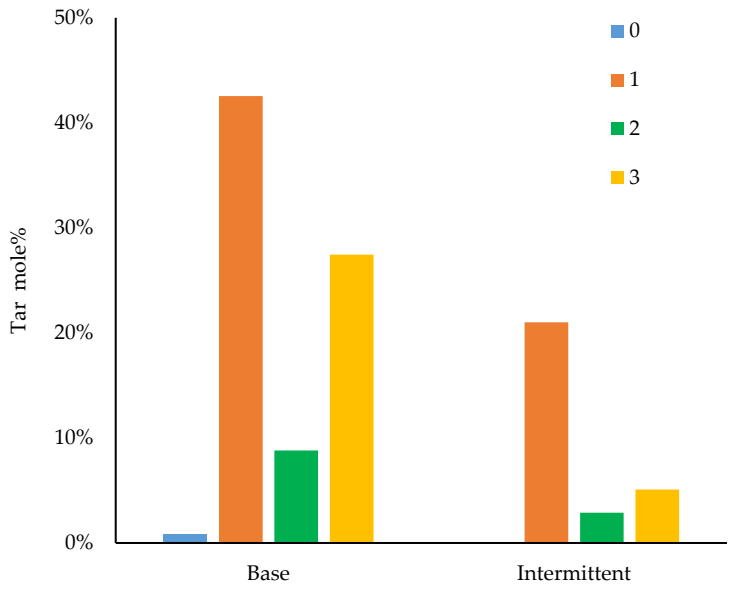

Figure 9.4: Mole percentage of aromatic tar compounds based on the number of rings.

Tar samples from both the base and intermittent regions were rich in oxygenated compounds since the fuel source is rich in oxygen. As seen in Fig. 9.5, increasing sampling height results in a higher concentration of oxygenated compounds. This phenomenon may be due to higher concentration of O_2 present at increased sampling heights.

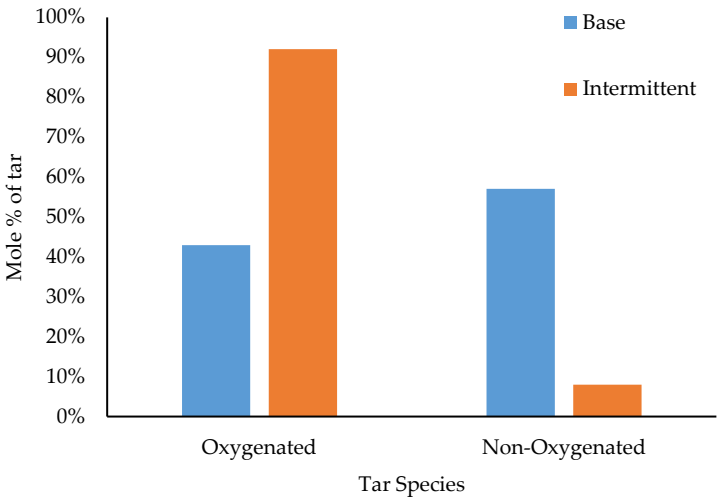

Figure 9.5: Concentration of oxygenated vs. non-oxygenated compounds observed in the Base and intermittent regions.

The average molecular weight of the tar from the flame base was 175.9 g/mol while the average molecular weight of compounds in the intermittent region was 284.2 g/mol. The average molecular formula for tar samples from the flame base was $C_{12.3}H_{12.4}O_{0.9}N_{0.09}$ while samples from the intermittent region had a molecular formula of $C_{18.3}H_{31.3}O_{1.7}N_{0.25}$.

9.4 Discussion

The interpretation of the results was hampered because quantitative tar yield was not measured during the experiment. However, observations of the glass wool in the tar trap indicated that tar yield decreased as sampling height increased. This result was expected, since tar is known to decompose at elevated temperatures and burn if O_2 is present in that region of the flame. The effect of temperature on tar yield has been studied relatively extensively. Several studies have reported that tar yield decreases as pyrolysis temperature increases. Lewis and Fletcher (2013) investigated the changes in the tar yield during sawdust pyrolysis as temperature increased. Their results showed that tar yield started to decrease as temperature increased beyond 500°C. Xiao and Yang (2013) showed that tar yield from pyrolysis of rice straw reached a maximum at around 500°C and started to decrease beyond that due to degradation. Scott et. al. (1985) found that tar yield during pyrolysis of aspen-polar wood started to decrease at around 500°C. Zhang et. al. (2006) studied tar yield resulting from rapid pyrolysis of Hinoki cypress sawdust over a relatively large temperature range (600°C-1400°C) and found that tar yield decreased as temperature increased. While the temperature at which tar yield reaches a maximum varies slightly with heating rate and type of biomass, reported tar yields always decrease with increasing gas temperature after that maximum point (Fagbemi et al., 2001; Gilbert et al., 2009; Zhang et al., 2010). The increasing temperature with sampling height in a flame partially explains why the observed tar yield in this experiment decreases as the sampling height changes from the base to the intermittent and plume region.

The low concentration of compounds found in samples from the plume region made identification and quantification of these chemicals unfeasible. This observation may be explained due to the higher presence of O_2 present in the plume region. Presence of O_2 will result in oxidative combustion of tar compounds causing a significant drop in concentration of these compounds as sample collection height increases from base to intermittent and subsequent plume region. Soot formation resulting from secondary tar compounds during biomass pyrolysis has been reported by Wang et. al (2018). Plume region tar is consumed and is converted to smoke/soot. The soot and smoke are not dissolvable and hence their composition was not analyzed as part of this study.

Quantitative analysis of tar samples revealed that 79.6% of the identified compounds in the base region were aromatic while only 29.0% of the tar species observed in the intermittent region were aromatic. The concentration of aromatic compounds decreased significantly as the concentration of non-aromatics increased. These non-aromatic compounds were high molecular weight ketones, aldehydes and cyclic compounds. There might be more than one explanation for this observation. First, degradation (e.g., dehydrogenation) of aromatic compounds present in tar at the base of the flame may result in formation of cyclic compounds. These cyclic compounds may be involved in further ring-opening reactions and form aliphatic compounds. A second possibility is that tar compounds may polymerize and form high molecular weight compounds that may not be detected by GC/MS, resulting in PAH and soot. Studying tar compounds present in samples collected from the base region of the flame in the current experiment showed that benzenoids and PAHs were the major constituents followed by non-aromatic compounds such as cyclo-alkanes and cyclo-alkenes, and ketones. This observation suggests that the tar species detected in the base region were associated with both primary and secondary pyrolysis. The small amount of aromatic compounds detected in the intermittent region seems to indicate that ring-opening reactions occurred, transforming aromatic species into ketones and aldehydes.

The average molecular formula for tar species detected in the samples collected from the flame base was $C_{12.3}H_{12.4}O_{0.9}N_{0.09}$ while samples from the intermittent region had a molecular formula of $C_{18.3}H_{31.34}O_{1.7}N_{0.25}$. Note the increase of carbon from 12.3 to 18.3, and the large increase in hydrogen from 12.4 to 31.34. Analysis of compounds present in samples from base and intermittent region shows that as sampling height increases, concentration of aromatics decreases. A closer look at the changes in the concentrations of multi-ring aromatic compounds present at various heights of flame reveals that as sampling height increases from base to intermittent region, concentration of three-ring and two-ring aromatic compounds decreased. This observation, along with decreasing concentration of aromatics as sampling height increased, suggests that aromatic compounds present in the base region may be involved in degradation and ring-opening reactions and then polymerize to form high molecular weight non-aromatic compounds such as alkanes, cyclic and aliphatic compounds. Comparing the average molecular weight of the non-aromatic fraction of tar extracted from base and intermittent region confirms this theory since the average molecular weight of tar compounds from the intermittent region was higher compared to the average molecular weight of tar from the base region.

9.5 Summary and Conclusion

Tar samples were obtained at three different heights in a stationary flame above a pine needle bed. A conveyor belt system permitted the flame to be stationary with respect to the probe location. This experimental setup was more similar to actual wildland fire conditions than controlled lab environments used in most research. Unfortunately, quantitative measurements of tar yields based on the mass release of pyrolysis products were not possible in this experiment. However, qualitative observations indicated that the tar yield from the base region was greater than from the intermittent region at the tip of the flame, and that tar yield was negligible in the plume region above the flame.

The qualitative decrease in tar yield was consistent with secondary reactions of tar as flame temperature increased from the flame base to the intermittent region. The concentration of aromatic compounds also decreased as sampling height increased due to (a) PAH and soot formation or (b) combustion due to increasing levels of O_2 at increased heights. The average molecular weight of tar compounds found in the intermittent region was higher than for compounds present in the base region. The decrease in the amount of aromatic compounds along with the increase in average molecular weight suggests that pyrolysis products detected in the base region may be involved in ring-opening reactions and later form heavy molecular weight non-aromatic compounds. An increase in the concentration of oxygenated compounds was also observed as height increased, consistent with increasing amounts of O_2 as sampling height increased. These findings help understand how pyrolyzed tars from wildland fuels behave in fires.

10 Summary and Conclusions

In this project, pyrolysis of plant samples from three regions- southern California and northern Utah (at 725 °C), and southeastern U.S. (at 765 °C) and 180 °C/s were studied. The effect of species type on characteristics of pyrolysis products, tar and light gases, was investigated. Also tar compounds in flames above a moving pine needle were analyzed.

The total yield of volatiles released from selected southeastern U.S. samples ranged from 78.0 ± 5.0 wt% (daf) in wax myrtle to 83.0 ± 6.6 wt% (daf) in yaupon. Northern Utah plants yielded between 80.0 ± 5.0 wt% (daf) to 82.0 ± 11.5 wt% (daf) of volatile compounds while southern California samples generated between 75.0 to 82.0 wt% (daf).

Tar obtained from southeastern U.S. samples varied from 53.0 ± 2.5 wt% (saw palmetto) to 62.0 ± 5.0 wt% (dwarf palmetto) while the yield of light gases changed respectively. Tar yield ranged from 53.0 ± 5.0 wt % (Gambel oak) to 58.0 ± 6.6 wt % (Bigtooth maple) for northern Utah samples while southern California samples exposed to similar pyrolysis conditions yielded between 48 wt % (manzanita twigs) to 59 wt % (chamise twigs with leaves) tar. The slight disparities in the tar yield of plants from different U.S. regions (southeastern U.S., northern Utah, and southern California) is likely due to inherent chemical and physical differences between various plant species. Tar from pyrolysis of plants during wildfires can be estimated to be between 48 wt% to 62 wt% of the plant.

Light gases released from southeastern U.S. samples ranged from 18.0 ± 5.0 wt% (dwarf palmetto) to 25.0 ± 5.0 wt% (saw palmetto) while the range of light gases from northern Utah species varied from 23.0 ± 5.0 wt% (bigtooth maple) to 29.0 ± 2.5 wt% (Gambel oak). Southern California samples generated approximately 23 wt% (chamise twig) to 31 wt% (hoaryleaf ceanothus). The overall yield of light gases from pyrolysis of plants in these experiments ranged from 18 wt% to 31 wt% of the plant.

Analysis of tar samples from southern California and northern Utah species showed, with the exception of Eastwood's manzanita, the majority of tar compounds were aromatics. Cycloalkenes were the major constituents of tar from Eastwood's manzanita. Among aromatics, benzenoids, especially phenol, were the most abundant tar compound from southern California species. The other primary tar compounds were 2-methyl phenol, 3-methyl phenol, 4-ethyl-2-methoxy phenol (4-ethyl guaiacol), 2,3- dihydro benzofuran, and 9,10-dihydro-11,12-diacetyl- 9,10-ethanoanthracene. Analysis of tar samples from Utah species, with the exception of Utah juniper, showed the primary compounds were PAHs.

The most abundant tar compounds in Utah samples were fluoranthene, 2-phenyl naphthalene, 3-methyl phenol, phenol, anthracene, and coumarin. Since operating conditions were the same during pyrolysis of southern California and northern Utah samples, the differences observed in their tar composition may be due to variations in ratios of major biopolymers (cellulose, hemicellulose and lignin) in biomass. As the concentration of benzenoids in tar decreased, concentration of PAHs increased.

The potential effect of foliage on pyrolysis of chamise samples was studied to investigate possible disparities in tar compounds and their concentration due to the presence of leaves. No significant differences were observed in the aromatic content of tar collected from chamise samples due to presence of foliage. Similar results were obtained from pyrolysis of Eastwood's manzanita foliage and twigs.

It was determined that CO, CO_2, CH_4 and H_2 were the major components of pyrolysis gases on a wt% dry, ash-free basis. CO was the main constituent of the pyrolysis gases followed by CO_2, CH_4 and H_2 on a wt% dry, ash-free basis. Analysis of tar from southern California samples showed that concentration of CO, CO_2 and H_2 in light gases depended on the species type while there was no statistically significant difference in the concentration of CH_4. For norther Utah samples, concentrations of CO, CH_4 and H_2 varied significantly due to species type. CO_2 was the only gas component with moderate changes in its concentration due to species type. This showed that in general, the concentration of major gas components may change due to species type as the ratios of major biopolymers in the biomass affect the composition of light gases. There was no difference in the concentration of major components of light gases between foliage and twigs of Eastwood's manzanita. For chamise samples, there was no difference in the composition of gases due to presence of foliage. This could be explained due to small differences in the ratios of major biopolymers composition of twigs and foliage belonging to the same plant species.

High heating values (HHV) for tar, light gases, and total volatiles released during pyrolysis of southern California and northern Utah samples were calculated for each plant species. The estimated values for HHV varied between approximately 19.37 to 23.68 MJ/kg of dry volatiles. Tar contribution to high heating value of volatiles was calculated and it was estimated that tar accounted between 81.99% (Eastwood's manzanita foliage) to 87.2% (chamise foliage) to HHV of volatiles. This shows the importance of tar analysis as better understanding of tar composition would lead to more precise estimations of its HHV and tar contribution to wildfires.

Simultaneous pyrolysis of chamise and scrub oak was studied in this project. The possible effect of mixing two different types of foliage on the yields of pyrolysis products, tar and light gases, and their composition was

investigated. The main findings are: No synergistic effects on the yields of tar and light gases due to co-pyrolysis of chamise and scrub oak were observed. Composition of tar from biomass blends was very similar to that collected from individual pyrolysis of chamise and scrub oak, with slight variations in compounds and their concentration in tar.

Tar yield collected from co-pyrolysis of chamise and scrub oak was slightly higher than the estimated values. Estimated values for tar yield were calculated based on the weighted averages of tar yields from individual pyrolysis of chamise and scrub oak. Since chamise had generated higher amounts of tar compared to scrub oak, it was expected that adding chamise to scrub oak would increase tar yield. While the recorded values for tar from co-pyrolysis of chamise and scrub oak were consistent with this theory, the deviations observed during co-pyrolysis experiments were not significant enough to suggest the presence of substantial synergistic effects.

The yields of light gases from co-pyrolysis of chamise and scrub oak were slightly lower than the estimated values. The estimated values for light gases from co-pyrolysis of chamise and scrub oak were calculated in the same manner as the estimated values for tar. Since chamise had lower gas yields compared to scrub oak, it was expected that adding chamise to scrub oak would lower gas yields. This was consistent with experiment results. However, the reduction in gas yields during co-pyrolysis experiments was not significant, suggesting slight synergistic effects.

The total yield of volatiles (tar and light gases combined) was not significantly affected due to co-pyrolysis of the two species. Overall, no synergetic effects from co-pyrolysis of chamise and scrub oak on pyrolysis product yields were reported.

Composition of tar from biomass blends was very similar to that collected from individual pyrolysis of chamise and scrub oak, with slight variations in compounds and their concentration in tar. Benzenoids and poly aromatic hydrocarbons (PAHs) were the main constituents of tar from co-pyrolysis of chamise and scrub oak blends. While majority of compounds detected in tar from blends were also present in tar from individual pyrolysis of each biomass, tar from blends contained compounds, such as acenaphthylene and 3-hydroxy dodecanoic acid, that were absent in tar from individual pyrolysis of chamise and scrub oak. These variations are minor and are not significant enough to suggest the presence of synergistic effects during pyrolysis processes. Analysis of light gases from pyrolysis of chamise, scrub oak and their blends revealed that in the cases of compounds such as H_2 and methane that there were no significant differences between the two plant species in the concentration of these two compounds, no synergistic effect was observed during co-pyrolysis experiments. For compounds such as CO and CO_2, which there

were significant differences between chamise and scrub oak, adding chamise to scrub oak would result in blends which generate light gases that contain concentrations of CO and CO_2 that are significantly different from those released during pyrolysis of chamise or scrub oak.

Analysis of tar samples from various flame heights revealed that tar yield and the concentration of its compounds decreased as the sampling height from flame base increased. Although tar yield was not measured during these experiments, the qualitative decrease in tar yield was consistent with secondary reactions of tar. This could be due to increase in flame temperature as the sampling height increased from flame base to the intermittent region. The concentration of aromatic compounds also decreased as sampling height increased due to (a) PAH and soot formation or (b) combustion due to increasing levels of O_2 at increased heights. The average molecular weight of tar compounds found in the intermittent region was higher than for compounds present in the base region. The decrease in the mole percentage of aromatic compounds in tar along with the increase in average molecular weight suggested that pyrolysis products detected in the base region may be involved in ring-opening reactions and later form heavy molecular weight non-aromatic compounds. An increase in the concentration of oxygenated compounds was also observed as height increased, consistent with increasing amounts of O_2 as sampling height increased. These findings help understand how pyrolyzed tars from wildland fuels behave in fires.

Reversed-phase HPLC with a C18 column and a water/acetonitrile gradient mobile phase was used to separate and detect both light and heavy portions of tar released during pyrolysis of longleaf pine litter and Utah juniper. It was observed that tar from longleaf pine litter had a higher proportion of heavy molecular weight tar compounds compared to Utah juniper.

A list of recommendations for future research on pyrolysis of plants is provided below:

- Measuring the weight fractions of major constituents of various plant species such as cellulose, hemicellulose, lignin, and extractives and looking for possible correlations between these weight fractions and the yields of pyrolysis products.
- Measuring the weight fractions of hemicellulose, lignin, and extractives and investigating correlations between these fractions and major constituents of tar and light gases
- Using standards for major tar compounds such as phenol, 2-methyl phenol, 2,3- dihydro benzofuran, fluoranthene, 2-phenyl naphthalene, anthracene, and coumarin to measure the concentration of each of these compounds in tar and correlating these concentrations to the initial mass of the biomass.

- Correlating the concentration of major tar compounds to the concentration of major gas compounds after combustion
- Conducting the experiments under various pyrolysis temperatures and investigating variations in concentration of major tar compounds and combustion products
- Using weight fractions of cellulose, hemicellulose, lignin, and extractives to tie biomass composition to a model that predicts fire spread and soot formation.

11 References

Abiven, S., A. Heim and M. W. I. Schmidt, "Lignin Content and Chemical Characteristics in Maize and Wheat Vary Between Plant Organs and Growth Stages: Consequences for Assessing Lignin Dynamics in Soil," *Plant and Soil,* **343**(1), 369-378 (2011).

Abnisa, F. and W. M. A. W. Daud, "A review on co-pyrolysis of biomass: an optional technique to obtain a high-grade pyrolysis oil," *Energy conversion and management,* **87**, 71-85 (2014).

Alizadeh, M., D. R. Weise and T. H. Fletcher, "Characteristics of Pyrolysis Products of California Chaparral and Their Potential Effect on Wildland Fires," *Fire,* **7**(8), 271 (2024).

Alizadeh, M. and T. H. Fletcher, "Pyrolysis of Foliage from 24 US Plant Species with Recommendations for Physics-Based Wildland Fire Models," *Fire,* **8**(11), 424 (2025).

Amini, E., "Characterization of Slow Pyrolysis Behavior of Live and Dead Vegetation," Ph.D. Dissertation, Chemical Engineering Department, Brigham Young University (2020).

Ansari, K. B., J. S. Arora, J. W. Chew, P. J. Dauenhauer and S. H. Mushrif, "Fast Pyrolysis of Cellulose, Hemicellulose, and Lignin: Effect of Operating Temperature on Bio-oil Yield and Composition and Insights into the Intrinsic Pyrolysis Chemistry," *Industrial & Engineering Chemistry Research,* **58**(35), 15838-15852 (2019).

Antal, M. J. and M. Grønli, "The art, science, and technology of charcoal production," *Industrial & engineering chemistry research,* **42**(8), 1619-1640 (2003).

Apicella, B., C. Russo, F. Cerciello, F. Stanzione, A. Ciajolo, V. Scherer and O. Senneca, "Insights on the Role of Primary and Secondary Tar Reactions in Soot Inception During Fast Pyrolysis of Coal," *Fuel,* **275**, 117957 (2020).

Bai, X., P. Johnston and R. C. Brown, "An Experimental Study of the Competing Processes of Evaporation and Polymerization of Levoglucosan in Cellulose Pyrolysis," *Journal of Analytical and Applied Pyrolysis,* **99**, 130-136 (2013).

Biagini, E. and L. Tognotti, "A Generalized Procedure for the Devolatilization of Biomass Fuels Based on the Chemical Components," *Energy & Fuels,* **28**(1), 614-623 (2014).

Boon, J. J., R. G. Wetzel and G. L. Godshalk, "Pyrolysis mass spectrometry of some Scirpus species and their decomposition products," *Limnology and Oceanography,* **27**(5), 839-848 (1982).

Brebu, M. and C. Vasile, "Thermal degradation of lignin—a review," *Cellulose Chemistry & Technology,* **44**(9), 353 (2010).

Burra, K. and A. Gupta, "Kinetics of Synergistic Effects in Co-pyrolysis of Biomass with Plastic Wastes," *Applied Energy,* **220**, 408-418 (2018).

Butler, B., J. Cohen, D. Latham, R. Schuette, P. Sopko, K. Shannon, D. Jimenez and L. Bradshaw, "Measurements of Radiant Emissive Power and Temperatures in Crown Fires," *Canadian Journal of Forest Research,* **34**(8), 1577-1587 (2004).

Caballero, J., R. Front, A. Marcilla and J. Conesa, "Characterization of Sewage Sludges by Primary and Secondary Pyrolysis," *Journal of Analytical and Applied Pyrolysis,* **40**, 433-450 (1997).

Cao, Q., X. Xie, J. Li, J. Dong and L. e. Jin, "A Novel Method for Removing Quinoline Insolubles and Ash in Coal Tar Pitch Using Electrostatic Fields," *Fuel,* **96**, 314-318 (2012).

City of Glendale, C., "Scrub Oak,," https://www.glendaleca.gov/government/departments/public-works/indigenous-tree-program/scrub-oak

Collard, F.-X. and J. Blin, "A review on pyrolysis of biomass constituents: Mechanisms and composition of the products obtained from the conversion of cellulose, hemicelluloses and lignin," *Renewable and sustainable energy reviews,* **38**, 594-608 (2014).

Collin, A., D. Bernardin and O. Sero-Guillaume, "A physical-based cellular automaton model for forest-fire propagation," *Combustion science and technology,* **183**(4), 347-369 (2011).

Colman, J. J. and R. R. Linn, "Separating combustion from pyrolysis in HIGRAD/FIRETEC," *International Journal of Wildland Fire,* **16**(4), 493-502 (2007).

Cruz, M. G., N. P. Cheney, J. S. Gould, W. L. McCaw, M. Kilinc and A. L. Sullivan, "An empirical-based model for predicting the forward spread rate of wildfires in eucalypt forests," *International Journal of Wildland Fire,* **31**(1), 81-95 (2021).

Debono, O. and A. Villot, "Nitrogen Products and Reaction Pathway of Nitrogen Compounds During the Pyrolysis of Various Organic Wastes," *Journal of Analytical and Applied Pyrolysis,* **114**, 222-234 (2015).

Demirbas, A., "Effect of Temperature on Pyrolysis Products from Biomass," *Energy Sources, Part A: Recovery, Utilization, and Environmental Effects,* **29**(4), 329-336 (2007).

Di Blasi, C., "Modeling chemical and physical processes of wood and biomass pyrolysis," *Progress in energy and combustion science,* **34**(1), 47-90 (2008).

Di Blasi, C., C. Branca, F. Sarnataro and A. Gallo, "Thermal runaway in the pyrolysis of some lignocellulosic biomasses," *Energy & fuels,* **28**(4), 2684-2696 (2014).

Dietenberger, M. A., C. R. Boardman and D. R. Weise, "New Methods for Pyrolysis and Combustion Properties of Forest Litter: Enhanced Cone Calorimetry with Longleaf Pine Needles," *In: Hood, Sharon M.; Drury, Stacy; Steelman, Toddi; Steffens, Ron,[eds.]. Proceedings of the Fire Continuum-Preparing for the Future of Wildland Fire; 2018 May 21-24; Missoula, MT. Proceedings RMRS-P-78. Fort Collins, CO: US Department of Agriculture, Forest Service, Rocky Mountain Research Station. p. 72-83.,* **78**, 72-83 (2020).

Dufour, A., P. Girods, E. Masson, Y. Rogaume and A. Zoulalian, "Synthesis Gas Production by Biomass Pyrolysis: Effect of Reactor Temperature on Product Distribution," *International Journal of Hydrogen Energy,* **34**(4), 1726-1734 (2009).

Esso, S. B. E., Z. Xiong, W. Chaiwat, M. F. Kamara, X. Longfei, J. Xu, J. Ebako, L. Jiang, S. Su and S. Hu, "Review on Synergistic Effects During Co-pyrolysis of Biomass and Plastic Waste: Significance of Operating Conditions and Interaction mechanism," *Biomass and Bioenergy,* **159**, 106415 (2022).

Evans, R. J. and T. A. Milne, "Molecular characterization of the pyrolysis of biomass. 2. Applications," *Energy & fuels,* **1**(4), 311-319 (1987).

Fagbemi, L., L. Khezami and R. Capart, "Pyrolysis Products from Different Biomasses: Application to the Thermal Cracking of Tar," *Applied Energy,* **69**(4), 293-306 (2001).

Fei, J., J. Zhang, F. Wang and J. Wang, "Synergistic effects on co-pyrolysis of lignite and high-sulfur swelling coal," *Journal of Analytical and Applied Pyrolysis,* **95**, 61-67 (2012).

Finney, M. A., J. D. Cohen, S. S. McAllister and W. M. Jolly, "On the need for a theory of wildland fire spread," *International journal of wildland fire,* **22**(1), 25-36 (2012).

Finney, M. A., S. S. McAllister, J. M. Forthofer and T. P. Grumstrup, Wildland fire behaviour: dynamics, principles and processes, CSIRO publishing (2021).

ForestWatch, "Chamise,," https://forestwatch.org/learn-explore/wildlife-plants/chamise/

Fusco, E. J., J. T. Finn, J. K. Balch, R. C. Nagy and B. A. Bradley, "Invasive grasses increase fire occurrence and frequency across US ecoregions," *Proceedings of the National Academy of Sciences,* **116**(47), 23594-23599 (2019).

Gallacher, J. R., "The Influence of Season, Heating Mode and Slope Angle on Wildland Fire Behavior," Ph.D. Dissertation, Chemical Engineering Department, Brigham Young University (2016).

Gilbert, P., C. Ryu, V. Sharifi and J. Swithenbank, "Tar Reduction in Pyrolysis Vapours from Biomass Over a Hot Char Bed," *Bioresource Technology,* **100**(23), 6045-6051 (2009).

Gollner, M., A. Trouve, I. Altintas, J. Block, R. de Callafon, C. Clements, A. Cortes, E. Ellicott, J. B. Filippi and M. Finney, "Towards data-driven operational wildfire spread modeling: A report of the NSF-funded WIFIRE workshop," (2015).

Gómez-Barea, A. and B. Leckner, "Modeling of biomass gasification in fluidized bed," *Progress in energy and combustion science,* **36**(4), 444-509 (2010).

Grasso, P. and M. S. Innocente, "Physics-based model of wildfire propagation towards faster-than-real-time simulations," *Computers & Mathematics with Applications,* **80**(5), 790-808 (2020).

Greenberg, J., H. Friedli, A. Guenther, D. Hanson, P. Harley and T. Karl, "Volatile organic emissions from the distillation and pyrolysis of vegetation," *Atmospheric Chemistry and Physics,* **6**(1), 81-91 (2006).

Guo, X.-j., S.-r. Wang, K.-g. Wang, Q. Liu and Z.-y. Luo, "Influence of Extractives on Mechanism of Biomass Pyrolysis," *Journal of Fuel Chemistry and Technology,* **38**(1), 42-46 (2010).

He, X., Z. Liu, W. Niu, L. Yang, T. Zhou, D. Qin, Z. Niu and Q. Yuan, "Effects of Pyrolysis Temperature on the Physicochemical Properties of Gas and Biochar Obtained from Pyrolysis of Crop Residues," *Energy,* **143**, 746-756 (2018).

Hoffman, C. M., J. Canfield, R. R. Linn, W. Mell, C. H. Sieg, F. Pimont and J. Ziegler, "Evaluating crown fire rate of spread predictions from physics-based models," *Fire Technology,* **52**, 221-237 (2016).

Hopa, D. Y., O. Alagöz, N. Yılmaz, M. Dilek, G. Arabacı and T. Mutlu, "Biomass co-pyrolysis: Effects of blending three different biomasses on oil yield and quality," *Waste Management & Research,* **37**(9), 925-933 (2019).

Jakab, E., G. Varhegyi and O. Faix, "Thermal decomposition of polypropylene in the presence of wood-derived materials," *Journal of Analytical and Applied Pyrolysis,* **56**(2), 273-285 (2000).

Jakab, E., M. Blazso and O. Faix, "Thermal decomposition of mixtures of vinyl polymers and lignocellulosic materials," *Journal of Analytical and Applied Pyrolysis,* **58**, 49-62 (2001).

Jegers, H. E. and M. T. Klein, "Primary and Secondary Lignin Pyrolysis Reaction Pathways," *Industrial & Engineering Chemistry Process Design and Development,* **24**(1), 173-183 (1985).

Johannes, I., L. Tiikma and H. Luik, "Synergy in co-pyrolysis of oil shale and pine sawdust in autoclaves," *Journal of Analytical and Applied Pyrolysis,* **104**, 341-352 (2013).

Kan, T., V. Strezov and T. J. Evans, "Lignocellulosic Biomass Pyrolysis: A Review of Product Properties and Effects of Pyrolysis Parameters," *Renewable and Sustainable Energy Reviews,* **57**, 1126-1140 (2016).

Keeley, J. E. and A. D. Syphard, "Climate change and future fire regimes: examples from California," *Geosciences,* **6**(3), 37 (2016).

Klemm, D., B. Heublein, H. P. Fink and A. Bohn, "Cellulose: fascinating biopolymer and sustainable raw material," *Angewandte chemie international edition,* **44**(22), 3358-3393 (2005).

Ku, C. S. and S. P. Mun, "Characterization of pyrolysis tar derived from lignocellulosic biomass," *JOURNAL OF INDUSTRIAL AND ENGINEERING CHEMISTRY-SEOUL-,* **12**(6), 853 (2006).

Lady Bird Johnson Wildflower Center, "Acer grandidentatum,," https://www.wildflower.org/gallery/result.php?id_image=89740 (2018).

Lady Bird Johnson Wildflower Center, "Artemisia tridentata," https://www.wildflower.org/plants/result.php?id_plant=artr2 (2019).

Leventon, I. T., J. Yang and M. C. Bruns, "Thermal decomposition of vegetative fuels and the impact of measured variations on simulations of wildfire spread," *Fire Safety Journal,* **137**, 103762 (2023).

Lewis, A. D. and T. H. Fletcher, "Prediction of Sawdust Pyrolysis Yields from a Flat-flame Burner Using the CPD Model," *Energy & Fuels,* **27**(2), 942-953 (2013).

Li, S., X. Chen, A. Liu, L. Wang and G. Yu, "Co-pyrolysis Characteristic of Biomass and Bituminous Coal," *Bioresource Technology,* **179**, 414-420 (2015).

Linn, R., J. Reisner, J. J. Colman and J. Winterkamp, "Studying wildfire behavior using FIRETEC," *International journal of wildland fire,* **11**(4), 233-246 (2002).

Liu, W.-J., K. Tian, H. Jiang, X.-S. Zhang and G.-X. Yang, "Preparation of liquid chemical feedstocks by co-pyrolysis of electronic waste and biomass without formation of polybrominated dibenzo-p-dioxins," *Bioresource technology,* **128**, 1-7 (2013).

Maggi, R. and B. Delmon, "Characterization and upgrading of bio-oils produced by rapid thermal processing," *Biomass and Bioenergy,* **7**(1-6), 245-249 (1994).

Manyà, J. J., E. Velo and L. Puigjaner, "Kinetics of Biomass Pyrolysis: a Reformulated Three-Parallel-Reactions Model," *Industrial & Engineering Chemistry Research,* **42**(3), 434-441 (2003).

Marsh, N. D., E. B. Ledesma, A. K. Sandrowitz and M. J. Wornat, "Yields of Polycyclic Aromatic Hydrocarbons from the Pyrolysis of Catechol [o rtho-Dihydroxybenzene]: Temperature and Residence Time Effects," *Energy & fuels,* **18**(1), 209-217 (2004).

Matt, F. J., M. A. Dietenberger and D. R. Weise, "Summative and Ultimate Analysis of Live Leaves from Southern U.S. Forest Plants for Use in Fire Modeling," *Energy & Fuels,* **34**(4), 4703-4720 (2020).

McAllister, S., I. Grenfell, A. Hadlow, W. Jolly, M. Finney and J. Cohen, "Piloted ignition of live forest fuels," *Fire Safety Journal,* **51**, 133-142 (2012).

McAllister, S. and D. Weise, "Effects of season on ignition of live wildland fuels using the forced ignition and flame spread test apparatus," *Combustion Science and Technology,* **189**(2), 231-247 (2017).

McGrattan, K., "Progress in Modeling Wildland Fires Using Computational Fluid Dynamics," *Proceedings of the 10th US National Combustion Meeting, College Park, MD, USA*, 23-26 (2017).

McKendry, P., "Energy production from biomass (part 1): overview of biomass," *Bioresource technology,* **83**(1), 37-46 (2002).

Mell, W., A. Maranghides, R. McDermott and S. L. Manzello, "Numerical simulation and experiments of burning douglas fir trees," *Combustion and Flame,* **156**(10), 2023-2041 (2009).

Mell, W. E., R. J. McDermott, G. P. Forney, C. Hoffman and M. Ginder, "Wildland Fire Behavior Modeling: Perspectives, New Approaches and Applications," proceedings of 3rd Fire Behavior and Fuels Conference (2010).

Miller, R. and J. Bellan, "Tar Yield and Collection from the Pyrolysis of Large Biomass Particles," *Combustion Science and Technology,* **127**(1-6), 97-118 (1997).

Morvan, D., "Physical phenomena and length scales governing the behaviour of wildfires: a case for physical modelling," *Fire technology,* **47**(2), 437-460 (2011).

Mount Diablo Interpretive Association, "Eastwood Manzanita,," https://www.mdia.org/wildflower-2/eastwood-manzanita

Mueller, E. V., N. S. Skowronski, K. L. Clark, M. R. Gallagher, W. E. Mell, A. Simeoni and R. M. Hadden, "Detailed physical modeling of wildland fire dynamics at field scale-An experimentally informed evaluation," *Fire Safety Journal,* **120**, 103051 (2021).

National Interagency Fire Center, "Wildfires and Acres,," https://www.nifc.gov/fire-information/statistics/wildfires (2026).

NIST, "NIST23: Updates to the NIST Tandem and Electron Ionization Spectral Libraries," https://www.nist.gov/programs-projects/nist23-updates-nist-tandem-and-electron-ionization-spectral-libraries (2023).

Novaes, E., M. Kirst, V. Chiang, H. Winter-Sederoff and R. Sederoff, "Lignin and Biomass: A Negative Correlation for Wood Formation and Lignin Content in Trees," *Plant Physiology,* **154**(2), 555-561 (2010).

Nunes, L. J., J. C. Matias, L. M. Loureiro, L. C. Sá, H. F. Silva, A. M. Rodrigues, T. P. Causer, D. B. DeVallance and D. E. Ciolkosz, "Evaluation of the potential of agricultural waste recovery: Energy densification as a factor for residual biomass logistics optimization," *Applied Sciences,* **11**(1), 20 (2020).

Olsen, S., D. Amundsen and S. Poudyal, "Gambel Oak Care,," Utah State University Extension (2021).

Paradela, F., F. Pinto, I. Gulyurtlu, I. Cabrita and N. Lapa, "Study of the Co-pyrolysis of Biomass and Plastic Wastes," *Clean Technologies and Environmental Policy,* **11**, 115-122 (2009).

Patwardhan, P. R., D. L. Dalluge, B. H. Shanks and R. C. Brown, "Distinguishing Primary and Secondary Reactions of Cellulose Pyrolysis," *Bioresource Technology,* **102**(8), 5265-5269 (2011).

Pereira, P., I. Bogunovic, W. Zhao and D. Barcelo, "Short-term effect of wildfires and prescribed fires on ecosystem services," *Current Opinion in Environmental Science & Health,* **22**, 100266 (2021).

Porterie, B., J.-L. Consalvi, J.-C. Loraud, F. Giroud and C. Picard, "Dynamics of Wildland Fires and Their Impact on Structures," *Combustion and Flame,* **149**(3), 314-328 (2007).

Prince, D., C. Shen and T. Fletcher, "Semi-empirical model for fire spread in shrubs with spatially-defined fuel elements and flames," *Fire technology,* **53**(3), 1439-1469 (2017).

Prince, D. R. and T. H. Fletcher, "Differences in burning behavior of live and dead leaves, Part 1: Measurements," *Combustion Science and Technology,* **186**(12), 1844-1857 (2014).

Rahimi Borujerdi, P., B. Shotorban, S. Mahalingam and D. R. Weise, "Influence of Pyrolysis Gas Composition and Reaction Kinetics on Leaf-Scale Fires," *Combustion Science and Technology*, 1-24 (2022).

Ranzi, E., A. Cuoci, T. Faravelli, A. Frassoldati, G. Migliavacca, S. Pierucci and S. Sommariva, "Chemical kinetics of biomass pyrolysis," *Energy & Fuels,* **22**(6), 4292-4300 (2008).

Raveendran, K. and A. Ganesh, "Heating value of biomass and biomass pyrolysis products," *Fuel,* **75**(15), 1715-1720 (1996).

Ren, Q., C. Zhao, X. Wu, C. Liang, X. Chen, J. Shen, G. Tang and Z. Wang, "TG–FTIR study on co-pyrolysis of municipal solid waste with biomass," *Bioresource technology,* **100**(17), 4054-4057 (2009).

Richards, A. P., D. Haycock, J. Frandsen and T. H. Fletcher, "A review of coal heating value correlations with application to coal char, tar, and other fuels," *Fuel,* **283**, 118942 (2021).

Safdari, M. S., "Characterization of Pyrolysis Products from Fast Pyrolysis of Live and Dead Vegetation," Ph.D. Dissertation, Chemical Engineering Department, Brigham Young University (2018).

Safdari, M. S., M. Rahmati, E. Amini, J. E. Howarth, J. P. Berryhill, M. Dietenberger, D. R. Weise and T. H. Fletcher, "Characterization of Pyrolysis Products from Fast Pyrolysis of Live and Dead Vegetation Native to the Southern United States," *Fuel,* **229**, 151-166 (2018).

Sainsbury, M., "The quinoline alkaloids," Rodd's Chemistry of Carbon Compounds, Eds. Elsevier, 171-255 (1964).

Scott, D. S., J. Piskorz and D. Radlein, "Liquid Products from the Continuous Flash Pyrolysis of Biomass," *Industrial & Engineering Chemistry Process Design and Development,* **24**(3), 581-588 (1985).

Shafizadeh, F., G. McGinnis and C. Philpot, "Thermal Degradation of Xylan and Related Model Compounds," *Carbohydrate Research,* **25**(1), 23-33 (1972).

Shafizadeh, F., "Introduction to pyrolysis of biomass," *Journal of analytical and applied pyrolysis,* **3**(4), 283-305 (1982).

Shen, D., S. Gu and A. Bridgwater, "The Thermal Performance of the Polysaccharides Extracted from Hardwood: Cellulose and Hemicellulose," *Carbohydrate Polymers,* **82**(1), 39-45 (2010a).

Shen, D. K., S. Gu and A. V. Bridgwater, "Study on the Pyrolytic Behaviour of Xylan-based Hemicellulose Using TG–FTIR and Py–GC–FTIR," *Journal of Analytical and Applied Pyrolysis,* **87**(2), 199-206 (2010b).

Shen, Y., J. Wang, X. Ge and M. Chen, "By-products recycling for syngas cleanup in biomass pyrolysis–An overview," *Renewable and Sustainable Energy Reviews,* **59**, 1246-1268 (2016).

Shotorban, C. A. B. Y. B. and S. Mahalingam, "Modeling dynamical and thermal behavior of firebrands in WFDS," *9th U. S. National Combustion Meeting,* (2015).

Smith, S. G., "Effects of Moisture on Combustion Characteristics of Live California Chaparral and Utah Foliage," M.S. Thesis, Chemical Engineering Department, Brigham Young University (2005).

Spörri, S., "Modelling of Timber Pyrolysis with FDS," Master's Thesis, Institute of Structural Engineering (IBK) ETH Zürich (2022).

Stefanidis, S. D., K. G. Kalogiannis, E. F. Iliopoulou, C. M. Michailof, P. A. Pilavachi and A. A. Lappas, "A Study of Lignocellulosic Biomass Pyrolysis via the Pyrolysis of Cellulose, Hemicellulose and Lignin," *Journal of Analytical and Applied Pyrolysis,* **105**, 143-150 (2014).

Stoliarov, S. I. and Y. Ding, "Pyrolysis model parameterization and fire growth prediction: the state of the art," *Fire safety journal,* **140**, 103905 (2023).

Sullivan, A. L., "A Review of Wildland Fire Spread Modelling, 1990-present 2: Empirical and Quasi-empirical Models," *International Journal of Wildland Fire* **18** (2007).

Sullivan, A. L., "Wildland Surface Fire Spread Modelling, 1990–2007. 1: Physical and Quasi-physical Models," *International Journal of Wildland Fire,* **18**(4), 349-368 (2009a).

Sullivan, A. L., "Wildland surface fire spread modelling, 1990–2007. 2: Empirical and quasi-empirical models," *International Journal of Wildland Fire,* **18**(4), 369-386 (2009b).

Sun, J.-P., S.-J. Sui, Z.-J. Zhang, S. Tan and Q.-W. Wang, "Study on the pyrolytic behavior of wood-plastic composites using Py-GC/MS," *BioResources,* **8**(4), 6196-6210 (2013).

Susott, R. A., "Characterization of the thermal properties of forest fuels by combustible gas analysis," *Forest Science,* **28**(2), 404-420 (1982).

Tao, J.-J., "Study on the Transition Mechanism for Broadleaf Foliage from Smoldering to Flaming Combustion Under External Hadiant Heat Flux," *Biomass Conversion and Biorefinery,* **10**(3), 765-773 (2020).

Taylor, S. W., D. G. Woolford, C. Dean and D. L. Martell, "Wildfire Prediction to Inform Fire Management: Statistical Science Challenges," *Statistical Science,* **28**(4), 586 - 615 (2013).

Tirmenstein, D. A., "Vaccinium arboreum,," Fire Sciences Laboratory, https://www.fs.usda.gov/database/feis/plants/shrub/vacarb/all.html (1991).

UC Irvine – Natural History of Orange County, "Hoary-leaved Ceanothus (Ceanothus crassifolius),," https://nathistoc.bio.uci.edu/plants/Rhamnaceae/Ceanothus%20crassifolius.htm (2009).

Uddin, M. N., K. Techato, J. Taweekun, M. M. Rahman, M. G. Rasul, T. M. I. Mahlia and S. M. Ashrafur, "An Overview of Recent Developments in Biomass Pyrolysis Technologies," *Energies,* **11**(11), 3115 (2018).

Utah State University Extension, "Utah Juniper," https://extension.usu.edu/botanicalcenter/trees-of-varga-arboretum/utah-juniper

Wang, S.-r., T. Liang, B. Ru and X.-j. Guo, "Mechanism of Xylan Pyrolysis by Py-GC/MS," *Chemical Research in Chinese Universities,* **29**(4), 782-787 (2013).

Wang, S., G. Dai, H. Yang and Z. Luo, "Lignocellulosic biomass pyrolysis mechanism: A state-of-the-art review," *Progress in energy and combustion science,* **62**, 33-86 (2017).

Wang, X., S. Bai, Q. Jin, S. Li, Y. Li, Y. Li and H. Tan, "Soot formation during biomass pyrolysis: Effects of temperature, water-leaching, and gas-phase residence time," *Journal of Analytical and Applied Pyrolysis,* **134**, 484-494 (2018).

Weise, D. R., T. H. Fletcher, T. J. Johnson, W. M. Hao, M. Dietenberger, M. Princevac, B. W. Butler, S. S. McAllister, J. J. O'Brien and E. L. Loudermilk, "Comparing gas composition from fast pyrolysis of live foliage measured in bench-scale and fire-scale experiments," *International Journal of Wildland Fire,* **33**(9) (2024).

Weise, D. R., T. H. Fletcher, T. J. Johnson, W. Hao, R. G. Tonkyn, C. A. Banach, J. Palarea-Albaladejo, M. Alizadeh and S. Baker, "The Composition of Gases from a Diffusion Flame Above Longleaf Pine Needle Fuel Beds," *Fuel,* **406**, 136681 (2026).

Willis, J. L., M. M. Bataineh, D. C. Clabo, E. D. Dickens, E. Galeano, S. B. Jack, J. S. Kush, C. D. Nelson, A. D. Polinko, K. M. Quigley, M. A. Sayer, J. M. Varner and W. C. Zipperer, "Longleaf Pine," USDA Forest Service (2026).

Xiao, R. and W. Yang, "Influence of Temperature on Organic Structure of Biomass Pyrolysis Products," *Renewable Energy,* **50**, 136-141 (2013).

Xiong, Z., H. Han, M. M. Azis, X. Hu, Y. Wang, S. Su, S. Hu and J. Xiang, "Formation of the Heavy Tar During Bio-oil Pyrolysis: A Study Based on Fourier Transform Ion Cyclotron Resonance Mass Spectrometry," *Fuel,* **239**, 108-116 (2019).

Yang, H., R. Yan, H. Chen, C. Zheng, D. H. Lee and D. T. Liang, "In-depth Investigation of Biomass Pyrolysis Based on Three Major Components: Hemicellulose, Cellulose and Lignin," *Energy & Fuels,* **20**(1), 388-393 (2006).

Yang, H., R. Yan, H. Chen, D. H. Lee and C. Zheng, "Characteristics of hemicellulose, cellulose and lignin pyrolysis," *Fuel,* **86**(12-13), 1781-1788 (2007).

Yang, X., H. Wang, P. J. Strong, S. Xu, S. Liu, K. Lu, K. Sheng, J. Guo, L. Che and L. He, "Thermal properties of biochars derived from waste biomass generated by agricultural and forestry sectors," *Energies,* **10**(4), 469 (2017).

Yokelson, R. J., D. W. T. Griffith and D. E. Ward, "Open-path Fourier Transform Infrared Studies of Large-scale Laboratory Biomass Fires," *Journal of Geophysical Research: Atmospheres,* **101**(D15), 21067-21080 (1996).

Yu, Q., C. Brage, G. Chen and K. Sjöström, "Temperature Impact on the Formation of Tar from Biomass Pyrolysis in a Free-fall Reactor," *Journal of Analytical and Applied Pyrolysis,* **40**, 481-489 (1997).

Zhang, L., S. Xu, W. Zhao and S. Liu, "Co-pyrolysis of biomass and coal in a free fall reactor," *Fuel,* **86**(3), 353-359 (2007).

Zhang, W., E. Zussman and A. Yarin, "Heat and mass transfer resulting in eruptive jetting from stems and leaves during distillation stage of forest fire," *Experimental Thermal and Fluid Science,* **116**, 110112 (2020).

Zhang, Y., S. Kajitani, M. Ashizawa and K. Miura, "Peculiarities of Rapid Pyrolysis of Biomass Covering Medium-and high-temperature Ranges," *Energy & Fuels,* **20**(6), 2705-2712 (2006).

Zhang, Y., S. Kajitani, M. Ashizawa and Y. Oki, "Tar Destruction and Coke Formation During Rapid Pyrolysis and Gasification of Biomass in a Drop-tube Furnace," *Fuel,* **89**(2), 302-309 (2010).

Zhou, H., C. Wu, A. Meng, Y. Zhang and P. T. Williams, "Effect of Interactions of Biomass Constituents on Polycyclic Aromatic Hydrocarbons (PAH) Formation During Fast Pyrolysis," *Journal of Analytical and Applied Pyrolysis,* **110**, 264-269 (2014).

Zhou, S., M. Garcia-Perez, B. Pecha, S. R. Kersten, A. G. McDonald and R. J. Westerhof, "Effect of the Fast Pyrolysis Temperature on the Primary and Secondary Products of Lignin," *Energy & Fuels,* **27**(10), 5867-5877 (2013).

Zhou, X., W. Li, R. Mabon and L. J. Broadbelt, "A Critical Review on Hemicellulose Pyrolysis," *Energy Technology,* **5**(1), 52-79 (2017).

Zhou, X., Y. Zhang, G. Chen and M. Zheng, "A model for physics-based fire simulation and analysis," *Virtual Reality,* **25**, 421-432 (2021).

Appendix

Analysis of heavy molecular weight tar compounds by HPLC

Introduction

This chapter focuses on separation of high molecular weight tar compounds and their detection using high performance liquid chromatography (HPLC). As noted in previous chapters, the GC/MS system could only measure molecules with a maximum molecular weight of about 300 amu. An HPLC system was therefore used to analyze the collected tar samples for higher molecular weight compounds. Tar samples from pyrolysis of Utah juniper and longleaf pine litter were analyzed for this purpose. The analysis of samples was performed in the Department of Chemistry and Biochemistry at Brigham Young University.

Materials and Methods

The experimental setup used for pyrolysis of biomass and the products' collection systems, including flat flame burner, ice bath, tar collection systems, and analysis instruments have been extensively explained in chapter 4.

Results and Discussion

Two tar samples, one collected from pyrolysis of longleaf pine litter and the other from Utah juniper were analyzed by this method to investigate the higher molecular wight compounds released during their pyrolysis. Among tar compounds detected from analysis with GC/MS, the heaviest compounds present in Utah juniper sample were dodecanoic acid (6.28 mol%) and 2-phenyl naphthalene (3.57 mol%) with molecular weights of 216 and 204 (g/mol) respectively. For longleaf pine litter, the heaviest tar compounds were benzo fluoranthene (1.45 mol%), and benzo phenanthrene (1.89 mol%) with molecular weights of 252 and 228 (g/mol) respectively. The focus of this chapter is to investigate whether any heavier tar compounds which could not be detected by GC/MS would be detected by HPLC.

Analysis of two tar spectrums (longleaf pine foliage and Utah juniper) from HPLC showed multiple unknown peaks. Tar analysis by GC/MS had already shown that phenol was one of the most abundant tar compounds with its concentration in longleaf pine litter and Utah juniper being 10.11 and 13.81 mol% respectively. A phenol standard performed under identical conditions eluted at approximately 4.8 minutes, confirming the method designed for HPLC was working, and that phenol peak was observed in the two unknown samples. Peaks at earlier retention times (<3 min) corresponded to column void volume (solvent front), and other very polar compounds present in tar samples. The gradual change in the concentration of acetonitrile in the mobile phase resulted in an effective separation of polar compounds from hydrophobic analytes. Peaks eluting earlier are the polar compounds which are more soluble in water. The hydrophobic compounds are more soluble in acetonitrile and elute at later retention times. Differences in the peak profiles of the two tar samples are due to variations in the biochemical compositions of longleaf pine litter and Utah juniper foliage. The spectrum resulting from longleaf pine litter tar showed stronger hydrophobic peaks eluting at later retention times compared to Utah juniper. This indicated tar from longleaf pine litter had a higher proportion of heavy molecular weight tar compounds compared to Utah juniper. Utah juniper tar resulted in fewer or smaller peaks in the same retention window, which may be due to lower concentration of heavy tar compounds or their lower solubility in acetonitrile. While this approach provided valuable preliminary insight into the distribution of higher molecular weight tar compounds, it could not identify compounds without comparing the unknown peaks to standards prepared under identical conditions. The preparation and use of such standards was deemed to be a separate Ph.D. project and beyond the scope of the current dissertation.

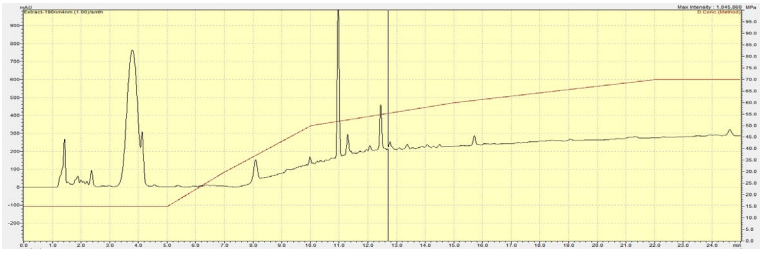

Figure A.0.1: HPLC spectrum for analysis of tar from Utah juniper

Figure A.0.2: HPLC spectrum for analysis of tar from longleaf pine litter

Conclusion

Despite these limitations, the present work shows that reversed-phase HPLC with a C18 column and a water/acetonitrile gradient mobile phase can separate and detect both light and heavy portions of tar released during pyrolysis of plant species. Tar from longleaf pine litter had a higher proportion of heavy molecular weight tar compounds compared to Utah juniper. If a library of reference standards of heavy molecular weight tar compounds such as pyrenes, anthracenes, coronenes, and other phenolic compounds is prepared, the identification of heavier tar compounds would also be possible. These efforts will improve the understanding of compounds released during pyrolysis of plant species and enhance modeling of wildland fires and associated smoke generation.

Table A1. Ultimate and proximate analysis for plant species

Region	Species	C	H	N	O	Moisture content	Ash	Volatile matter	Fixed C
northern Utah	Big sagebrush	48.52	6.46	2.25	42.77	100-195	3.9	85.2	n.a
northern Utah	Utah juniper	49.92	6.88	1.33	41.87	40-100	4	84.8	n.a
northern Utah	Gambel oak	49.15	6.23	2.52	42.10	50-125	2.9	83.5	n.a
northern Utah	Bigtooth maple	48.52	6.46	2.25	42.77	55-160	3.5	83.9	n.a
southern California	Chamise	51.48	6.61	1.31	40.60	76-85	2.8	76.9	n.a
southern California	Eastwood's manzanita	52.77	6.32	0.78	40.13	45-105	2.2	76.9	n.a
southern California	Scrub oak	51.47	6.50	1.99	40.03	45-75	5.1	74.5	n.a
southern California	Hoaryleaf ceanothus	52.94	6.30	1.08	39.67	35-105	3.2	75.8	n.a

Table A2. Complete list of tar compounds, their chemical class, molecular formula, and molecular weight

No.	Component name	Chemical class	Ar/Non-Ar	Mol. Formula	MW(g/mol)
1	Triethylamine	Amine	Non-Ar	$C_6H_{15}N$	101
2	Pyridine	Heterocyclic Ar	Ar	C_5H_5N	79.1
3	1,3-Diazine	Heterocyclic Ar	Ar	$C_4H_4N_2$	80
4	1-Hydroxy-2-butanone	Ketones	Non-Ar	$C_4H_8O_2$	88
5	Pyrimidine,2-methyl	Heterocyclic Ar	Ar	$C_5H_6N_2$	94
6	2-Cyclopenten-1-one	Cyclic Ketone	Non-Ar	C_5H_6O	82
7	2-Furanmethanol	Alcohols	Ar	$C_5H_6O_2$	98
8	Butyrolactone	Cyclo-Ester	Non-Ar	$C_4H_6O_2$	86
9	p- Benzoquinone	Cyclo-alkene	Non-Ar	$C_6H_4O_2$	108
10	2-cyclopenten-1- one, 2- methyl	Cyclic Ketone	Non-Ar	C_6H_8O	96
11	Phenol	Benzenoid Aromatic	Ar	C_6H_6O	94
12	2-cyclopenten-1- one, 3- methyl	Cyclic Ketone	Non-Ar	C_6H_8O	96
13	3- pyridine carbonitrile	Cyclo-alkene	Non-Ar	$C_6H_4N_2$	104
14	1,2-Cyclopentanedione, 3-methyl-	Cyclic Ketone	Non-Ar	$C_6H_8O_2$	112
15	Benzene, 1-ethyl-3-methyl	Benzenoid Aromatic	Ar	C_9H_{12}	120
16	Benzyl Alcohol (α-cresol)	Benzenoid Aromatic	Ar	C_7H_8O	108
17	Hexanoic acid, 4-methyl	Acid	Non-Ar	$C_7H_{14}O_2$	130
18	6- Heptenoic acid	Acid	Non-Ar	$C_7H_{12}O_2$	128
19	Phenol, 4-methyl-	Benzenoid Aromatic	Ar	C_7H_8O	108
20	Phenol, 2-methyl-	Benzenoid Aromatic	Ar	C_7H_8O	108
21	1-Octen-3-ol	Alcohols	Non-Ar	$C_8H_{16}O$	128
22	Phenol, 2-methoxy- (guaiacol)	Benzenoid Aromatic	Ar	$C_7H_8O_2$	124

Table A2 continued.

No.	Component name	Chemical class	Ar/Non-Ar	Molecular formula	MW(g/mol)
23	Phenol, 3,4-dimethyl- (Xylenol)	Benzenoid Aromatic	Ar	$C_8H_{10}O$	122
24	Phenol, 4-ethyl-	Benzenoid Aromatic	Ar	$C_8H_{10}O$	122
25	7-octenoic acid	Acid	Non-Ar	$C_8H_{14}O_2$	142
26	Benzoic Acid	Benzenoid Aromatic	Ar	$C_7H_6O_2$	122
27	1,2-Benzenediol(catechol)	Benzenoid Aromatic	Ar	$C_6H_6O_2$	110
28	1,3-Benzenediol, 4-ethyl-	Benzenoid Aromatic	Ar	$C_8H_{10}O_2$	138
29	Naphthalene	PAH	Ar	$C_{10}H_8$	128
30	Benzofuran, 2,3-dihydro-	Benzenoid Aromatic	Ar	C_8H_8O	120
31	3-hydroxy phenyl acetylene	Benzenoid Aromatic	Ar	C_8H_6O	118
32	1,4-Benzenediol(Hydroquinone, Quinol, Benzene- 1,4-diol)	Benzenoid Aromatic	Ar	$C_6H_6O_2$	110
33	1,2-Benzenediol, 3-methyl-	Benzenoid Aromatic	Ar	$C_7H_8O_2$	124
34	Quinoline	Benzenoid Aromatic	Ar	C_9H_7N	129
35	1,2-Benzenediol, 3-methoxy-	Benzenoid Aromatic	Ar	$C_7H_8O_3$	140
36	8-Nonenoic acid	Acid	Non-Ar	$C_9H_{16}O_2$	156
37	1,2-Benzenediol, 4-methyl-	Benzenoid Aromatic	Ar	$C_7H_8O_2$	124
38	Phenol, 4-ethyl-2-methoxy- (4-ethyl guaiacol)	Benzenoid Aromatic	Ar	$C_9H_{12}O_2$	152
39	Indole	Benzenoid Aromatic	Ar	C_8H_7N	117
40	Ethanone, 1-(2-hydroxy-5-methylphenyl)-	Ketones	Ar	$C_9H_{10}O_2$	150
41	Indolizine	Heterocyclic Non-Ar	Non-Ar	C_8H_7N	117
42	2-Methoxy-6-methylphenol	Benzenoid Aromatic	Ar	$C_8H_{10}O_2$	138

Table A2 continued.

No.	Component name	Chemical class	Ar/Non-Ar	Molecular formula	MW(g/mol)
43	2,2'- Bifuran	Heterocyclic Ar	Ar	$C_8 H_6 O_2$	134
44	Phenol, 2,6-dimethoxy-	Benzenoid Aromatic	Ar	$C_8 H_{10} O_3$	154
45	1,2,3-Benzenetriol(Benzene-1,2,3- triol)	Benzenoid Aromatic	Ar	$C_6 H_6 O_3$	126
46	1,2-Benzenediol, 4-ethyl-	Benzenoid Aromatic	Ar	$C_8 H_{10} O_2$	138
47	1-H-indenol	Benzenoid Aromatic	Ar	$C_9 H_8 O$	132
48	Benzeneethanol, 4-hydroxy-	Benzenoid Aromatic	Ar	$C_8 H_{10} O_2$	138
49	1-Heptatriacotanol	Alcohols	Non-Ar	$C_{37} H_{76} O$	537
50	1-Methylnaphthalene	PAH	Ar	$C_{11} H_{10}$	142
51	1,2,3-Benzenetriol, 5-methyl-	Benzenoid Aromatic	Ar	$C_7 H_8 O_3$	140
52	2-[4-methyl-6-(2,6,6-trimethylcyclohex-1-enyl)hexa-1,3,5-trienyl]cyclohex-1-en-1-carboxaldehyde	Cyclo-alkene	Non-Ar	$C_{23} H_{32} O$	324.5
53	Coumarin	Benzenoid Aromatic	Ar	$C_9 H_6 O_2$	146
54	Acenaphthylene	PAH	Ar	$C_{12} H_8$	152
55	2-Methylnaphthalene	PAH	Ar	$C_{11} H_{10}$	142
56	6,7-Epoxypregn-4-ene-9,11,18-triol-3,20-dione, 11,18-diacetate	Cyclo-alkene	Non-Ar	$C_{25} H_{32} O_8$	460.57
57	Ethyl iso-allocholate	Cyclo-alkane	Non-Ar	$C_{27} H_{48} O_5$	452.67
58	Dodecanoic acid, 3-hydroxy	Acid	Non-Ar	$C_{12} H_{24} O_3$	216
59	Dodecanoic acid	Acid	Non-Ar	$C_{12} H_{24} O_2$	200
60	Fluorene	PAH	Ar	$C_{13} H_{10}$	166
61	Phorbol	Cyclo-alkene	Non-Ar	$C_{20} H_{28} O_6$	364.44

Table A2 continued.

No.	Component name	Chemical class	Ar/Non-Ar	Molecular formula	MW(g/mol)
62	Naphthalene, 2,6-diisopropyl-	PAH	Ar	$C_{16}H_{20}$	212
63	5H-Cyclopropa[3,4]benz[1,2-e]azulen-5-one, 9a-(acetyloxy)-1,1a,1b,4,4a,7a,7b,8,9,9a-decahydro-4a,7b,9-trihydroxy-3-(hydroxymethyl)-1,1,6,8-tetramethyl-, [1aR-(1aa,1bß,4aß,7aa,7ba,8a,9ß,9aa)]-	Cyclo-alkene	Non-Ar	$C_{26}H_{34}O_{10}$	506
64	3-Hydroxy biphenyl	Benzenoid Aromatic	Ar	$C_{12}H_{10}O$	170
65	Anthracene	PAH	Ar	$C_{14}H_{10}$	178
66	Phenanthrene	PAH	Ar	$C_{14}H_{10}$	178
67	9H Fluorene-9-one	PAH	Ar	$C_{13}H_{8}O$	180
68	9,10-Ethanoanthracene, 9,10-dihydro-11,12-diacetyl-	PAH	Ar	$C_{20}H_{18}O_{2}$	290.38
69	4H Cyclopenta[def]phenanthrene	PAH	Ar	$C_{15}H_{10}$	190
70	Naphthalene, 2-phenyl-	PAH	Ar	$C_{16}H_{12}$	204
71	Fluoranthene	PAH	Ar	$C_{16}H_{10}$	202

Table A2 continued.

No.	Component name	Chemical class	Ar/Non-Ar	Molecular formula	MW(g/mol)
72	Benzo[e]pyrene	PAH	Ar	$C_{20}H_{12}$	252
73	Pyrene	PAH	Ar	$C_{16}H_{10}$	202
74	7H-Benzo[c]fluorene	PAH	Ar	$C_{17}H_{12}$	216
75	11H-Benzo[a]fluorene	PAH	Ar	$C_{17}H_{12}$	216
76	Benzo[c]phenanthrene	PAH	Ar	$C_{18}H_{12}$	228
77	Benzo(a)fluoranthene	PAH	Ar	$C_{20}H_{12}$	252
78	Cyclopenta[cd]pyrene	PAH	Ar	$C_{18}H_{10}$	226
79	Naphthacene	PAH	Ar	$C_{18}H_{12}$	228
80	Benz(a)anthracene	PAH	Ar	$C_{18}H_{12}$	228
81	Chrysene	PAH	Ar	$C_{18}H_{12}$	228

Table A3. Tar compounds and their concentration from pyrolysis of California chaparral.

No.	Component name	Chamise twigs with foliage (Mol%)	Chamise twigs w/o foliage (Mol%)	Manzanita foliage (Mol%)	Manzanita twig (Mol%)	Scrub oak (Mol%)	Hoaryleaf Ceanothus (Mol%)
1	Pyridine	2.1	0.0	0.0	0.0	2.5	0.0
2	p- Benzoquinone	0.0	2.6	0.0	0.0	0.0	0.0
3	Phenol	40.7	31.6	10.5	18.3	34.5	27.2
4	Benzene, 1-ethyl-3-methyl	0.0	0.0	0.0	0.0	0.0	2.2
5	Phenol, 4-methyl-	13.3	12.9	1.1	5.5	11.6	13.3
6	Phenol, 2-methyl-	3.3	2.3	2.1	6.2	2.8	7.4
7	Benzofuran, 2,3-dihydro-	6.5	8.0	3.1	3.6	17.4	9.5

Table A3 continued.

No.	Component name	Chamise twigs with foliage (Mol%)	Chamise twigs w/o foliage (Mol%)	Manzanita foliage (Mol%)	Manzanita twig (Mol%)	Scrub oak (Mol%)	Hoaryleaf Ceanothus (Mol%)
8	3-hydroxy phenyl acetylene	0.0	1.8	0.0	0.0	0.0	0.0
9	1,4-Benzenediol(Hydroquinone, Quinol, Benzene- 1,4-diol)	4.5	2.2	0.0	0.0	0.0	0.0
10	Quinoline	4.7	2.5	0.0	0.0	4.5	6.2
11	Phenol, 4-ethyl-2-methoxy- (4-ethyl guaiacol)	1.7	1.8	0.0	0.0	0.0	0.0
12	Indolizine	2.4	2.0	3.0	5.8	0.0	0.0
13	1-Heptatriacotanol	0.0	1.5	6.9	5.5	4.3	7.4
14	2-[4-methyl-6-(2,6,6-trimethylcyclohex-1-enyl)hexa-1,3,5-trienyl]cyclohex-1-en-1-carboxaldehyde	0.0	0.0	2.4	6.1	0.0	0.0
15	Acenaphthylene	0.0	0.0	0.0	0.0	0.0	3.6
16	6,7-Epoxypregn-4-ene-9,11,18-triol-3,20-dione, 11,18-diacetate	3.3	4.9	2.9	2.0	5.0	4.3
17	Ethyl iso-allocholate	2.2	1.8	4.6	2.5	1.4	2.0
18	Phorbol	0.0	3.6	34.1	16.4	2.7	0.0
19	9,10-Ethanoanthracene, 9,10-dihydro-11,12-diacetyl-	11.6	13.7	1.4	9.2	4.9	6.3
20	Fluoranthene	3.8	7.0	19.3	7.8	8.5	9.2

Table A3 continued.

No.	Component name	Chamise twigs with foliage (Mol%)	Chamise twigs w/o foliage (Mol%)	Manzanita foliage (Mol%)	Manzanita twig (Mol%)	Scrub oak (Mol%)	Hoaryleaf Ceanothus (Mol%)
21	5H-Cyclopropa[3,4]benz[1,2-e]azulen-5-one, 9a-(acetyloxy)-1,1a,1b,4,4a,7a,7b,8,9,9a-decahydro-4a,7b,9-trihydroxy-3-(hydroxymethyl)-1,1,6,8-tetramethyl-, [1aR-(1aa,1bß,4aß,7aa,7ba,8a,9ß,9aa)]-	0.0	0.0	8.8	11.2	0.0	0.0

Table A4a. Complete list of tar compounds and their concentration from pyrolysis of selected southeastern species.

No.	Component name	Darrow's blueberry (live)	Dwarf palmetto (live)	Fetterbush(live)	Inkberry (live)	Live oak (live)	Little Bluestem(live)	Longleaf pine (live)
		Mol%	Mol%	Mol%	Mol%	Mol%	Mol%	Mol%
1	Phenol	14.5	33.2	21.3	16.2	27.2	6.4	13.1
2	1,2-Cyclopentanedione, 3-methyl-	0.0	2.2	0.0	0.0	0.0	0.0	0.0

Table A4a continued.

No.	Component name	Darrow's blueberry (live)	Dwarf palmetto (live)	Fetterbush(live)	Inkberry (live)	Live oak (live)	Little Bluestem(live)	Longleaf pine (live)
		Mol%	Mol%	Mol%	Mol%	Mol%	Mol%	Mol%
3	Benzyl Alcohol (α-cresol)	0.1	0.0	0.4	0.3	0.0	0.0	0.0
4	Phenol, 4-methyl-	1.3	2.4	4.1	0.6	6.7	0.1	3.7
5	Phenol, 2-methyl-	0.0	0.0	0.8	0.1	0.0	0.0	0.0
6	1-Octen-3-ol	0.1	0.0	0.1	0.0	0.0	0.0	0.0
7	Phenol, 2-methoxy- (guaiacol)	0.2	0.0	1.3	0.3	0.0	0.0	0.0
8	Phenol, 3,4-dimethyl- (Xylenol)	0.0	0.0	0.9	0.0	0.0	0.0	0.0
9	Phenol, 4-ethyl-	0.0	0.0	0.4	0.0	0.0	0.0	0.0
10	1,2-Benzenediol(catechol)	13.0	3.0	5.3	7.2	5.2	2.6	2.0
11	1,3-Benzenediol, 4-ethyl-	0.0	0.0	0.0	0.0	0.0	0.1	0.0
12	Naphthalene	2.1	3.9	1.9	0.3	4.7	0.8	0.3
13	Benzofuran, 2,3-dihydro-	3.1	0.0	1.0	1.0	0.0	0.0	0.0
14	1,4-Benzenediol(Hydroquinone, Quinol, Benzene- 1,4-diol)	9.3	3.3	2.9	5.3	2.2	0.3	0.1
15	1,2-Benzenediol, 3-methyl-	1.8	0.0	0.9	1.4	1.6	0.0	0.0
16	Quinoline	1.0	1.1	0.0	1.2	3.2	0.0	0.0

Table A4a continued.

No.	Component name	Darrow's blueberry (live)	Dwarf palmetto (live)	Fetterbush(live)	Inkberry (live)	Live oak (live)	Little Bluestem(live)	Longleaf pine (live)
		Mol%	Mol%	Mol%	Mol%	Mol%	Mol%	Mol%
17	1,2-Benzenediol, 3-methoxy-	2.1	0.0	0.0	1.3	0.0	0.0	0.0
18	1,2-Benzenediol, 4-methyl-	4.1	0.0	0.0	2.0	1.1	0.0	0.0
19	Phenol, 4-ethyl-2-methoxy- (4-ethyl guaiacol)	0.0	0.0	0.0	0.0	0.0	0.8	1.1
20	Indole	0.6	3.5	2.6	0.4	4.1	0.0	0.0
21	Ethanone, 1-(2-hydroxy-5-methylphenyl)-	0.0	0.1	0.0	0.0	0.0	0.0	0.0
22	2-Methoxy-6-methylphenol	0.0	0.0	0.0	0.0	0.0	0.0	1.7
23	Phenol, 2,6-dimethoxy-	1.9	5.9	1.4	0.5	6.9	0.8	2.5
24	1,2,3-Benzenetriol(Benzene-1,2,3- triol)	0.3	0.0	0.1	0.4	1.3	0.0	1.3
25	1,2-Benzenediol, 4-ethyl-	7.3	0.0	0.0	0.4	0.0	0.0	0.0
26	Benzeneethanol, 4-hydroxy-	0.0	0.0	0.0	0.0	0.0	0.0	1.3
27	1-Methylnaphthalene	3.0	2.0	1.6	1.4	0.9	0.2	1.4

Table A4a continued.

No.	Component name	Darrow's blueberry (live) Mol%	Dwarf palmetto (live) Mol%	Fetterbush(live) Mol%	Inkberry (live) Mol%	Live oak (live) Mol%	Little Bluestem(live) Mol%	Longleaf pine (live) Mol%
28	1,2,3-Benzenetriol, 5-methyl-	0.2	0.0	0.0	0.1	0.0	0.0	0.0
29	Acenaphthylene	2.7	2.6	1.8	2.7	1.9	1.9	1.8
30	2-Methylnaphthalene	1.5	1.4	1.0	1.5	2.2	9.5	8.0
31	Fluorene	3.0	3.1	1.3	2.3	2.8	25.6	10.6
32	Naphthalene, 2,6-diisopropyl-	0.8	1.5	1.1	0.6	1.4	4.8	3.9
33	Anthracene	3.3	2.0	2.2	5.1	1.8	3.1	2.1
34	Phenanthrene	1.5	4.6	5.3	2.6	2.2	3.1	3.9
35	4H Cyclopenta[def]phenanthrene	1.5	1.1	2.7	2.2	1.8	2.5	2.2
36	Naphthalene, 2-phenyl-	1.3	1.0	0.8	1.6	1.0	3.7	4.1
37	Fluoranthene	4.5	2.1	6.8	5.2	3.0	3.6	2.6
38	Benzo[e]pyrene	2.1	2.4	2.5	5.6	2.4	1.3	1.2
39	Pyrene	5.3	5.1	9.9	8.3	3.0	12.0	13.0
40	7H-Benzo[c]fluorene	1.3	2.8	2.9	7.2	4.2	10.6	11.7
41	11H-Benzo[a]fluorene	1.4	1.0	3.1	2.0	3.0	3.0	2.9
42	Benzo[c]phenanthrene	0.3	2.2	2.5	2.1	3.1	1.0	1.6
43	Benzo(a)fluoranthene	0.4	2.5	2.5	2.5	0.2	1.0	0.9
44	Cyclopenta[cd]pyrene	0.3	1.4	2.4	2.6	0.3	0.3	0.1
45	Naphthacene	1.5	1.0	0.9	2.1	0.3	0.3	0.3
46	Benz(a)anthracene	1.3	1.2	2.1	2.5	0.1	0.2	0.2
47	Chrysene	0.4	0.8	1.1	0.7	0.2	0.2	0.4

Table A4b. Complete list of tar compounds and their concentration from pyrolysis of selected southeastern species.

No.	Component name	Saw Palmetto (live) Mol%	Sparkleberry (live) Mol%	Swamp bay (live) Mol%	water oak (live) Mol%	Wax myrtle (live) Mol%	wire grass(live) Mol%	Yaupon(live) Mol%	Longleaf pine litter Mol%
1	Phenol	0.2	0.0	0.0	0.0	0.0	0.0	0.0	10.1
2	1,2-Cyclopentanedione, 3-methyl-	0.0	0.3	0.0	0.0	0.0	0.0	0.0	0.0
3	Benzyl Alcohol (α-cresol)	1.8	2.5	3.0	5.9	3.1	2.8	3.0	0.0
4	Phenol, 4-methyl-	0.0	0.0	0.0	0.0	0.0	0.0	0.0	3.0
5	Phenol, 2-methyl-	0.0	0.0	0.0	0.0	0.0	0.0	1.1	0.0
6	1-Octen-3-ol	0.0	0.3	1.1	0.0	1.3	0.8	1.9	0.0
7	Phenol, 2-methoxy-(guaiacol)	0.0	0.0	0.0	0.0	0.5	0.0	0.0	0.0
8	Phenol, 3,4-dimethyl-(Xylenol)	0.0	0.0	0.0	0.0	0.0	0.9	0.0	0.0
9	Phenol, 4-ethyl-	1.5	8.7	7.3	6.5	14.3	4.0	2.4	0.0
10	1,2-Benzenediol(catechol)	0.0	0.0	0.0	0.0	0.0	0.5	0.0	2.3
11	1,3-Benzenediol, 4-ethyl-	2.2	0.8	1.8	3.6	2.8	0.4	1.7	0.0
12	Naphthalene	0.0	2.2	2.2	0.0	0.0	0.0	0.9	0.2

Table A4b continued.

No.	Component name	Saw Palmetto (live)	Sparkleberry (live)	Swamp bay (live)	water oak (live)	Wax myrtle (live)	wire grass(live)	Yaupon(live)	Longleaf pine litter
		Mol%	Mol%	Mol%	Mol%	Mol%	Mol%	Mol%	Mol%
13	Benzofuran, 2,3-dihydro-	0.0	2.2	2.2	0.0	0.0	0.0	0.9	0.0
14	1,4-Benzenediol(Hydroquinone, Quinol, Benzene- 1,4-diol)	2.0	7.2	5.2	1.9	1.5	0.1	1.2	0.2
15	1,2-Benzenediol, 3-methyl-	0.0	1.3	1.8	1.3	2.0	0.0	0.0	0.0
16	Quinoline	1.5	1.0	2.0	2.2	0.5	0.0	0.8	0.0
17	1,2-Benzenediol, 3-methoxy-	0.0	2.5	0.0	0.0	3.4	0.0	0.0	0.0
18	1,2-Benzenediol, 4-methyl-	0.0	4.1	3.1	1.3	1.1	0.0	0.0	0.0
19	Phenol, 4-ethyl-2-methoxy-(4-ethyl guaiacol)	0.0	0.0	0.0	0.0	0.0	0.7	0.0	1.2
20	Indole	2.5	0.5	1.5	3.2	1.3	0.0	2.2	0.0
21	Ethanone, 1-(2-hydroxy-5-methylphenyl)-	0.5	0.0	0.0	0.0	0.0	0.0	0.0	0.0

Table 4Ab continued.

No.	Component name	Saw Palmetto (live)	Sparkleberry (live)	Swamp bay (live)	water oak (live)	Wax myrtle (live)	wire grass(live)	Yaupon(live)	Longleaf pine litter
		Mol%	Mol%	Mol%	Mol%	Mol%	Mol%	Mol%	Mol%
22	2-Methoxy-6-methylphenol	0.0	0.0	0.0	0.0	0.0	1.8	0.0	2.0
23	Phenol, 2,6-dimethoxy-	3.9	2.9	3.5	5.3	3.3	2.9	3.4	2.8
24	1,2,3-Benzenetriol(Benzene-1,2,3- triol)	0.0	1.3	1.1	0.9	0.1	1.3	0.0	1.1
25	1,2-Benzenediol, 4-ethyl-	0.0	2.9	0.0	0.0	0.0	0.0	0.0	0.0
26	Benzeneethanol, 4-hydroxy-	0.0	0.0	0.0	0.0	0.0	1.1	0.0	1.3
27	1-Methylnaphthalene	1.2	1.7	2.4	1.0	1.4	1.0	1.9	1.1
28	1,2,3-Benzenetriol, 5-methyl-	0.0	0.1	0.5	0.0	0.0	0.6	2.2	0.0

Table 4Ab continued.

No.	Component name	Saw Palmetto (live)	Sparkleberry (live)	Swamp bay (live)	water oak (live)	Wax myrtle (live)	wire grass(live)	Yaupon(live)	Longleaf pine litter
		Mol%	Mol%	Mol%	Mol%	Mol%	Mol%	Mol%	Mol%
29	Acenaphthylene	2.5	2.8	4.2	2.4	4.0	1.3	1.7	1.6
30	2-Methylnaphthalene	1.2	1.3	4.5	2.0	0.0	7.1	1.7	5.9
31	Fluorene	4.7	2.2	1.2	2.0	3.3	10.0	1.1	10.3
32	Naphthalene, 2,6-diisopropyl-	1.6	0.9	1.2	0.8	0.0	3.3	1.3	3.0
33	Anthracene	2.2	5.7	5.2	1.1	2.5	2.1	3.3	2.0
34	Phenanthrene	2.6	3.5	3.3	3.8	5.0	3.8	4.0	3.5
35	4H Cyclopenta[def]phenanthrene	2.5	1.4	2.4	2.3	2.6	2.6	2.4	2.1

Table 4Ab continued.

No.	Component name	Saw Palmetto (live)	Sparkleberry (live)	Swamp bay (live)	water oak (live)	Wax myrtle (live)	wire grass(live)	Yaupon(live)	Longleaf pine litter
		Mol%	Mol%	Mol%	Mol%	Mol%	Mol%	Mol%	Mol%
36	Naphthalene, 2-phenyl-	1.2	3.8	2.2	1.9	0.4	4.8	3.7	6.2
37	Fluoranthene	3.6	6.6	5.1	6.1	2.9	4.0	5.7	2.7
38	Benzo[e]pyrene	4.3	2.3	2.3	1.8	0.5	2.5	5.2	1.7
39	Pyrene	8.2	5.7	7.8	6.0	8.0	6.9	6.8	14.3
40	7H-Benzo[c]fluorene	3.4	1.4	1.4	4.5	2.2	7.5	4.6	12.9
41	11H-Benzo[a]fluorene	1.7	2.4	2.2	2.5	1.4	2.9	3.0	3.1
42	Benzo[c]phenanthrene	1.5	1.1	1.8	2.6	2.0	2.3	2.7	1.9

Table 4Ab continued.

No.	Component name	Saw Palmetto (live)	Sparkleberry (live)	Swamp bay (live)	water oak (live)	Wax myrtle (live)	wire grass(live)	Yaupon(live)	Longleaf pine litter
		Mol%	Mol%	Mol%	Mol%	Mol%	Mol%	Mol%	Mol%
43	Benzo(a)fluoranthene	1.4	0.9	0.8	0.3	1.4	1.9	2.0	1.4
44	Cyclopenta[cd]pyrene	1.4	0.8	1.0	0.6	1.3	2.0	2.9	0.6
45	Naphthacene	1.5	1.3	1.1	0.1	1.7	2.6	1.4	0.4
46	Benz(a)anthracene	1.1	1.7	1.4	0.5	1.2	2.1	0.8	0.2
47	Chrysene	0.1	0.1	0.2	0.3	0.8	1.2	0.9	0.7

Table A5. Complete list of compounds and their concentration in tar from co-pyrolysis of biomass blends.

Fuel Type	β	Compound Name	Mole %	Ar/Non-AR	Compound Type
Chamise-SO 2.5	0.29	Pyridine	2.5%	Ar	Non-Benzenoid Ar
Chamise-SO 2.5	0.29	Phenol	35.2%	Ar	Benzenoid
Chamise-SO 2.5	0.29	Phenol, 2-methyl-	3.1%	Ar	Benzenoid
Chamise-SO 2.5	0.29	Phenol,3-methyl	12.5%	Ar	Benzenoid
Chamise-SO 2.5	0.29	3-Hydroxyphenylacetylene	1.0%	Ar	Benzenoid
Chamise-SO 2.5	0.29	Benzofuran, 2,3-dihydro-	14.2%	Ar	Benzenoid
Chamise-SO 2.5	0.29	Quinoline	4.6%	Ar	PAH
Chamise-SO 2.5	0.29	Phenol,4-ethyl-2-methoxy	1.0%	Ar	Benzenoid
Chamise-SO 2.5	0.29	1-Heptatriacotanol	2.9%	Non-Ar	Alcohol
Chamise-SO 2.5	0.29	Acenaphthylene	1.2%	Ar	PAH
Chamise-SO 2.5	0.29	6,7-Epoxypregn-4-ene-9,11,18-triol-3,20-dione, 11,18-diacetate	4.5%	Non-Ar	Cyclo-alkene
Chamise-SO 2.5	0.29	Dodecanoic acid, 3-hydroxy	1.3%	Non-Ar	Acid
Chamise-SO 2.5	0.29	Ethyl iso-allocholate	1%	Non-Ar	Cyclo-alkane
Chamise-SO 2.5	0.29	Phorbol	2.5%	Non-Ar	Cyclo-alkene
Chamise-SO 2.5	0.29	Fluoranthene	4.2%	Ar	PAH
Chamise-SO 2.5	0.29	9,10-Ethanoanthracene, 9,10-dihydro-11,12-diacetyl-	8.2%	Ar	PAH

Table A5 continued.

Fuel Type	β	Compound Name	Mole %	Ar/Non-AR	Compound Type
Chamise1-SO1	0.5	Pyridine	2.4%	Ar	Non-Benzenoid Ar
Chamise1-SO1	0.5	Phenol	36.2%	Ar	Benzenoid
Chamise1-SO1	0.5	Phenol, 2-methyl-	3.1%	Ar	Benzenoid
Chamise1-SO1	0.5	Phenol,3-methyl	14.2%	Ar	Benzenoid
Chamise1-SO1	0.5	Benzofuran, 2,3-dihydro-	10.1%	Ar	Benzenoid
Chamise1-SO1	0.5	Hydroquinone	2.1%	Ar	Benzenoid
Chamise1-SO1	0.5	Quinoline	4.2%	Ar	PAH
Chamise1-SO1	0.5	Phenol,4-ethyl-2-methoxy	1.0%	Ar	Benzenoid

Table A5 continued.

Fuel Type	β	Compound Name	Mole %	Ar/Non-AR	Compound Type
Chamise1-SO1	0.5	Indolizine	1.5%	Ar	Hetrocyclic
Chamise1-SO1	0.5	Acenaphthylene	1.4%	Ar	PAH
Chamise1-SO1	0.5	6,7-Epoxypregn-4-ene-9,11,18-triol-3,20-dione, 11,18-diacetate	4.2%	Non-Ar	Cyclo-alkene
Chamise1-SO1	0.5	Dodecanoic acid, 3-hydroxy	2.3%	Non-Ar	Acid
Chamise1-SO1	0.5	Ethyl iso-allocholate	2%	Non-Ar	cyclo-alkane
Chamise1-SO1	0.5	Phorbol	2.3%	Non-Ar	Cyclo-alkene
Chamise1-SO1	0.5	Fluoranthene	6.5%	Ar	PAH
Chamise1-SO1	0.5	9,10-Ethanoanthracene, 9,10-dihydro-11,12-diacetyl-	6.3%	Ar	PAH

Table A5 continued.

Fuel Type	β	Compound Name	Mole %	Ar/Non-AR	Compound Type
Chamise2.5-SO1	0.71	Pyridine	2.2%	Ar	Non-Benzenoid Aromatic
Chamise2.5-SO1	0.71	p-Benzoquinone	1.3%	Non-Ar	Cyclo-alkene
Chamise2.5-SO1	0.71	Phenol	39.0%	Ar	Benzenoid
Chamise2.5-SO1	0.71	Phenol, 2-methyl-	3.3%	Ar	Benzenoid
Chamise2.5-SO1	0.71	Phenol,3-methyl	12.1%	Ar	Benzenoid
Chamise2.5-SO1	0.71	3-Hydroxyphenylacetylene	1.1%	Ar	Benzenoid
Chamise2.5-SO1	0.71	Benzofuran, 2,3-dihydro-	9.1%	Ar	Benzenoid
Chamise2.5-SO1	0.71	Hydroquinone	3.1%	Ar	Benzenoid

Table A5 continued.

Fuel Type	β	Compound Name	Mole %	Ar/Non-AR	Compound Type
Chamise2.5-SO1	0.71	Quinoline	4.9%	Ar	PAH
Chamise2.5-SO1	0.71	Phenol,4-ethyl-2-methoxy	1.5%	Ar	Benzenoid
Chamise2.5-SO1	0.71	Indolizine	1.1%	Ar	Hetrocyclic
Chamise2.5-SO1	0.71	1-Heptatriacotanol	1.0%	Non-Ar	Alcohol
Chamise2.5-SO1	0.71	Acenaphthylene	2.1%	Ar	PAH
Chamise2.5-SO1	0.71	6,7-Epoxypregn-4-ene-9,11,18-triol-3,20-dione, 11,18-diacetate	3.7%	Non-Ar	Cyclo-alkene
Chamise2.5-SO1	0.71	Dodecanoic acid, 3-hydroxy	1.5%	Non-Ar	Acid
Chamise2.5-SO1	0.71	Ethyl iso-allocholate	1%	Non-Ar	cyclo-alkane

Table A5 continued.

Fuel Type	β	Compound Name	Mole %	Ar/Non-AR	Compound Type
Chamise2.5-SO1	0.71	Quinoline	4.9%	Ar	PAH
Chamise2.5-SO1	0.71	Phenol,4-ethyl-2-methoxy	1.5%	Ar	Benzenoid
Chamise2.5-SO1	0.71	Indolizine	1.1%	Ar	Hetrocyclic
Chamise2.5-SO1	0.71	1-Heptatriacotanol	1.0%	Non-Ar	Alcohol
Chamise2.5-SO1	0.71	Acenaphthylene	2.1%	Ar	PAH
Chamise2.5-SO1	0.71	6,7-Epoxypregn-4-ene-9,11,18-triol-3,20-dione, 11,18-diacetate	3.7%	Non-Ar	Cyclo-alkene
Chamise2.5-SO1	0.71	Dodecanoic acid, 3-hydroxy	1.5%	Non-Ar	Acid
Chamise2.5-SO1	0.71	Ethyl iso-allocholate	1%	Non-Ar	cyclo-alkane

Table A5 continued.

Fuel Type	β	Compound Name	Mole %	Ar/Non-AR	Compound Type
Chamise2.5-SO1	0.71	9,10-Ethanoanthracene, 9,10-dihydro-11,12-diacetyl-	5.2%	Ar	PAH
Chamise2.5-SO1	0.71	Phorbol	1.1%	Non-Ar	Cyclo-alkene
Chamise2.5-SO1	0.71	Fluoranthene	5.5%	Ar	PAH

Table A6. Compounds in tar and their HHV.

No.	Component name	Each Tar component HHV(MJ/Kg)	Each Tar Component HHV (KJ/mol)
1	Triethylamine	45.077	4552.8
2	Pyridine	32.142	2542.5
3	1,3-Diazine	27.29	2183.2
4	1-Hydroxy-2-butanone	26.624	2342.94
5	Pyrimidine,2-methyl	30.542	2871

Table A6 continued.

No.	Component name	Each Tar component HHV(MJ/Kg)	Each Tar Component HHV (KJ/mol)
6	2-Cyclopenten-1-one	32.289	2647.7
7	2-Furanmethanol	25.044	2454.3
8	Butyrolactone	24.036	2067.1
9	p- Benzoquinone	25.406	2746.2
10	2-cyclopenten-1- one, 2- methyl	34.711	3332.29
11	Phenol	32.45	3053.9
12	2-cyclopenten-1- one, 3- methyl	34.711	3332.29
13	3- pyridine carbonitrile	28.758	2990.8
14	1,2-Cyclopentanedione, 3-methyl-	27.971	31342.83
15	Benzene, 1-ethyl-3-methyl	43.337	5208.7
16	Benzyl Alcohol (α-cresol)	34.537	3729.96
17	Hexanoic acid, 4-methyl	33.689	4380
18	6- Heptenoic acid	34.22	4380.5
19	Phenol, 4-methyl-	34.54	3729.96
20	Phenol, 2-methyl-	34.54	3729.96
21	1-Octen-3-ol	41.17	5269.76
22	Phenol, 2-methoxy- (guaiacol)	28.47	3530.35

Table A6 continued.

No.	Component name	Each Tar component HHV(MJ/Kg)	Each Tar Component HHV (KJ/mol)
23	Phenol, 3,4-dimethyl- (Xylenol)	36.211	4417.7
24	Phenol, 4-ethyl-	36.211	4417.7
25	7-octenoic acid	33.653	4778.7
26	Benzoic Acid	26.442	3225.9
27	1,2-Benzenediol(catechol)	25.91	2850.01
28	1,3-Benzenediol, 4-ethyl-	30.523	4212.2
29	Naphthalene	39.064	5000
30	Benzofuran, 2,3-dihydro-	34.884	4191.4
31	3-hydroxy phenyl acetylene	32.625	3849.76
32	1,4-Benzenediol(Hydroquinone, Quinol, Benzene-1,4-diol)	25.91	2850.01
33	1,2-Benzenediol, 3-methyl-	28.47	3530.35
34	Quinoline	35.88	4628.2
35	1,2-Benzenediol, 3-methoxy-	23.88	3343.13
36	8-Nonenoic acid	35.01	5461.9
37	1,2-Benzenediol, 4-methyl-	28.471	3530.35
38	Phenol, 4-ethyl-2-methoxy- (4-ethyl guaiacol)	32.205	4895.15
39	Indole	36.106	4224.4
40	Ethanone, 1-(2-hydroxy-5-methylphenyl)-	30.745	4611.8
41	Indolizine	36.1	4224.4
42	2-Methoxy-6-methylphenol	30.523	4212.2
43	2,2'- Bifuran	27.21	3645.78
44	Phenol, 2,6-dimethoxy-	26.11	4020.3
45	1,2,3-Benzenetriol(Benzene-1,2,3- triol)	26.142	3293.92
46	1,2-Benzenediol, 4-ethyl-	30.52	4212.2
47	1-H-indenol	34.375	4537.56

Table A6 continued.

No.	Component name	Each Tar component HHV(MJ/Kg)	Each Tar Component HHV (KJ/mol)
48	Benzeneethanol, 4-hydroxy-	30.523	4212.2
49	1-Heptatriacotanol	47.48	25499.96
50	1-Methylnaphthalene	40.545	5757.49
51	1,2,3-Benzenetriol, 5-methyl-	23.88	3343.13
52	2-[4-methyl-6-(2,6,6-trimethylcyclohex-1-enyl)hexa-1,3,5-trienyl]cyclohex-1-en-1-carboxaldehyde	41.91	13598.76
53	Coumarin	27.706	4045.12
54	Acenaphthylene	39.352	5981.6
55	2-Methylnaphthalene	40.545	5757.49
56	6,7-Epoxypregn-4-ene-9,11,18-triol-3,20-dione, 11,18-diacetate	28.074	12928.1
57	Ethyl iso-allocholate	36.653	16591.78
58	Dodecanoic acid, 3-hydroxy	35.153	7593.01
59	Dodecanoic acid	38.995	7799.07
60	Fluorene	38.881	6454.3
61	Phorbol	29.521	10758.9
62	Naphthalene, 2,6-diisopropyl-	43.871	9300.8
63	5H-Cyclopropa[3,4]benz[1,2-e]azulen-5-one, 9a-(acetyloxy)-1,1a,1b,4,4a,7a,7b,8,9,9a-decahydro-4a,7b,9-trihydroxy-3-(hydroxymethyl)-1,1,6,8-tetramethyl-, [1aR-(1aa,1bß,4aß,7aa,7ba,8a,9ß,9aa)]-	26.123	13231.25
64	3-Hydroxy biphenyl	36.058	6130
65	Anthracene	38.297	6816.99
66	Phenanthrene	38.298	6816.99
67	9H Fluorene-9-one	34.182	6152.76
68	9,10-Ethanoanthracene, 9,10-dihydro-11,12-diacetyl-	35.009	10166.7
69	4H Cyclopenta[def]phenanthrene	39.352	7476.99

Table A6 continued.

No.	Component name	Each Tar component HHV(MJ/Kg)	Each Tar Component HHV (KJ/mol)
70	Naphthalene, 2-phenyl-	40.023	8164.8
71	Fluoranthene	37.3	7534.6
72	Benzo[e]pyrene	38.809	9779.99
73	Pyrene	39.014	7880.81
74	7H-Benzo[c]fluorene	39.669	8568.59
75	11H-Benzo[a]fluorene	39.669	8568.59
76	Benzo[c]phenanthrene	37.315	8507.8
77	Benzo(a)fluoranthene	38.809	9779.99
78	Cyclopenta[cd]pyrene	38.444	8688.4
79	Naphthacene	37.089	8456.41
80	Benz(a)anthracene	37843	8628.2
81	Chrysene	37.414	8530.3

Table A7. List of tar compounds detected from the flame base.

No.	Compound Name	Average mol%	Compound class	Compound Type	M W (g/mol)	Rings
1	Phenol	6.03%	Benzenoid Ar	Ar	94.11	1
2	Benzene, 1-ethyl-3-methyl-	0.04%	Benzenoid Ar	Ar	120.19	1
3	Phenol, 2-methyl-	1.34%	Benzenoid Ar	Ar	108.14	1
4	Phenol, 3-methyl-	6.76%	Benzenoid Ar	Ar	108.14	1
5	Phenol, 3,4-dimethyl-	1.19%	Benzenoid Ar	Ar	122.16	1
6	Phenol, 4-ethyl-	2.22%	Benzenoid Ar	Ar	122.16	1
7	Phenol, 3-ethyl-	0.08%	Benzenoid Ar	Ar	122.16	1
8	Catechol	3.38%	Benzenoid Ar	Ar	110.1	1

Table A7 continued.

No.	Compound Name	Average mol%	Compound class	Compound Type	M W (g/mol)	Rings
9	6-Methylenebicyclo[3.2.0]hept-3-en-2-one	2.52%	Ketone	Ketone	120.15	N/A
10	Azulene	0.85%	Non-benzenoid Ar	Ar	128.174	0
11	1H-Indene, 1-methylene-	0.37%	Benzenoid Ar	Ar	128.17	1
12	Propoxur	1.11%	Benzenoid Ar	Ar	209.24	1
13	1H-2,8a-Methanocyclopenta[a]cyclopropa[e]cyclodecen-11-one, 1a,2,5,5a,6,9,10,10a-octahydro-5,5a,6-trihydroxy-1,4-bis(hydroxymethyl)-1,7,9-trimethyl-, [1S-(1a,1aa,2a,5ß,5aß,6ß,8aa,9a,10aa)]-	0.18%	Cyclo-alkene	Non-Ar	364.4	N/A
14	Caprolactam	4.49%	Cyclo-alkane	Non-Ar	113.16	N/A
15	1,2-Benzisothiazole	1.60%	Benzenoid Ar	Ar	135.19	1
16	9,10-Secocholesta-5,7,10(19)-triene-3,24,25-triol, (3ß,5Z,7E)-	0.14%	Cyclo-alkane	Non-Ar	416.71	N/A
17	Cyclopropanebutanoic acid, 2-[[2-[[2-[(2-pentylcyclopropyl)methyl]cyclopropyl]methyl]cyclopropyl]methyl]-, methyl ester	0.47%	Cyclo-alkane	Non-Ar	374.6	N/A
18	Bicyclo[4.4.1]undeca-1,3,5,7,9-pentaene	4.94%	Cyclo-alkene	Non-Ar	142.2	N/A
19	6,7-Epoxypregn-4-ene-9,11,18-triol-3,20-dione, 11,18-diacetate	0.24%	Cyclo-alkene	Non-Ar	460.57	N/A
20	Biphenyl	2.74%	Benzenoid Ar	Ar	154.21	1
21	Ethyl iso-allocholate	7.17%	Cyclo-alkane	Non-Ar	436.7	N/A
22	Naphthalene, 2-ethenyl-	4.43%	PAH	Ar	154.21	2
23	Quinoline, 1,2-dihydro-2,2,4-trimethyl-	1.70%	Benzenoid Ar	Ar	173.25	1
24	1-Heptatriacotanol	0.20%	Alcohol	Non-Ar	537	N/A

Table A7 continued.

No.	Compound Name	Average mol%	Compound class	Compound Type	M W (g/mol)	Rings
25	Acenaphthylene	4.37%	PAH	Ar	152.19	2
26	Biphenylene	14.65%	Benzenoid Ar	Ar	152.19	3
27	Fluorene	8.59%	PAH	Ar	166.22	1
28	9,10-Ethanoanthracene, 9,10-dihydro-11,12-diacetyl-	5.40%	Benzenoid Ar	Ar	290.38	1
29	Phenanthrene	12.80%	PAH	Ar	178.23	3

Table A8. List of tar compounds detected from the intermittent region.

No.	Compound Name	Average mol%	Compound class	Compound Type	M W (g/mol)	Rings
1	5,9-Dodecadien-2-one, 6,10-dimethyl-, (E,E))-	2.32%	Ketone	Non-Ar	208.34	0
2	2-Ethylhexanal	11.20%	Aldehyde	Non-Ar	128.21	0
3	Ethanone, 1-(3-methylphenyl)-	4.34%	Benzenoid Ar	Ar	134.18	1
4	Caprolactam	8.11%	Cyclo-Alkane	Non-Ar	113.16	0
5	1,2-Benzisothiazole	6.58%	Benzenoid Ar	Ar	135.19	1
6	Ethanol, 2-(9,12-octadecadienyloxy)-, (Z,Z)-	2.88%	Alcohol	Non-Ar	310.58	0
7	1-Heptatriacotanol	7.16%	Alcohol	Non-Ar	537.00	0
8	9,10-Secocholesta-5,7,10(19)-triene-3,24,25-triol, (3ß,5Z,7E)-	1.42%	Cyclo-Alkane	Non-Ar	416.71	0
9	Quinoline, 1,2-dihydro-2,2,4-trimethyl-	10.09%	Benzenoid Ar	Ar	173.25	1
10	Ethyl iso-allocholate	25.50%	Cyclo-Alkane	Non-Ar	436.70	0
11	Acenaphthylene	2.88%	PAH	Ar	152.19	2
12	Octadecane, 3-ethyl-5-(2-ethylbutyl)-	12.40%	Alkane	Non-Ar	366.70	0
13	Phenanthrene	5.09%	PAH	Ar	178.23	3